PUTTING THE SELF IN CONTEXT: AN INTEGRATIVE ANALYSIS OF INTEROCEPTION IN AUTISM

By

Alisa Rose Zoltowski

Dissertation

Submitted to the Faculty of the

Graduate School of Vanderbilt University

in partial fulfillment of the requirements

for the degree of

DOCTOR OF PHILOSOPHY

in

Neuroscience

December 16, 2023

Nashville, Tennessee

Approved:

Blythe Corbett, Ph.D.

Baxter Rogers, Ph.D.

Jennifer Blackford, Ph.D.

Carissa Cascio, Ph.D.

This dissertation is dedicated to my triplet brother, Matthew Zoltowski. You are and will always be my inspiration.

ACKNOWLEDGMENTS

This work was supported by the National Institutes of Health under awards: 2T32MH064913-16, R01MH102272 and the National Science Foundation under award: NRT DGE 19-22697. I would further like to thank all of the members of the Laboratory of Affective Sensory Research (LASR) and all of our research participants for making this work possible.

TABLE OF CONTENTS

LIST OF TABLES

LIST OF FIGURES

CHAPTER 1

Introduction

1.1 The bird's eye view: Sensory issues in autism

The earliest definitions of autism were described in terms of differences in language, social behaviors, observed motor behaviors, and interests (Asperger, 1944; Kanner, 1943; Rosen et al., 2021). Altered sensory behaviors were described in some early definitions of autism, including in Ritvo and Freeman (1977) as "Abnormal responses to sensations. Any one or a combination of sight, hearing, touch, pain, balance, smell, taste, and the way a child holds his or her body are affected." However, until recently, autism diagnostic criteria previously focused on social/communicative and motor behaviors; sensory behaviors were only listed as a standardized diagnostic criterion in the latest diagnostic manual revision (American Psychiatric Association, 2013). Though autism is still primarily diagnosed through behavioral observation and thus has often been described by these types of observer perspectives, the research field has gained more insight into the internal experiences of autism from the growing voices of autistic self-advocates (Force, 2019; Savarese, 2010). As awareness of sensory differences has increased, they are increasingly seen as fundamental to the autistic experience (Savarese, 2010).

Indeed, the evidence to date suggests broad differences in how autistic individuals experience and respond to sensory information. Autistic sensory differences have been reported across different modes of inquiry (e.g., by sensory testing or self-report) and different sensory modalities, especially auditory and tactile (Ausderau et al., 2014; Baranek et al., 2006; Minshew and Hobson, 2008). Efforts to create a taxonomy of altered sensory processing have commonly done so by the nature of the observable behavioral response. Most prominently, strong, affectively negative behavioral reactions to typical sensations are termed "hyper-responsiveness", reduced reactions to salient sensations are termed "hypo-

responsiveness", and increased intentional engagement with sensory stimuli is termed "sensory seeking" (Baranek, 1999; Baranek et al., 2006; Boyd et al., 2010). On the surface, these might seem mutually exclusive such that an individual would be either hyper- or hypo- responsive to sensory stimuli. However, many individuals show both of these types of patterns (Ausderau et al., 2016; Baranek et al., 2022; Lee et al., 2022; Williams et al., 2018). This suggests that the relationship between behavioral and brain patterns is not as simple as a single mapping between neural and behavioral sensitivity (e.g., enhanced neural processing always leading to enhanced behavioral sensitivity and vice versa), but that some of these behavioral patterns may be inter-related at the neural level.

Individual variability is also a complicated part of understanding sensory processing in autism. Though it is common for autistic individuals to show some type of sensory difference, the types of differences vary between individuals across behavioral responsiveness categories and different sensory modalities. Thus, researchers have attempted to identify different sub-types of autistic sensory experiences. The sensory subtypes that have emerged for autistic individuals often first identify groups by the overall level of sensory symptoms (mild, moderate, or highly elevated), then other features include relative hypo- versus hyper- responsiveness and how these features change over time (Ausderau et al., 2016; Chen et al., 2022a). Across each of these categories, autistic children are more likely to show levels of altered responsiveness that increase from birth to early childhood than their non-autistic peers (Chen et al., 2022a,b). Though sensory processing/integration treatments for autistic individuals are commonly prescribed due to these pervasive challenges, their evidence base for long term outcomes is limited (Camarata et al., 2020). This suggests a need for greater understanding of the underlying brain differences.

1.2 Sensory processing over development

One key part of understanding autistic sensory experiences is autism's classification as a neurodevelopmental condition. The biology of autism starts in earliest development, as

autism-linked genes have predominant expression during early to late fetal development (Krishnan et al., 2016). Autistic individuals show different patterns of brain development from non-autistic peers starting in infancy (Hazlett et al., 2011; The IBIS Network et al., 2017) and continuing throughout their lives (MRC AIMS Consortium et al., 2020; Nickl-Jockschat et al., 2012). Though autism diagnoses may still be made into adolescence and adulthood, the DSM specifies that symptom onset must be in the early developmental period, even if only identified retrospectively (American Psychiatric Association, 2013). This developmental lens gives another window to view individual variability in autism. Some biological heterogeneity occurs inherently, reflected in the numerous different genes that have been linked to autism (Geschwind and Levitt, 2007; Sestan and State, 2018). On the other hand, diverse life experiences may also contribute to variations in how sensory processing differences with similar etiologies may present differentially, across individuals and within individuals at different stages of their lives.

One prominent theory in explaining sensory differences in autism also follows from a developmental lens, describing how individuals predict their incoming sensations based on prior experiences (Palmer et al., 2017; Pellicano and Burr, 2012). Systems neuroscience has exposed the anticipation of incoming sensory input as a critical part of our nervous system structure, allowing for efficient processing of an overwhelming (and often redundant) amount of receptor input (Bastos et al., 2012; Huang and Rao, 2011). Learning from past experience is a fundamental part of this process, as incoming real-time input is compared with expectations based on prior sensory experiences. In mathematical modeling terms, this has been described by Bayesian modeling. Bayesian theories of autism have suggested that autistic individuals rely less on their past experience to interpret current sensations than non-autistic individuals do (Palmer et al., 2017; Pellicano and Burr, 2012). The proposed consequences are that autistic individuals process sensory information more veridically than non-autistic individuals, but with a cost in terms of efficient interpretation.

There has indeed been evidence that autistic individuals show more detailed percep-

tion ("local") at the expense of bigger-picture integration ("global"), particularly in visual processing (Behrmann et al., 2006; Flevaris and Murray, 2015) but also in tactile (Puts et al., 2014; Tavassoli et al., 2016) and auditory processing (Kwakye et al., 2011), reviewed across modalities in Robertson and Baron-Cohen (2017). Other evidence in line with Bayesian theories of autism extends to the different types of sensory cues that people may use to predict their sensations. For example, what someone is expecting to see is not just influenced by past visual experience, but by learned relationships between sights and related sounds, touch, or smells. Combining sensory information from different modalities to increase understanding of the current situation, such as lip reading when you cannot fully hear what someone is saying, is known as multisensory integration. As part of relying less on prior experience, there is evidence that autistic individuals also rely less on multisensory information to interpret current sensory cues (Baum et al., 2015; Feldman et al., 2018). This includes reduced susceptibility to multisensory illusions, such as the "McGurk effect," an illusion created by mismatched auditory and visual speech cues (Stevenson et al., 2014; Zhang et al., 2019) , or the rubber hand illusion, created by mismatched visual and tactile cues, (Cascio et al., 2012a). Added together, the unimodal and multimodal evidence support Bayesian theories of autism. However, the scope of this theory across different sensory systems and different individuals has yet to be determined, as well as thorough testing of how this is proposed to occur within specific neural circuits.

Lastly, understanding autistic sensory processing as developmental includes how early sensory experiences lay the foundation for later skills. Proposed as a developmental cascade, early sensory differences in autism may impact increasingly complex skills over time (Cascio et al., 2016). For example, auditory processing is one foundation for verbal language development; other foundations include mapping between visual cues and the relevant sounds (Baum et al., 2015; Woynaroski et al., 2013). Our social worlds include many such sensory components, including the visual cues of familiar faces (McGugin and Gauthier, 2016; Schultz, 2005) and the sensorimotor skills we use to interact with oth-

ers (Iverson, 2021). Reduced sensory predictive processing in autism may also cascade onto increased preference for routines and sameness, to reduce what might otherwise be an overwhelming amount of new sensory information to interpret (Pellicano and Burr, 2012; Pellicano, 2013). Making sense of sensory processing in autism requires thoughtful consideration of these potential developmental relationships.

1.3 Interoception: The ultimate developmental cascade

Arguably, our primary sensation for survival is the sense of interoception, i.e., the ability to perceive and respond to physiological cues such as hunger, thirst, cardiac sensations, pain, and respiration (Craig, 2002, 2004, 2008). Due to this primacy, interoceptive brain responses are reliable before other sensory areas in human infants (Jönsson et al., 2018) and these brain areas are wired to receive diverse input summarizing the external sensory environment (linking specific sights, sounds, etc. with a given bodily state, (Craig, 2009)). In turn, this lends interoceptive processing the ability to pervade many other areas of functioning that rely on self-referential thinking and relating "self" and "other" (Palmer and Tsakiris, 2018). Theories of embodied cognition propose that interoceptive signals provide a stable sense of self that serves as backdrop for interpreting all other information (Montirosso and McGlone, 2020; Park and Tallon-Baudry, 2014; Tallon-Baudry et al., 2018). Park and Tallon-Baudry (2014) describe this as forming the "I" in "I saw that." On the social side, the degree to which humans are a social species has neurobiological links to the role human caregivers play in initially meeting the physiological needs of their infants (Atzil et al., 2018; Fotopoulou et al., 2022).

Interoception and health outcomes intersect across multiple domains of health and wellness. Critical implications of altered interoception for health were described in rare patients with greatly reduced or non-existent pain perception, who often developed severe injuries and physical disorders since these patients did not react to signals of tissue injury (Dearborn, 1932; Nagasako et al., 2003). Experiences of fatigue during illness have also been

shown to be an interoceptive process, driving individuals to appropriately rest and recover until their body is healed (Harrison et al., 2009; Lekander et al., 2016). Researchers have started to study links between interoception and physical activity, with studies supporting positive bidirectional effects: physical activity may help refine interoceptive signal processing and interoceptive awareness may help optimizing an activity plan (Amaya et al., 2021; McMorris, 2021; Wallman-Jones et al., 2021; Zarza-Rebollo et al., 2019). On the other hand, negative bidirectional effects may be seen in cases of disordered eating: reduced interoception predicts propensity towards a later eating disorder (Leon et al., 1995; Lilenfeld et al., 2006), whereas disordered eating may also reduce one's ability to adaptively process and perceive one's internal cues (Adams et al., 2022b; Khalsa et al., 2022).

Further, interoception has been theorized to prominently impact mental health, prompting multidisciplinary initiatives to better understand its role in anxiety, depression, and addiction as well as eating disorders (Khalsa et al., 2018). Paulus and Stein (2006) first conceptualized anxiety as disordered interoceptive predictions, i.e., predicting a "threat" to bodily state even when interoceptive sensations were within homeostatic range. The organization of interoceptive-emotional brain systems provides further support for how the circuitry of anxiety closely overlaps with the circuitry for predicting and responding to interoceptive sensations (Barrett and Simmons, 2015; Kleckner et al., 2017). This framework has been expanded to also describe interoceptive system changes that occur in depression, wherein the interoceptive system predicts a state of scarcity and directs this system to heavily conserve energy resources (Barrett et al., 2016). The ability for artificially altered interoceptive signaling to cause anxiety-related behaviors has now been shown compellingly in rodent research (Hsueh et al., 2023) and is also supported in human lesion patients (Khalsa et al., 2016). However, correlative relationships between interoceptive processing and anxiety have been harder to characterize in more natural settings, leaving a limited evidence base to understand how interoception and anxiety relate in practice. Though several studies have supported links between measures of interoceptive processing and anxiety in human

research, there have been largely mixed/inconclusive findings at the level of perceptual tasks (Adams et al., 2022a; Domschke et al., 2010), likely attributable to measurement challenges in this area and a need to break down the relevant aspects of interoception and anxiety more precisely.

1.4 The history of interoceptive measurement

There has been a growing interest to measure individual differences in interoception, emerging first in the 1970s and 1980s. Studies in this time period were inspired by studies from other sensory systems, using psychophysics approaches to carefully map relationships between sensory stimulus levels and participant perception (Dale and Anderson, 1978; Schandry, 1981; Whitehead et al., 1977). Of the different types of interoceptive stimuli, heartbeats have been the most popular choice for psychophysics task design, as they occur rapidly, frequently, and are straightforward to objectively measure, easing the adaptation of paradigms designed for exteroceptive stimuli such as visual flashes or auditory tones. Thus, early research focused on individuals' ability to perceive their heartbeats, either by counting them (Dale and Anderson, 1978; Schandry, 1981) or by discriminating them from other sensations (Whitehead et al., 1977). Though these tasks provided the framework for interoceptive perceptual understanding, many participants find them difficult to complete and thus both tasks were plagued by low participant accuracy, and many confounds in their interpretation (Brener and Ring, 2016; Desmedt et al., 2018). This limited researchers in using these tasks to study their relationships with other individual features, such as mental health outcomes.

These challenges inspired a broader scope of interoceptive task design. Certain tasks have focused on addressing some of the confounds present in prior heartbeat tracking tasks (Fittipaldi et al., 2020; Körmendi et al., 2022). Researchers have also considered the ecological relevance of different types of internal signals, designing tasks that might reflect the levels at which interoceptive sensations more readily reach awareness. This focus has

been applied to cardiac sensation, shifting towards measuring perception of heart rate rather than individual beats (Legrand et al., 2022) or induced cardiac changes pharmacologically (Khalsa et al., 2016). There have also been creative efforts to study interoceptive submodalities other than cardiac sensation, including respiration (Walsh et al., 2019) and gastrointestinal perception (Khalsa et al., 2022). Due to the recency of their development, the psychometric properties of these tasks and their relationship to individual features are ripe to explore.

There has also been an interest in understanding more detailed representations of how people report their interoceptive experiences. Porges' Body Perception Questionnaire was an early endeavor in this area, focusing on the frequency and strength to which individuals report feeling their interoceptive sensations (Porges, 1993). However, this did not readily distinguish the extent to which interoceptive awareness (or lack thereof) corresponded with challenges or distress to the individual. Later, multiple other questionnaires were developed to distinguish different aspects of interoceptive experiences, such as the Interoception Sensory Questionnaire (Fiene et al., 2018) that measures confusion resulting from reduced awareness of bodily sensations. When analyzing the content structure of the most commonly used questionnaires, Desmedt et al. (2022) found that they represented at least five distinct aspects of interoceptive experiences. As with perceptual tasks, self-report of daily interoceptive experiences seems best understood as multifaceted.

A few different frameworks have been proposed to organize interoceptive measures more broadly, across both objective and subjective domains. Garfinkel et al. (2015) proposed an early taxonomy of these distinctions, dividing interoception into objective measures ("accuracy"), subjective measures ("sensibility"), and their concordance ("awareness", reflecting self-insight about interoceptive processing). A more recent 2 x 2 model was then proposed that built in the role that attention might play in interoceptive perception and experience (Murphy et al., 2019). The first domain of this model describes what is measured, as attention or accuracy. The second domain describes how it is measured, via

task performance or self-report. Though these taxonomies are still evolving, they highlight the different nuances that need to be considered when measuring interoception in clinical populations.

1.5 Status: Interoception in autism

Qualitative self-report data suggests that many autistic individuals are concerned with their interoception, providing statements such as "The best way I can describe this to health professionals is that I receive a signal from somewhere I'm not exactly sure, and I have difficulties interpreting what they might mean" or "I'm super sensitive to little changes in how my body feels" (Trevisan et al., 2021b). However, interoceptive questionnaires that attempt to quantify these reported patterns do not necessarily suggest a single pattern of differences in autism (Williams et al., 2022). Instead, autistic individuals may report feeling like they are either more or less aware of their interoceptive cues than neurotypical peers depending on the situation and study (Failla et al., 2020; Gargouri et al., 2016; Mul et al., 2018; Palser et al., 2018; Pickard et al., 2020), similar to findings in other sensory modalities. Thus, there remain many questions about the scope and degree of interoceptive differences in autism and what may explain the types of challenges that autistic individuals report qualitatively.

Perceptual studies of interoception in autism have similarly been mixed. Due to their dominance in the literature until recently, interoception studies in autism so far have typically used either heartbeat counting or heartbeat discrimination paradigms. Williams et al. (2022) meta-analysis of these studies found evidence for significantly reduced heartbeat counting, but not heartbeat discrimination accuracy, in autistic compared to neurotypical samples. This type of finding has led to the suggestion that primary interoception is reduced in autism (Garfinkel et al., 2016; Palser et al., 2018). However, Williams et al. (2022) note the potential for these findings to be explained by non-interoceptive factors, including their finding that the degree of intellectual quotient (IQ) matching explains 38% of the

variance in between-group effect size estimates in studies using this task (**??**). Failla et al. (2020) found no significant differences in the brain areas that autistic participants recruited to complete the task, compared to neurotypical peers, using functional magnetic resonance imaging (fMRI). However, they did find significant associations between brain responses and age across groups, suggesting that a developmental framework may be fruitful for a better understanding of interoception and autism.

1.6 Making sense of interoception: A closer look at interoceptive brain systems

To better explain these inconclusive findings, a key path forward is to re-evaluate what constitutes adaptive interoceptive processing. Initial perceptual studies have focused on accurate detection of cardiac sensations, implicitly equating increased detection with "better" interoception. Estimates of only 50% of healthy adults detecting their heartbeats above chance (Brener and Ring, 2016), however, would imply that not all interoceptive cues are adaptive to perceive. Predictive coding frameworks, following from Bayesian models of sensory processing, have refined models of interoceptive processing to account for this distinction. Successfully predicted sensory stimuli need not rise to conscious awareness, which provides an adaptive filter for our limited cognitive resources (Barrett and Simmons, 2015). Our interoceptive stimuli are especially predictable compared to other sensations for two reasons: we have the most learned experience with these stimuli and many of these signals can be subconsciously adjusted, by signals from the brain back to the body.

Within this framework, adaptive interoception might be considered as awareness necessary for bodily needs that require intentional action, such as hunger or thirst. For cardiac functioning, which is generally subconsciously controlled, adaptive awareness may be situational. For example, ideal cardiac awareness may depend on whether a heart rate increase occurs in the context of physical activity or in a calm, home environment. Only changes that are unexpected for the given environment may signal an actionable threat. Thus, efficient prediction of heartbeats may be a more relevant measure than accurate detection.

As mentioned, sensory predictions may be formed from a variety of cues, based on past experiences and associations with other sensory information. One way we can study how these often-implicit associations get formed is by looking more closely at interoceptive brain systems.

The Embodied Predictive Interoception Coding (EPIC) model proposed by Barrett and Simmons (2015) describes these brain systems. Sensory information from internal organs travel through brainstem and thalamic regions to reach primary interoceptive cortex in the posterior insula, which controls perception of these signals (Barrett and Simmons, 2015; Kleckner et al., 2017). This information reaches visceromotor brain regions, specifically, anterior insula, dorsal amygdala, and anterior cingulate, that coordinate responses to bodily needs. These adjustments may include physiological adjustments within the body or planning movements towards these needs, such as going to the pantry to get food. Rather than simply reacting to physiological sensations, however, visceromotor brain regions continually generate and update predictive models for which physiological adjustments may be necessary in each moment. Predicted physiological sensations are sent to primary interoceptive cortex in the posterior insula; thus, it is mainly unpredicted sensations that rise to our awareness. This serves two purposes: we can then meet the newly-perceived physiological need and learn from this experience for the future.

The middle part of insular cortex, between posterior and anterior insula, also plays a fascinating role in interoceptive integration and learning. It receives diverse multimodal sensory inputs which may then be associated with interoceptive cues. At the cell circuit level, the insular cortex implements associative processing via a laminar gradient from its dorsal posterior to ventral anterior axis. The cell circuits in the posterior insula involve the greatest number of cortical layers ("hypergranular"), which allows this area to process detailed sensory information. This number of layers is reduced in the middle insula and then further in the anterior insula, ultimately reflecting an abstracted "gist" of bodily state as interpreted within the current environmental context (Barrett and Simmons, 2015; Kleckner

Figure 1.1: An overview of interoceptive brain systems

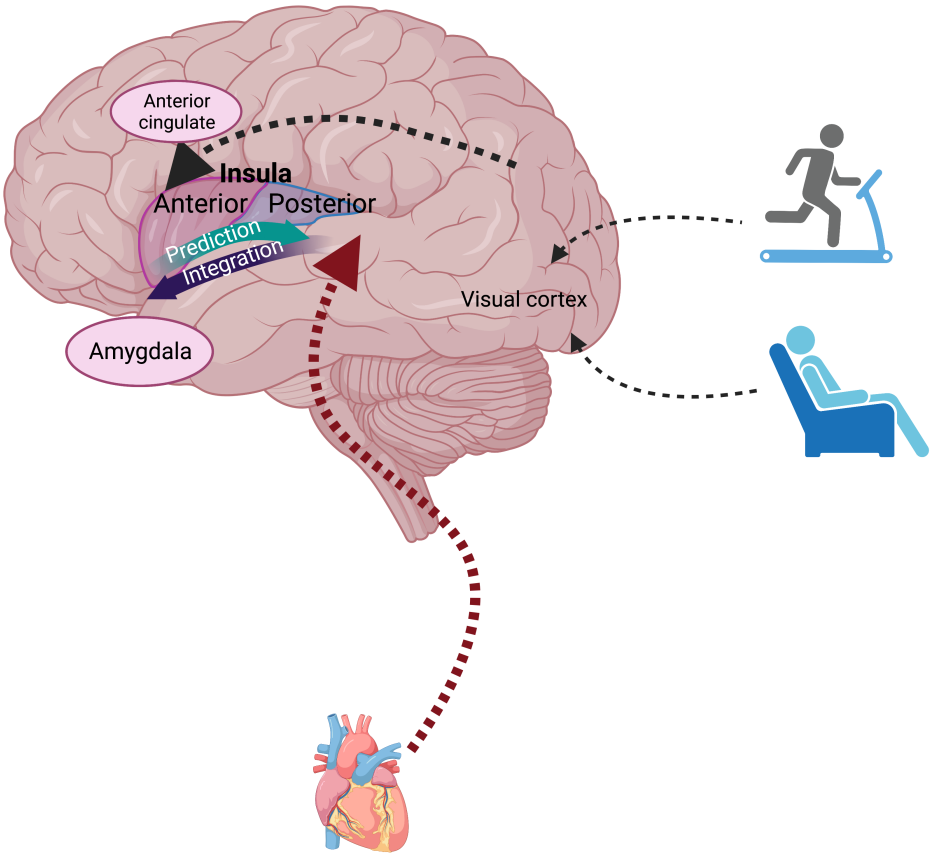

This figure overviews the predictive integration of interoceptive information (e.g., as from the heart) and exteroceptive information (e.g., within different visual contexts of a treadmill versus chair) within the insular cortex. Created with Biorender.com.

et al., 2017).

1.7 The path forward: A contextual, systems-based analysis of interoception in autism

We have thus far highlighted sensory processing as a foundational part of autism and interoception as a foundational sensory modality among sensory systems. Though there has been a long history and varied approaches to understanding interoception, we propose several features that must be considered to move this progress forward. The first is development: our sensory processing patterns are established based on sensory experiences, and any clinically relevant processing differences must be considered within a developmental

lens. Further, we must use tools that account for the often subconscious, situational ways that we process these stimuli. Thus, the study of interoceptive processing within this multisensory, contextual framework will fill gaps that were left by the study of this system in attempted isolation.

To examine broader network features of interoception, we will study the properties of interoceptive brain systems that reflect the scaffold of how we perceive and integrate interoceptive information. In Chapter 2, we will examine structural morphology, which will give us clues as to how the underlying cell circuits are arranged within the insula. This in turn will inform how autistic compared to non-autistic individuals process interoceptive information along the gradient of detail within the insula. In Chapter 3, we will look at communication patterns between the insula and other sensory brain areas, to examine how bodily state information is processed relative to other environmental cues. Then, to relate brain findings back to perceptual experiences, we will examine interoceptive processing at the perceptual task level in Chapter 4, but by using a new generation of tasks that measure interoception relative to other sensory information that might guide its interpretation. Importantly, in each of these three chapters, we will consider how each of these measures vary by age, giving insight into potential developmental patterns of interoception. Lastly, we will connect each of these approaches back to the behavioral experience, analyzing dimensional relationships between these updated measures and reported daily interoceptive experiences, anxiety, and broader autism-related behaviors. Taken together, these approaches will extend beyond a theoretical framework for the interoceptive predictive process and characterize these processes in autistic and non-autistic individuals. These relationships may provide ideas for novel sensory-based supports for autistic individuals, such as explicit teaching of internal and external integration if our hypotheses of broader patterns are confirmed.

CHAPTER 2

Cortical morphology in autism: Findings from a cortical shape-adaptive approach to gyrification indexing

[1]

2.1 Introduction

Autism is increasingly recognized as a diverse spectrum of behavioral phenotypes, with significant biological variability across individuals (e.g., Geschwind and Levitt, 2007; Jeste and Geschwind, 2014; Mottron and Bzdok, 2020). Though individuals diagnosed with autism show some common patterns of social and communicative challenges, repetitive behaviors, and sensory processing (American Psychiatric Association, 2013), the high degree of individual variability has made it particularly challenging to identify biological mechanisms of autistic features. While there is evidence that autism-linked genes show some converging effects on sensory systems (e.g., Gilman et al., 2011; Sestan and State, 2018), the resulting brain differences in autism that contribute to specific sensory processing patterns remain poorly understood. As brain structure provides an intermediary endophenotype between genetic and behavioral phenotypes, a more thorough understanding of structural brain differences in autism may help bridge the link between biological and behavioral profiles in autism. Identifying detailed patterns including the nature, spatial location, and developmental timing of structural brain changes in autism may help dissociate specific biological and environmental processes that contribute to each of these patterns. This may be particularly helpful for understanding features of the autistic experience that

[1]This chapter is adapted from "Cortical Morphology in Autism: Findings from a Cortical Shape-Adaptive Approach to Local Gyrification Indexing" published in *Cerebral Cortex*, Volume 31, Issue 11, DOI: doi.org/10.1093/cercor/bhab151 and has been reproduced with the permission of the publisher and my co-authors: Ilwoo Lyu, Michelle Failla, Lisa E. Mash, Kacie Dunham, Jacob I. Feldman, Tiffany G. Woynaroski, Mark T. Wallace, Laura A. Barquero, Tin Q. Nguyen, Laurie E. Cutting, Hakmook Kang, Bennett A. Landman, and Carissa J. Cascio. It may be found online at: https://academic.oup.com/cercor/article/31/11/5188/6311002.

are difficult to measure and self-report, such as challenges with perceiving and interpreting bodily cues (i.e., interoception, Trevisan et al., 2021b). Since these cues often are processed implicitly, the structural patterns of this brain system inform how these cues reach conscious awareness and when this awareness (or lack thereof) may lead to challenges.

Previous studies of brain development in autism have identified consistent differences in total brain volume in studies employing both longitudinal designs and cross-sectional samples across the lifespan. These studies have suggested a trajectory of brain overgrowth in early childhood followed by exaggerated volumetric decreases in adolescence and adulthood (e.g., Courchesne et al., 2007, 2001; Shen et al., 2013). Further, the degree of early overgrowth has been related to autism-related behaviors in individuals as young as 12-24 months old (The IBIS Network et al., 2017). Consistently identified areas of cortical volumetric differences in autism at the brain lobe level include frontal and parietal lobes (Carper, 2002; Schumann et al., 2010; Hazlett et al., 2011). More specific regions of volumetric difference identified across large samples include lateral occipital cortex, medial temporal gyrus, left superior temporal gyrus, and right parietal operculum (Nickl-Jockschat et al., 2012; Riddle et al., 2017), which are each involved in primary and associative sensory processing. Though these patterns of brain volume have illuminated broad properties of cortical development in autism, ongoing research is focused on dissociating more specific properties of cortical volumetric changes in order to link them to brain function, and thus, behavior.

Cortical structure can be captured on a more granular scale by measuring cortical thickness, surface area, and degree of cortical folding (i.e., gyrification). These indices are thought to closely reflect both shared and distinct aspects of early cortical development, including early neuronal proliferation (Caviness et al., 1995), lateral neural progenitor cell expansion (surface area), and radial progenitor cell expansion (cortical thickness; Rakic, 1995; Lui et al., 2011). In terms of resulting cortical architecture, the radial unit hypothesis posits that increased cortical thickness reflects increased cell body size or count and that in-

creased surface area reflects a greater number of cortical columns (Rakic, 1995). However, these indices do not exclusively measure gray matter; for example, increased myelination also results in decreased indices of cortical thickness (Natu et al., 2019) and relate closely to gliogenesis as well (Rash et al., 2019). Though there are multiple theories regarding cortical gyrification, most agree that the degree of gyrification reflects a complex interplay between the aforementioned cortical processes (i.e., scaling with increased cortical surface area and inversely with increased thickness (Mota and Herculano-Houzel, 2015); axonal tension (Essen, 1997); and cytoarchitectural features (Bayly et al., 2014; Ronan and Fletcher, 2015). Lastly, increased gyrification indexed along a specific fold may occur in multiple dimensions (e.g., either increased width or increased depth of that fold).

Thus, nuanced alterations in these structural indices may implicate specific features both in local neuronal circuitry and in broader network organization. For example, in the previously mentioned longitudinal work, early hyper-expansion of cortical surface area was implicated as a more specific property contributing to brain overgrowth in individuals who later received an autism diagnosis, which in turn points to lateral neural progenitor cell expansion as a likely affected process (The IBIS Network et al., 2017). As gyrification in particular reflects a combination of surface area and cortical thickness, which themselves are relatively independent indices, a more detailed understanding of gyrification patterns in autism may therefore help bridge the understanding between early developmental processes and resulting differences in brain circuitry. Early studies of finer-grained cortical structure in autism started to pinpoint differences in folding as indexed by sulcal depth (e.g., Hardan et al., 2004; Nordahl et al., 2007). Studies of gyrification indices as a ratio of folded cortex at whole-brain or brain lobe levels have provided further evidence that cortical folding patterns do indeed differ in autism (Levitt, 2003; Jou et al., 2010; Bos et al., 2015).

To more precisely localize regions of gyrification differences, a local gyrification index (LGI) was developed to measure the ratio of folded cortex in specific cortical patches, as influenced by both the width and depth of sulci in that patch (Schaer et al., 2008). Studies

of LGI in autism across childhood, adolescence, and adulthood suggest atypical trajectories in autism relative to neurotypical controls, in particular for gyrification in frontal, parietal, and temporal regions (e.g., Wallace et al., 2013; Schaer et al., 2013, 2015; Ecker et al., 2014, 2016; Libero et al., 2014, 2019; Bos et al., 2015; Dierker et al., 2015; Yang and Hofmann, 2016; Kohli et al., 2019a,b). A recent large-scale study has suggested that heterogeneity in factors such as age, biological sex, intellectual quotient (IQ), and the degree of autism-related behaviors may contribute to mixed morphological findings by region and direction of change across diverse samples, including a trend of greater differences in cortical thickness in autism at younger ages and several regions of sex-specific changes in autism (MRC AIMS Consortium et al., 2020). Thus, additional studies with large samples may further help identify morphological patterns across these varying features.

Though resolution is improved relative to whole-brain studies, common approaches to local gyrification indexing may still blur findings across regions with distinct cytoarchitecture, which may make these behavioral relationships harder to identify. For instance, a widely used and established method to compute LGI employs a uniform spherical patch of cortex within which the area ratio is measured. This approach, however, can result in over-smoothing across functionally distinct regions (Power et al., 2011; Wig et al., 2014). Given the relationship between cytoarchitecture and gyrification (Bayly et al., 2014; Ronan and Fletcher, 2015), indexing gyrification with improved resolution may help clarify these mixed findings and provide insights into the brain bases of behavioral features in autism. Thus, in this study, we implement a new method of local gyrification indexing developed by Lyu et al. (2018b) to better characterize differences in cortical morphology in autism. To address the limited resolution of prior approaches, the approach of Lyu et al. (2018b) uses a cortical folding pattern-aware patch rather than a sphere, which permits computation of LGI within single sulci/gyri and provides greater focal quantification of this index across the cortex (Figure 1a). There is emerging evidence that, as intended, this approach identifies regions of group differences that are more precisely localized to specific curves

than the frequently used FreeSurfer approach (Płonka et al., 2020).

The approach of Lyu et al. (2018b) further addresses an important potential confound influencing the interpretation of the LGI. As LGI defines the degree of cortical folding by "area ratio", LGI should have the same value across brains of different scales for a given cortical shape. However, this does not hold in existing methods that use absolute patch size (Figure 1b). Therefore, the adaptive approach automatically adjusts for individual brain size, minimizing this confounding factor, which may be particularly relevant for autism given the previously discussed differences in brain volume (e.g., Courchesne et al., 2007, 2001; Redcay and Courchesne, 2005; Shen et al., 2013; The IBIS Network et al., 2017). In this study, we expand upon prior findings regarding gyrification in autism by using this spatially precise, focal approach to local gyrification indexing. We also consider complementary indices of cortical thickness and sulcal depth, to differentiate patterns between the multiple features that contribute to gyrification. We employ a data-driven approach in a large sample spanning a broad age range to identify cortical features that may be common across heterogeneous individuals with autism and, given the broad age range of our sample, features that may vary by age. We also investigate the relationship between cortical indices and combined social, communicative, and motor behaviors, to provide preliminary links between autism-associated behavioral profiles and precise cortical structure.

Though we will analyze morphology across the whole brain, we will particularly focus on potential implications for interoceptive brain regions, including insular cortex and anterior cingulate (Craig, 2002; Barrett and Simmons, 2015). The insular cortex is among the deepest folds in the cortex, thus LGI and sulcal depth indices are especially high in this area. Further, the insula shows some unique morphological features, as fetal developmental studies suggest that this region defies physics-predicted patterns of gyrification; instead, the rest of the cortex develops around the insula (Türe et al., 1999; Mallela et al., 2023). Thus, examining the unique gyrification patterns of the insula with our refined LGI technique will provide an interesting window into how interoceptive development compares in autis-

Figure 2.1: Rationale for adaptive local gyrification indexing

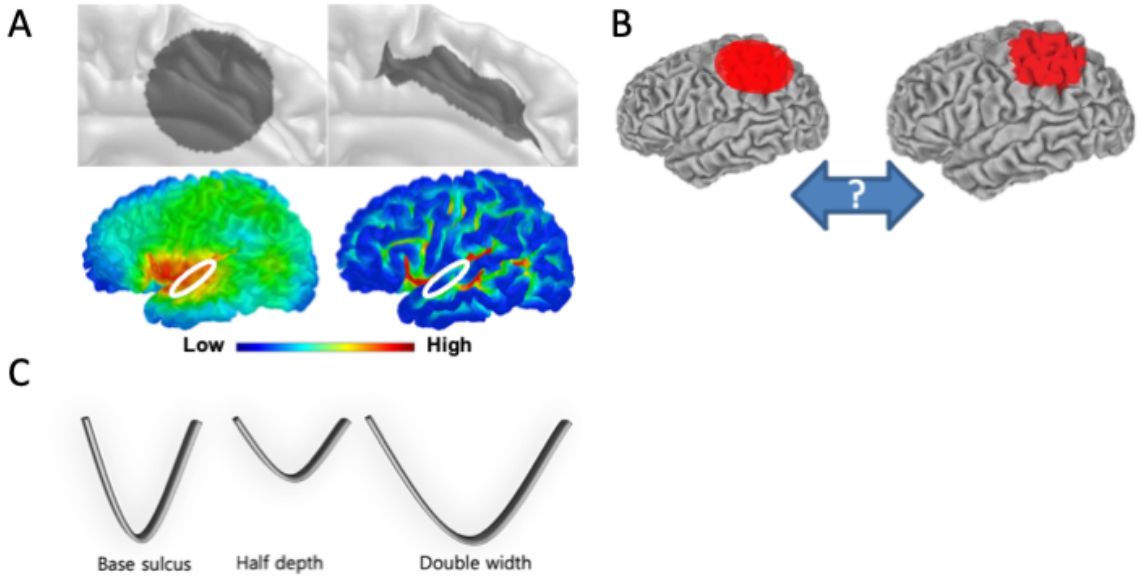

Panel A: Different patch shapes (top) and corresponding gyrification index (bottom); conventional circular patch (left) and our cortical folding-adaptive patch (right). Conventional methods use a large size with a simple circular shape, resulting in moderate gyrification values across most of the cortex (bottom). Our novel patch captures the amount of cortical folding within a sulcus and resulting gyrification index values more focally represent cortical folds. To illustrate resulting differences, gyrification index is high within the circled region computed using conventional approaches (in this instance, standard settings applied in Freesurfer), but low using the adaptive patch approach. Panel B: Importance of patch size adjustment. By definition, local gyrification index measures amount of folds as area ratio. The resulting ratio should be identical for the same cortical folding patterns regardless of brain size. The patch size thus needs to be adjusted rather than fixed, which otherwise yields different area ratio (see example above and conventional approaches). Panel C: Influence of sulcal width and depth on gyrification index. The same degree of changes in local gyrification index of different scenarios: half depth and double width. Local gyrification index measures structural changes on both sulcal depth and width, which is implicit, i.e., the index is changed due to either sulcal depth or width or both. Thus, sulcal depth and local gyrification index need to be considered together to explicitly explain cortical fold differences.

tic and non-autistic individuals. These results will be interpreted within the framework of cascading effects of sensory processing, particularly of interoception (Cascio et al., 2016; Zoltowski et al., 2022).

2.2 Methods

2.2.1 Participants

The data for this study were collected under multiple imaging cohorts focused on functional and diffusion magnetic resonance imaging (MRI) conducted between 2007 and 2019. Structural analyses have been previously published on subsets of this data (i.e., Huo et al., 2016; Price et al., 2016; Aboud et al., 2019). The Vanderbilt University Medical Center Institutional Review Board approved each individual study comprising this dataset. Informed consent was obtained for each adult participant and by a parent or legal guardian of child participants. Child participants additionally provided oral and/or written assent to procedures. Participants completed one to four structural scan sessions, based on i) protocol for each imaging cohort and ii) potential participation in multiple of these cohorts, since participating in one of these studies was not an exclusionary criterion for participating in others. Exclusionary criteria for participating in any of these imaging cohorts include histories of epilepsy, traumatic brain injury, and any MRI contraindications as determined by MRI staff technicians (such as implanted metal, severe claustrophobia, or medical conditions known to interact with scanning, but see Supplemental Material for full possible list). Of the 835 scan sessions considered for inclusion in the study, sessions were excluded from analyses based on failed quality assessment procedures (i.e., T1-weighted image was jittered or cropped, results of automated surface reconstruction were jagged, or tissue boundaries were not clearly matched to the volume, n = 121 scans) or missing age, diagnostic group, or biological sex (n = 141 scans). Therefore, a total of n = 573 scans from n = 369 subjects were included in final analyses. Age between repeated scans is summarized in Supplemental Table 1, but most commonly repeated scans occurred within 2 years of the initial visit. Per diagnostic group, there were n = 115 diagnosed with autism (AUT, n = 136 scans) and n = 254 neurotypical (NT, n = 437 scans) participants. For inclusion in the AUT group, autism diagnoses were confirmed via research-reliable administration of the Autism Diagnostic Observation Scale, General or 2nd edition (ADOS-G or ADOS-2, Lord et al., 2000,

2012), administered within 2 years of scan date, and judgment of a licensed clinician on the research team who was experienced in evaluating persons with autism. Individuals were excluded from the NT group if they had no prior diagnoses of autism or another psychiatric disorder, which was determined prior to MRI scanning (i.e., no additional scans were excluded for this reason).

In addition to these factors for inclusion/exclusion, participant intellectual quotient (IQ) was characterized across protocols. Participant demographics are summarized in Table 1. Group comparisons on demographic features indicate our autistic group was slightly older (Cohen's d = 0.22), included a higher proportion of males than the neurotypical group (Cohen's d = 0.56), and had somewhat lower average IQ (d = -0.28 and -0.32 for non-verbal and verbal IQ, respectively). Participant age and biological sex were covaried in analyses; however, the approaches used to characterize IQ were too varied across protocols to consider this a covariate for analyses. Out of 369 participants, n = 60 participants had only non-verbal IQ (NVIQ) scores from Test of Nonverbal Intelligence (4th edition; Brown et al., 2010) or Leiter International Performance Scale (3rd edition; Roid et al., 2013), n = 103 participants had only full-scale IQ (FSIQ) scores from the 2-subtest Wechsler Abbreviated Scale of Intelligence (WASI, 1st or 2nd edition; Wechsler, 1999, 2011), and n = 148 participants had both NVIQ and FSIQ scores from the 4-subtest WASI, with n = 58 participants missing an IQ score.

Links with autism-associated features in the AUT group were explored using ADOS total calibrated severity scores (CSS; Gotham et al., 2009 for Modules 1-3; Hus and Lord, 2014 for Module 4). These scores are derived from combined social, communicative, and repetitive behaviors as observed during the ADOS and calibrated by age and administration module on a 1-10 scale, with 10 indicating the greatest degree of autism-associated behaviors. Thus, they represent a broad index of autism-associated behaviors that can be compared across individuals of different ages and verbal abilities. Eight individuals with autism with missing CSS scores were excluded from these analyses. Of the 107 individ-

Table 2.1: Participant characteristics by diagnostic group

	AUT (total n = 115)			NT (total n = 254)			
	n	M (SD)	Range	n	M (SD)	Range	d (p)
Age at Scan	115	14.97 (8.69)	5-54	254	13.13 (8.43)	5-43	0.22 (.03)
FSIQ	72	105.5 (17.3)	63-142	181	110.6 (15.2)	81-144	–0.32 (.02)
NVIQ	96	105.6 (21.7)	61-143	114	110.7 (15.0)	83-160	–0.28 (.05)
ADOS CSS	107	7.47 (1.95)	3-10	NA			NA
Sex	88 male, 27 female			137 male, 117 female			0.56 (<.01)

Participant characteristics are summarized by count for categorical variables and mean, standard deviation for continuous variables. Differences between groups are summarized by Cohen's d. AUT: autism; NT: neurotypical; FSIQ: full-scale intellectual quotient and NVIQ = non-verbal intellectual quotient as assessed using either the Wechsler Abbreviated Scale of Intelligence 2- or 4-subtest (1st or 2nd edition), the Test of Nonverbal Intelligence (4th edition) or Leiter International Performance Scale (3rd edition); ADOS: Autism Diagnostic Observation Schedule, General or 2nd version; CSS: calibrated severity score.

uals included in these analyses, n = 21 had a repeated scan session, resulting in n = 128 total scans. Across the cohorts, the ADOS was re-administered after 1-2 years for children and after 2-3 years for adults. Fifteen of the 21 repeated scans occurred within this re-administration window. The six repeated scans that occurred outside this window had a repeated ADOS score corresponding to the new scan.

2.2.2 Image acquisition

All images were acquired on one of two 3.0 Tesla Phillips Achieva MRI scanners with a 32-channel SENSE head coil. The participants in this study were pooled from seven different imaging cohorts, which each had distinct acquisition parameters and/or were collected under distinct study protocols. To control for effects of the differing protocols, acquisition protocol type was included as a covariate in subsequent analyses.

Cohort one (n = 40 NT subjects (n = 48 scans) and n = 24 AUT subjects (n = 24 scans)). Cohort one's high-resolution T1-weighted anatomical images were acquired via sagittal slices with 0.89 x 0.89 x 1.2 millimeter (mm) voxel resolution, TR = 8.7 milliseconds (msec), TE = 4.6 msec, flip angle = 9o, and acquisition matrix = 288 x 288 x 142.

Cohort two (n = 38 NT subjects (n = 38 scans) and n = 32 AUT subjects (n = 32

scans)). Cohort two's high-resolution T1-weighted anatomical images were acquired via sagittal slices with 1mm^3 voxel resolution, TR = 9.0 msec, TE = 4.6 msec, flip angle = 8o, and acquisition matrix = 256 x 256 x 170.

Cohort three (n = 9 NT subjects (n = 9 scans) and n = 13 AUT subjects (n = 13 scans)). Cohort three's high-resolution T1-weighted anatomical images were acquired via sagittal slices with 1mm^3 voxel resolution, TR = 7.9 msec, TE = 3.7 msec, flip angle = 7o, and acquisition matrix = 256 x 256 x 170.

Cohort four (n = 21 NT subjects (n = 22 scans) and n = 20 AUT subjects (n = 20 scans)) and *five* (n = 69 NT subjects (n =76 scans) and n = 47 AUT subjects (n = 47 scans)). Cohort four and five's high-resolution T1-weighted anatomical images were acquired via sagittal slices with 1mm^3 voxel resolution, TR = 8.0 msec, TE = 3.7 msec, flip angle = 7o, and acquisition matrix = 256 x 256 x 170.

Cohort six (n = 71 NT subjects (n = 173 scans)) and *seven* (n = 37 NT subjects (n = 71 scans)). Cohort six and seven were collected with identical protocols, at the first and second of the two scanners, respectively. These were acquired via sagittal slices with 1mm^3 voxel resolution, TR = 7.975 msec, TE = 3.67 msec, flip angle = 7o, and acquisition matrix 256 x 256 x 170.

2.2.3 Imaging pre-processing

Cortical surface reconstruction and registration. T1-weighted images were segmented using Multi Atlas segmentation (Asman and Landman, 2012), and the whole cortical surface was reconstructed via the Multi-atlas Cortical Reconstruction Using Implicit Surface Evolution (MaCRUISE) pipeline (Huo et al., 2016). The Multi-atlas Cortical Reconstruction Using Implicit Surface Evolution (MaCRUISE) pipeline is designed for cortical surface reconstruction (Huo et al., 2016). The tool is based on the original CRUISE pipeline that employs a level set approach to trace the tissue boundaries with fuzzy tissue segmentation (Han et al., 2004). MaCRUISE extends the original CRUISE pipeline

specifically by simultaneously updating tissue segmentation and cortical surface boundaries, which minimizes cortical surface reconstruction errors and boosts the accuracy of volumetric tissue segmentation. We used the gray/CSF boundary (pial surface). The pipeline has been previously validated on both control and patient datasets. Also, prior findings show that CRUISE offers comparable or better reconstruction quality in both control and white matter pathology groups to FreeSurfer (Shiee et al., 2014; Huo et al., 2016). See Huo et al. (2016) for more technical details. The software is publicly available at https://github.com/MASILab/MaCRUISE.

Once cortical surfaces were reconstructed, spherical registration for cortical surface using hierarchical spherical deformation (HSD) was applied (Lyu et al., 2019). The shape correspondence was then established via the registered spheres, and each surface was resampled into the same number of vertices (# = 163,842) via icosahedral subdivision. Only resampled surfaces were used for statistical shape analysis. Surface-related processing used the originally reconstructed surfaces to avoid any potential loss of information from the resampling process.

Cerebral hull. For LGI and sulcal depth, the cerebral hull surface (i.e., reference surface for those metrics) is required. For this purpose, we first voxelized the cortical surfaces to make a binary volume (Patil and Ravi, 2005), and then applied a three-dimensional morphological closing operation to close sulci. We employed a sphere of 15 mm diameter as a structural element of the morphological operation. We followed existing studies to choose the size of the morphological operation in Schaer et al. (2008) andLyu et al. (2018b). Although the size was experimentally determined on the adult brain (Schaer et al., 2008), the size was sufficient to cover the main cortical sulci, and as discussed in Schaer et al. (2008), 50% increase or decrease in this diameter does not alter the gyrification index consequently. Though our cohort includes young children, they do not exhibit more than 50% volumetric difference from the adult brain, which, as noted by Schaer et al. (2008), can be still suffi-

ciently covered by a sphere of 15 mm diameter for the cerebral hull creation. This results in a cerebral hull in the volumetric space. Finally, we used a standard marching cube to generate a cerebral hull surface by finding the largest connected component (Lorensen and Cline, 1987).

2.2.4 Cortical morphological measures

Local gyrification index. The local gyrification index was computed as a proportion of cortex within the cerebral fold compared to the hull surface. As described in Lyu et al. (2018b), we first established a spatial correspondence between the cortical surface and its hull by tracing streamlines in the Laplacian field of their intermediate volume via the Runge-Kutta method (Lee et al., 2016). At the same time, we computed sulcal/gyral curves along cortical folds for regional segmentation of sulcal fundi and gyral crowns (Lyu et al., 2018a). From the regional segmentation, we computed an anisotropic velocity field modeled by solving stationary Hamilton-Jacobi partial differential equations that propagate fast in the parallel directions to sulcal/gyral curves, along which patch shape is adaptively determined (elongated along sulci/gyri). Finally, we computed an area ratio between the cortical surface and its cerebral hull per each vertex within the adaptively elongated patch. We used the same amount of anisotropy (η=0.2) for the patch size as proposed in Lyu et al. (2018b).

A non-scaled brain size could yield inconsistent results even for the same brain structures at different scales. Introducing an extra covariate (e.g., brain size) in a statistical model is unnatural to handle scaling effects in LGI as the measure is defined by an area ratio and introducing brain size (surface area) to normalize the measure could be misleading because such post-normalization only adjusts the area on the outer hull while its corresponding cortical regions in pial surface is not adjusted accordingly. For these reasons, we normalized the kernel size first and find the corresponding area within the adjusted kernel rather than directly adjusting the measures. This way guarantees that the resulting index is consistent for the same shape patterns at different scales. We adapted a minimal patch size

(316 mm2) that minimally covers the healthy adult cohort studied in Lyu et al. (2018b). We then adjusted the patch size with respect to a surface area ratio between average surface area in the adult cohort and that of individual participants in our cohorts.

The software used to compute LGI can be found at https://hub.docker.com/r/ilwoolyu/cmorph, a Docker image that is a collection of surface processing techniques developed by the authors, which as a part of its implementation, contains a pre-compiled version of the source code available at https://github.com/ilwoolyu/LocalGyrificationIndex; HSD, as used for surface registration (Lyu et al., 2019), at https://github.com/ilwoolyu/HSD; and TRACE for computing the proposed LGI by defining sulcal/gyral regions, at https://github.com/ilwoolyu/CurveExtraction.

Sulcal depth. As the interpretation of LGI as defined by area ratio alone cannot distinguish between sulcal depth and width changes given a constant area change (Figure 1c), consideration of the sulcal depth index in addition to LGI helps distinguish between these features. The sulcal depth measure was computed as the geodesic distance between the pial cortical surface and its cerebral hull, as generated previously for local gyrification indexing. Per each vertex, we computed the shortest distance between the cerebral hull to its corresponding cortical surface as proposed in Lyu et al. (2018c). Briefly, we voxelized both cortical surface and its hull and then defined intermediate volume between them as a domain of the geodesics. We then solved the Eikonal equation with uniform speed in the intermediate volume from the hull to the cortical surface. We finally projected volumetric measures back onto the cortical surface for vertex-wise measurements. However, the reconstructed cortical surfaces do not necessarily guarantee unique voxel-to-vertex matching (normally, more than one vertex belongs to a single voxel) even if they perfectly trace the cerebrospinal fluid (CSF) and gray-matter boundary. This potentially degenerates vertex-to-voxel mapping without a voxel-wise resampling scheme. Therefore, the sulcal depth to a given vertex was obtained by tri-linear resampling of the associated voxel for sub-voxel

accuracy. Spatial smoothing was performed on the cortical surfaces with a standard Gaussian kernel (full width at half maximum (FWHM) = 6 mm). For spatial smoothing, we followed a conservative strategy to avoid overly smoothing the signals (to maximize sensitivity) with a minimal kernel size as suggested by Han et al. (2006), unlike other studies using more aggressive smoothing kernel size (FWHM=30 mm, Chung et al., 2005; Lerch and Evans, 2005). As our approach focuses on surface representation, the voxel resolution is independent of the processing except for the surface reconstruction. The structural images were isotropically interpolated to run the cortical surface reconstruction pipeline for consistent results (Shiee et al., 2014; Huo et al., 2016).

Cortical thickness. Using the MaCRUISE pipeline, cortical thickness was obtained by measuring distances between pial and white matter surfaces (Huo et al., 2016). Spatial smoothing was performed on the cortical surfaces with a standard Gaussian kernel (FWHM = 6 mm).

2.2.5 Statistical models

Mixed effects models were implemented using SurfStat and Worsley toolboxes (Worsley et al. 2009) in MATLAB (MathWorks, Natick, MA). The code used to implement these models can be found at
https://github.com/casciolab/CorticalMorphologyAutism2021. For each of the three structural indices of interest, we analyzed the following three models:

- Diagnostic (Dx) group model testing the effects of AUT versus NT status on average, controlling for age, biological sex, and scanning protocol:

  $measure = (\beta_0 + b_0) + \beta_1 Dx + \beta_2 Age + \beta_3 Sex + (\beta_4 + b_1) Scanner + \varepsilon$ and evaluating $H_0 : \beta_1 = 0$

- Age by diagnosis interaction model testing the degree to which the effect of diagnostic group varied according to age, controlling for biological sex and scan-

ning protocol: $measure = (\beta_0 + b_0) + \beta_1 Dx + \beta_2 Age + \beta_3 Dx * Age + \beta_4 Sex + (\beta_5 + b_1) Scanner + \varepsilon$ and evaluating $H_0 : \beta_3 = 0$

- Autism-related behaviors model (AUT group only) testing associations with broader autism-related behaviors controlling for age, biological sex, and scanning protocol: $measure = (\beta_0 + b_0) + \beta_1 Age + \beta_2 Sex + \beta_3 ADOS + (\beta_4 + b_1) Scanner + \varepsilon$ and evaluating $H_0 : \beta_3 = 0$

In each model,b_0 and b_1 represent subject-specific random intercept and random slope for scanner effect on the dependent variable, respectively, and ε represents random error.

The first two models were assessed using the full cohort. Because participant age was skewed in our sample such that a few older individuals may have highly influenced results, we assessed influence for age by diagnosis interaction models by calculating Cook's D for models of age by diagnosis interactions on averaged indices in significant regions, and reran final models without i) participants with extreme influence in a particular region and contrast (i.e., D $>$ 20% of F(4, 569) distribution, n=2 participants for sulcal depth model, Age*NT $>$ AGE*AUT contrast) and ii) participants with outlying influence in all contrasts (n=1 participant). As only the AUT group received the ADOS and had calibrated severity scores, the autism-related behaviors model only included scans from the n = 107 AUT individuals with ADOS CSS scores. Statistical significance of parameters was corrected for multiple comparisons using random field theory (RFT) at the level of 0.05 and cluster threshold (raw p) = 0.01 (Hagler et al., 2006).

2.3 Results

A complete list of significant clusters per contrast for group differences, including the number of associated vertices and unstandardized coefficient estimate at the maximum vertex, is contained in Table 2.

2.3.1 Group differences for AUT >NT contrast

There were three clusters in which LGI was significantly higher in the AUT group compared to the NT group on average, controlling for age, biological sex, and scan protocol: one cluster localized to the right middle frontal gyrus, one localized to the right inferior temporal gyrus, and one localized to the right middle occipital gyrus (Figure 2a, right panel). To illustrate the correspondence between these indices, LGI is plotted in relation to sulcal depth and cortical thickness for each of these clusters in Supplemental Figure 1. Sulcal depth was significantly greater in AUT in two regions of spatial concordance with gyrification changes, in the right middle frontal gyrus and right middle occipital gyrus. Consistent with this spatial correspondence, Supplemental Figure 2 shows a particularly high correspondence between LGI and sulcal depth in these two regions. Three additional clusters in which sulcal depth was significantly greater in the AUT group were localized to right precentral gyrus, right postcentral gyrus, and left medial orbital gyrus (Figure 2b, right panel). The cortical thickness index was significantly greater on average in the AUT group in clusters in right anterior insula, right anterior cingulate, right planum temporale/-superior temporal gyrus, and six additional clusters in occipital and temporal areas (Figure 2c, left panel).

2.3.2 Group differences for NT >AUT contrast

Conversely, there were three clusters in which LGI was significantly lower in the AUT group on average: bilateral clusters in central/parietal operculum areas (including the posterior insula in the left hemisphere) and one cluster localized to the right precuneus (Figure 2a, left panel). There were seven clusters in which sulcal depth was significantly lower in the AUT group, localized to a variety of sensory and motor regions, including sub-regions of the precentral and postcentral gyri bilaterally, as well as the left fusiform gyrus and a region in the right hemisphere spanning the planum polare, planum temporale, superior temporal gyrus, and superior temporal gyrus (Figure 2b, left panel). There were three

clusters in which cortical thickness was significantly lower in the AUT group on average: one cluster localized to the left precentral gyrus, one cluster localized to the left postcentral gyrus, and one cluster localized to the right superior parietal lobule (Figure 2c, right panel). However, the sub-regions of the precentral and postcentral gyri that were significant for the cortical thickness model were spatially distinct from the sub-regions that were significant for the sulcal depth model.

2.3.3 Interacting effects of age and diagnostic group

A complete list of significant clusters per contrast for group by age interactions, including the number of associated vertices and unstandardized coefficient estimate at the maximum vertex, is contained in Table 3. On average across diagnostic groups, each of the cortical metrics of interest to the present report decreased with age (Supplemental Figure 2 a-c).

The only cluster in which the AUT group showed significantly greater decreases in LGI with increasing age relative to the NT group was localized to a right medial frontal cortex region (Figure 3a, left panel). The AUT group showed significantly greater decreases in sulcal depth with age relative to NT (Figure 3b, left panel) and greater increases in cortical thickness with age relative to NT in a similar medial frontal region (Figure 3c, left panel), consistent with expected correspondence between these indices.

For the sulcal depth index, there were multiple additional clusters of interacting findings in either direction (i.e., where the AUT group showed either significantly greater or significantly lesser decreases in sulcal depth than the NT group with increasing age, Figure 3b). Regions of significantly greater decreases in sulcal depth with age for AUT versus NT included two clusters in the left middle and superior frontal gyri, and large bilateral regions (i.e., more than 6 times the size of other significant regions) comprising multiple functional regions between the Sylvian fissure and superior temporal gyrus. In addition to the right medial frontal cluster, regions of significantly lesser decreases in sulcal depth with age for AUT as compared to the NT group included clusters localized to the right precentral gyrus,

Figure 2.2: Group differences in cortical surface metrics

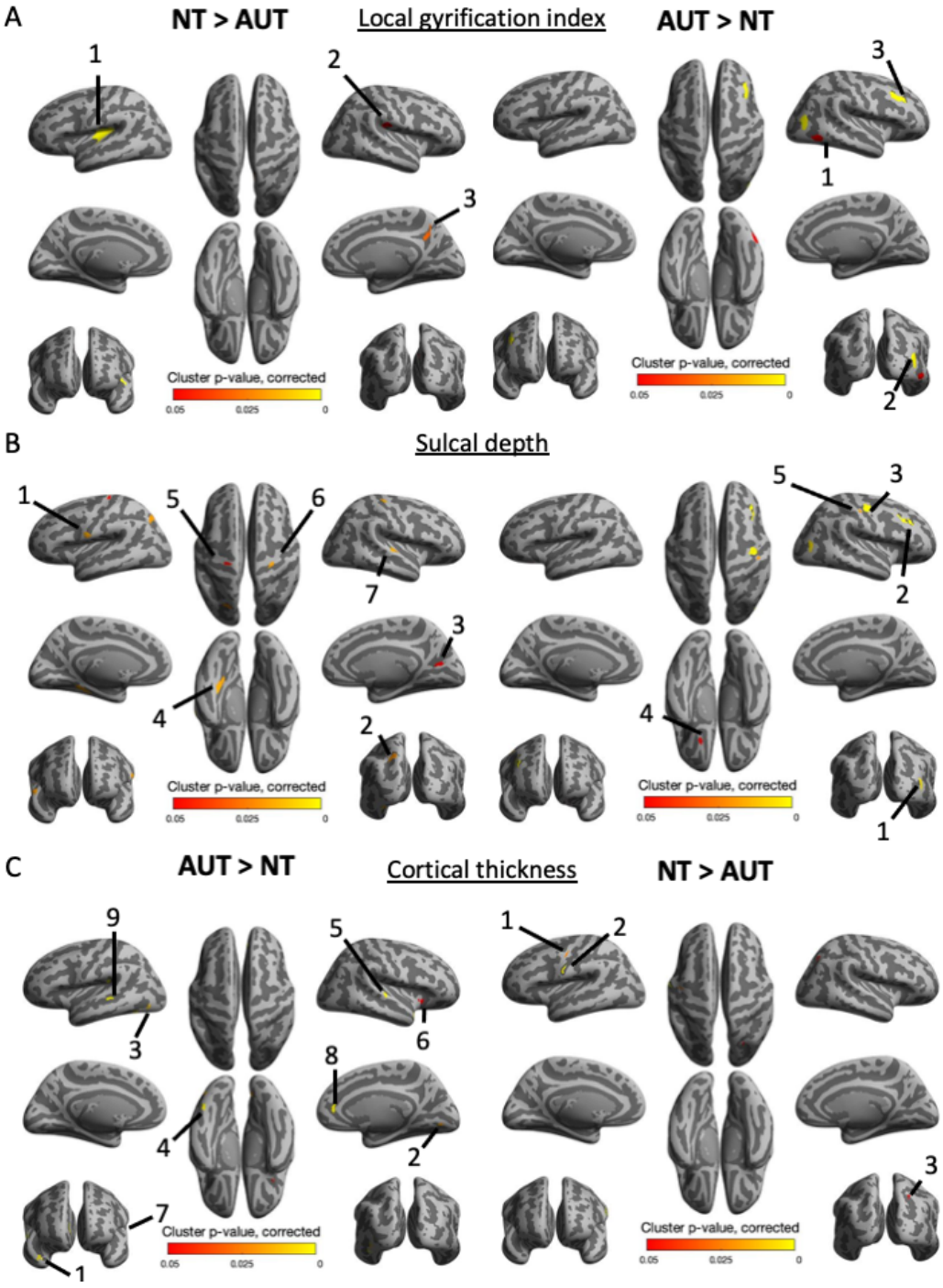

Regions of significant group differences in local gyrification index (LGI, panel A), sulcal depth (SD, panel B), and cortical thickness (CT, panel C) are shown, colored according to cluster p-value (bottom scale). Left panels indicate regions of greater LGI, greater SD, and reduced CT (arranged by expected correspondence between the indices) in the neurotypical (NT) group than autism (AUT) group, and vice versa in right panels, at the p $<$0.05 level after correcting for multiple comparisons via random field theory. CT is presented inversely from LGI and SD (i.e., as labeled, AUT $>$NT is on the left panel rather than right) due to its inverse correspondence with these indices. Regions are labeled by corresponding structure.

Table 2.2: Clusters of significant regions for group differences

Index	Cluster	Region	# Vertices	Max. Coeff.
AUT>NT				
LGI	1	Right inferior temporal gyrus	361	0.558
LGI	2	Right middle occipital gyrus	489	0.531
LGI	3	Right middle frontal gyrus	658	0.473
SD	1	Right inferior / middle occipital gyrus	223	1.732
SD	2	Right middle frontal gyrus	352	1.662
SD	3	Right precentral gyrus	541	0.813
SD	4	Left medial orbital gyrus	83	0.599
SD	5	Right postcentral gyrus	140	0.492
CT	1	Right temporal pole	136	0.343
CT	2	Right lingual gyrus	87	0.307
CT	3	Left inferior occipital gyrus	85	0.275
CT	4	Left fusiform gyrus / occipital fusiform gyrus	109	0.274
CT	5	Right planum temporale / superior temporal gyrus	139	0.273
CT	6	Right anterior insula	106	0.242
CT	7	Left parietal operculum	160	0.236
CT	8	Right anterior cingulate gyrus	92	0.230
CT	9	Left superior temporal gyrus	132	0.206
NT>AUT				
LGI	1	Left central/parietal operculum / posterior insula / planum polare / transverse temporal gyrus	2632	1.234
LGI	2	Right central/parietal operculum	511	0.642
LGI	3	Right precuneus	403	0.290
SD	1	Left postcentral gyrus / precentral gyrus	363	1.612
SD	2	Left superior parietal lobule	416	1.281
SD	3	Right cuneus	214	1.236
SD	4	Left fusiform gyrus / lingual gyrus	468	1.121
SD	5	Left precentral gyrus	190	0.829
SD	6	Right precentral gyrus	306	0.813
SD	7	Right planum polare / planum temporale / superior temporal gyrus / transverse temporal gyrus	278	0.772
CT	1	Left precentral gyrus	81	0.206
CT	2	Left postcentral gyrus / precentral gyrus	155	0.184
CT	3	Right superior parietal lobule	79	0.184

By column: Morphological index, cluster number per contrast (in descending order by maximum coefficient), regions of cluster localization, number of vertices per cluster, and the maximum coefficient, i.e. the unstandardized coefficient estimate of the diagnostic group term at the maximum vertex in each cluster. Direction of contrast AUT>NT indicates measure is greater in AUT and vice versa. Significance was assessed after correcting for multiple comparisons using random field theory at $p < 0.05$. Abbreviations: CT=cortical thickness; LGI=local gyrification index; SD=sulcal depth, AUT=autism, NT=neurotypical.

left lingual gyrus, right superior parietal lobule, and multiple subregions of the postcentral gyrus, bilaterally.

There were also several clusters in which the AUT group showed significantly greater decreases in cortical thickness with increasing age relative to the NT group, including clusters in bilateral lingual gyri and in several frontal and limbic regions, as well as a cluster comprising left angular gyrus/supramarginal gyrus (Figure 3c, right panel).

2.3.4 Regions of increased indices associating with greater autism-related behaviors

A complete list of significant clusters per contrast for ADOS CSS associations, including the number of associated vertices and unstandardized coefficient estimate at the maximum vertex, is contained in Table 4.

Both increased LGI and increased sulcal depth significantly covaried with greater ADOS CSS scores (indicating a greater degree of autism-related behaviors) in sub-regions of the left superior temporal gyrus (Figure 4a-b, left panels). There were no regions in which increased cortical thickness significantly covaried with greater ADOS CSS scores.

2.3.5 Regions of decreased indices associating with great autism-related behaviors

There was one cluster in which decreased LGI significantly covaried with greater ADOS CSS scores, localized to right anterior insula and orbital/frontal gyri (Figure 4a, right panel). There were four clusters in which decreased sulcal depth significantly covaried with greater ADOS CSS scores, including right middle temporal gyrus, left precentral and postcentral gyrus, left superior parietal lobule/precuneus, and right anterior insula (Figure 4b, right panel). There were nine clusters in which decreased cortical thickness significantly covaried with increased ADOS CSS scores, including frontal, parietal, and occipital regions (Figure 4c, left panel).

Though scanner protocol and biological sex were not analyzed as outcomes of interest in the current study, qualitative patterns of these variables per cortical index are visualized in Supplemental Figure 3. The random effect of scanner protocol was low in most regions

Figure 2.3: Significant regions of age by group interactions by cortical surface index

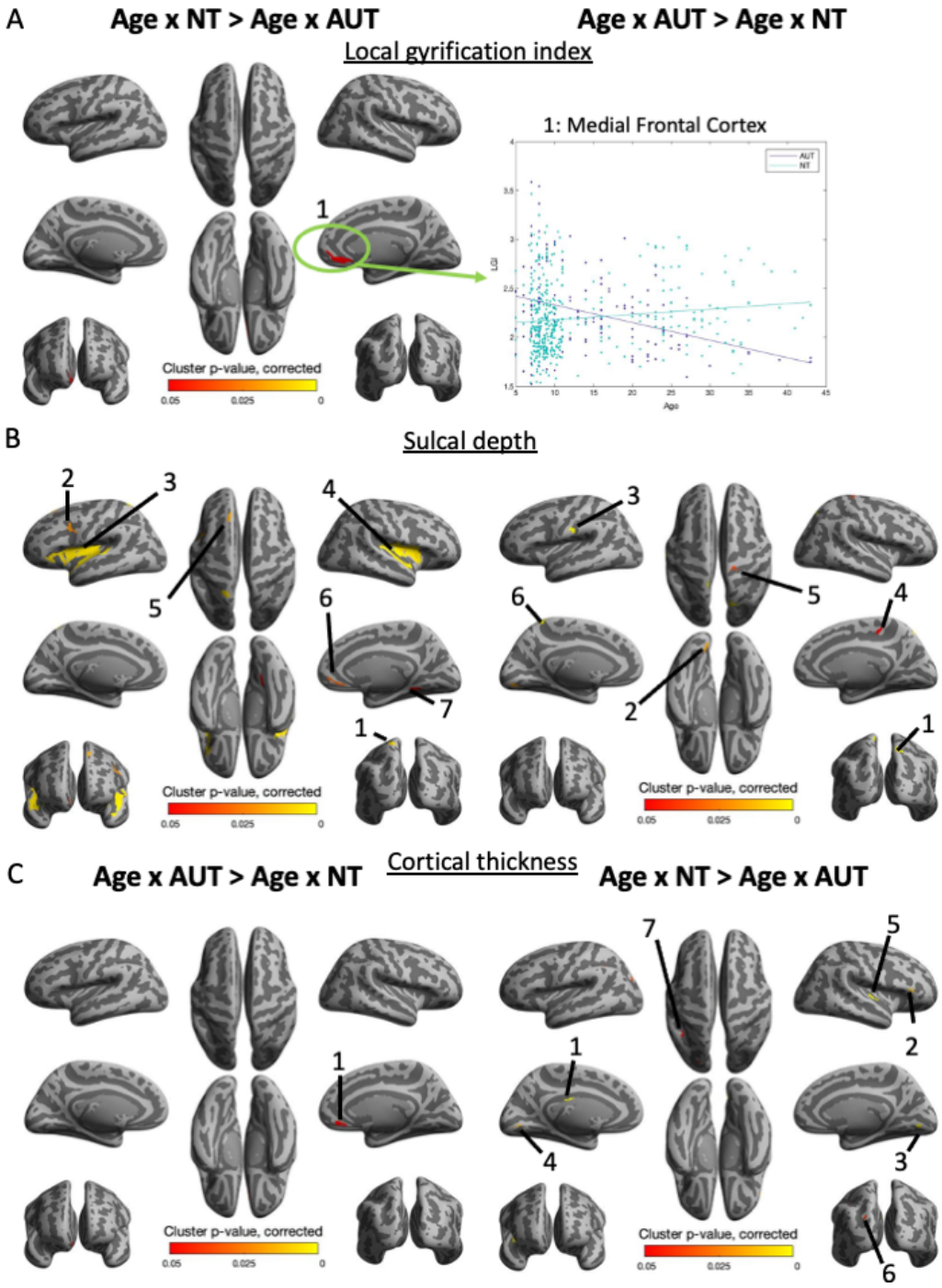

Regions of significant age by group differences in local gyrification index (LGI, panel A), sulcal depth (SD, panel B), and cortical thickness (CT, panel C) are shown, colored according to cluster p-value (bottom scale). Left panels indicate regions of greater slope with age in the NT group than AUT group for LGI, SD and regions of greater slope with age in the AUT than NT group for CT and vice versa in the right panels, at the $p < 0.05$ level after correcting for multiple comparisons via random field theory. CT is presented inversely from LGI and SD (i.e., as labeled, Age * AUT >Age * NT is on the left panel rather than right) due to its inverse correspondence with these indices. Regions are labeled in Table 2.3. The inset on panel B displays LGI by age and group, averaged within the indicated medial frontal cortex region. Points are colored by by NT=neurotypical (turquoise) and AUT=autism (purple) group.

Table 2.3: Clusters of significant regions for group by age interactions

Index	Cluster	Region	# Vertices	Max. Coeff.
Contrast: Age*AUT>Age*NT				
LGI		n/a		
SD	1	Right superior parietal lobule	248	0.142
SD	2	Left lingual gyrus	149	0.137
SD	3	Left postcentral gyrus	227	0.130
SD	4	Right precentral gyrus medial segment	120	0.090
SD	5	Right postcentral gyrus / precentral gyrus	146	0.063
SD	6	Left postcentral gyrus / precuneus	166	0.057
CT	1	Right medial frontal cortex	131	0.032
Contrast: Age*NT>Age*AUT				
LGI	1	Right anterior cingulate gyrus / medial frontal cortex / superior frontal gyrus medial segment	390	0.031
SD	1	Left precuneus / postcentral gyrus / superior parietal lobule	359	0.186
SD	2	Left middle frontal gyrus / precentral gyrus	291	0.170
SD	3	Left posterior/anterior insula, central/frontal/ parietal operculum, lateral/posterior orbital gyrus, orbital/triangular part of the inferior frontal gyrus / planum polare / planum temporale / temporal pole / transverse temporal gyrus	6394	0.163
SD	4	Right posterior/anterior insula, central/frontal/parietal operculum, opercular part of the inferior frontal gyrus / planum polare / planum temporale / temporal pole / transverse temporal gyrus	6125	0.156
SD	5	Left superior frontal gyrus	159	0.148
SD	6	Right medial frontal cortex / superior frontal gyrus medial segment	129	0.127
SD	7	Right lingual gyrus	222	0.122
CT	1	Left middle cingulate gyrus	66	0.040
CT	2	Right triangular part of the inferior frontal gyrus	82	0.032
CT	3	Right lingual gyrus	100	0.029
CT	4	Left lingual gyrus	72	0.028
CT	5	Right posterior insula / planum polare	243	0.028
CT	6	Left superior occipital gyrus	74	0.025
CT	7	Left angular gyrus / supramarginal gyrus	99	0.023

By column: Morphological index, cluster number per contrast (in descending order by maximum coefficient), regions of cluster localization, number of vertices per cluster, and the maximum coefficient, i.e. the unstandardized coefficient estimate for the age by diagnostic group term of the maximum vertex in each cluster. Direction of contrast Age*AUT>Age*NT indicates slope with age is greater in AUT and vice versa. Significance was assessed after correcting for multiple comparisons using random field theory at $p<0.05$. Abbreviations: CT=cortical thickness; LGI=local gyrification index; SD=sulcal depth, AUT=autism, NT=neurotypical.

(i.e., r $<$0.2).

2.4 Discussion

This study analyzed cortical morphology in autism using a newly developed approach which quantifies LGI adaptively in relation to specific sulci/gyri and further analyzed the complementary indices of sulcal depth and cortical thickness. Overall, these findings add to the extant literature in that they suggest a complex pattern of cortical morphological differences in autism, with higher confidence in the localization of these regions due to our adaptive approach to local gyrification indexing. Further, by including indices of local gyrification, sulcal depth, and cortical thickness, we provide findings that begin to disentangle specific, more granular dimensions of morphological changes associated with autism. Lastly, by applying these indices in a large sample and considering effects of age and autism-related behaviors, we provide findings that inform how cortical structure in autism may vary with development and behavior.

This approach identified a number of sensory, associative, limbic, and frontal regions in which one or more of these indices differed in autistic participants compared to neurotypical participants. In many of these regions, gyrification increases corresponded with expected increases in sulcal depth, whereas regions of gyrification decreases were spatially distinct from sulcal depth decreases. This suggests that increases on these indices may be explained by a common mechanism, whereas there may be distinct factors contributing to gyrification versus sulcal depth decreases. On the other hand, regions of group differences in cortical thickness did not spatially overlap with regions of group differences in LGI, though one region showed the expected inverse correspondence between these two indices in analyses of age.

Analyses of age-specific effects revealed several regions in which group differences depended on age, predominantly in frontal and/or limbic regions such as anterior insula, anterior cingulate, and orbitofrontal cortex, though these findings are within the context

Figure 2.4: Significant regions of association with ADOS CSS by cortical index

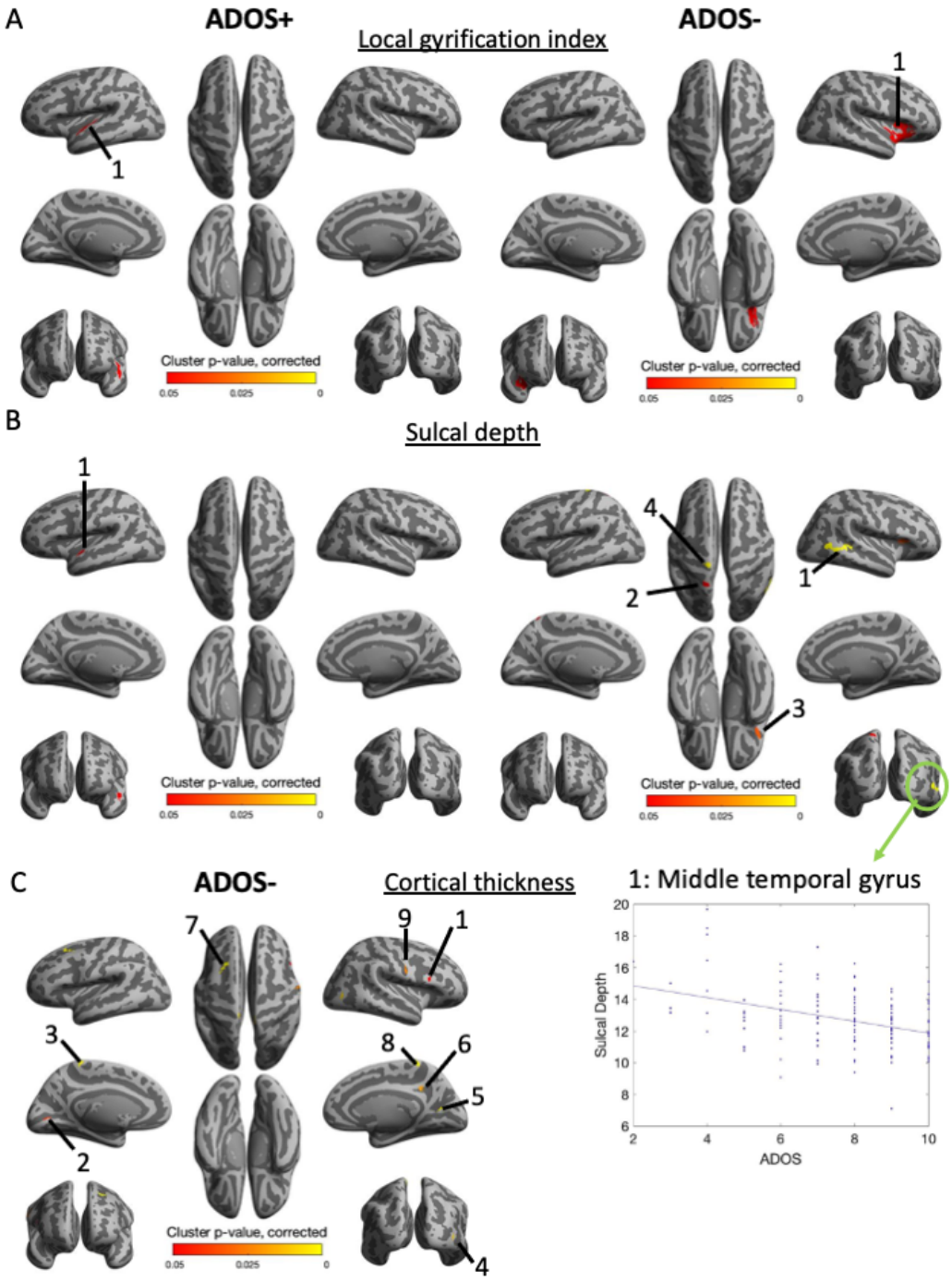

Regions of significant associations with autism-related behaviors for local gyrification index (LGI, panel A), sulcal depth (SD, panel B), and cortical thickness (CT, panel C) are shown, colored according to cluster p-value (bottom scale). Left panels indicate regions of positive associations (i.e., increased index value corresponds with greater symptomatology) for LGI, SD and negative associations (i.e., decreased index value corresponds with greater symptomatology) for CT (arranged by expected correspondence between the indices) and vice versa in the right panels, at the $p < 0.05$ level after correcting for multiple comparisons via random field theory. CT is presented inversely from LGI and SD (i.e., as labeled, ADOS- is on the left panel rather than right) due to its inverse correspondence with these indices. Regions are labeled by corresponding structure. The inset on panel C displays sulcal depth (in mm) by ADOS CSS, averaged within the indicated middle/superior temporal gyrus region.

Table 2.4: Clusters of regions significantly associated with ADOS CSS

Index	Cluster	Region	# Vertices	Max. Coeff.
ADOS+				
LGI	1	Left planum polare / superior temporal gyrus / transverse temporal gyrus	598	0.276
SD	1	Left planum polare / superior temporal gyrus / temporal pole	284	0.462
CT	n/a			
ADOS-				
LGI	1	Right posterior, anterior insula / entorhinal area / frontal operculum / lateral, posterior orbital gyrus / orbital, triangular part of the inferior frontal gyrus / planum polare	2564	0.422
SD	1	Right middle temporal gyrus	911	0.879
SD	2	Left precuneus / postcentral gyrus / superior parietal lobule	283	0.579
SD	3	Right anterior insula, frontal operculum	354	0.294
SD	4	Left precentral / postcentral gyrus	232	0.184
CT	1	Right opercular part of the inferior frontal gyrus	80	0.116
CT	2	Left calcarine cortex	78	0.113
CT	3	Left postcentral, precentral gyrus medial segment	137	0.110
CT	4	Right inferior occipital gyrus	69	0.107
CT	5	Right cuneus	82	0.103
CT	6	Right posterior cingulate gyrus / precuneus	111	0.100
CT	7	Left middle frontal gyrus / superior frontal gyrus	175	0.088
CT	8	Right postcentral, postcentral gyrus medial segment	186	0.085
CT	9	Right postcentral gyrus / precentral gyrus	145	0.072

By column: Morphological index, cluster number per contrast (in ascending order by maximum coefficient), regions of cluster localization, number of vertices per cluster, and the maximum coefficient, i.e. the unstandardized coefficient estimate for the ADOS term at the maximum vertex in each cluster. Direction of contrast ADOS+ indicates correspondence such that increased index corresponded with greater autism-related behaviors and ADOS- indicating inverse correspondence with index such that decreased index corresponded with greater behaviors. Significance was assessed after correcting for multiple comparisons using random field theory at $p<0.05$. Abbreviations: CT=cortical thickness; LGI=local gyrification index; SD=sulcal depth, AUT=autism, NT=neurotypical, ADOS=Autism Diagnostic Observation Schedule, General or 2nd version.

of having a wide sample age range but denser data at younger ages. On the other hand, analyses of autism-related behaviors identified several regions in which morphological indices covaried with autism-related behaviors, predominantly in sensory and motor regions such as temporal gyri, somatosensory cortex, and motor cortex. The pattern of structural changes in auditory, visual, somatosensory, and motor regions are largely congruent with previously reported structural changes in sensory processing regions in autism (Ecker et al., 2014; Libero et al., 2014; Yang and Hofmann, 2016; Kohli et al., 2019a; Libero et al., 2019; MRC AIMS Consortium et al., 2020). Our results extend prior findings linking cortical indices in temporal regions to autism-related behaviors (Libero et al., 2019; MRC AIMS Consortium et al., 2020) by identifying several additional sensory regions in which structural patterns with autism-related behaviors, including primary interoceptive, somatosensory, and visual cortices. Further, there were several regions of overlap between age and behavioral analyses such that morphological patterns in these regions of overlap depended on both age and autism-related behaviors.

2.4.1 Sensory region morphology in autism: Support for a developmental cascade

Temporal gyri. We found a multiple group differences in cortical indices in temporal areas related to auditory, language, and multisensory processing, including consistent relationships across indices with autism-related behaviors in the middle and superior temporal gyrus. Two recent studies have found correlations between enhanced gyrification in subsets of the temporal gyri and social traits in autism, although in the smaller study of 3-5 year olds this correlation did not survive correction for multiple comparisons (Libero et al., 2019; MRC AIMS Consortium et al., 2020). Our present results complement and extend these findings, providing evidence for the structural brain features that may underlie multisensory processing differences in autism.

Occipital cortex. Regions of association with autism-related behaviors in occipital cor-

tex included one region in which decreased cortical thickness significantly correlated with greater autism-related behaviors localized to inferior occipital cortex. There was also a superior occipital clusters of significant association between decreased sulcal depth with greater autism-related behaviors. These structural changes, as spread across different areas of the visual processing stream, may relate more broadly to evidence for enhanced visual feature processing in autism relative to global integration (Behrmann et al., 2006; Baum et al., 2015).

Somatosensory and motor cortices. In primary motor cortex along the precentral gyrus, both significant group differences in structural indices and relations between such indices and autism-related behaviors were spatially similar to those seen in somatosensory cortex, often in overlapping regions between the two gyri. This concordance emphasizes close relationships between tactile and motor development. Cortical thickness and sulcal depth within somatosensory cortex also covaried by autism-related behaviors. Differences in tactile reactivity in autism are commonly reported and these findings are further consistent with prior studies that suggest dimensional relationships between measures of somatosensory function and autism behaviors (Cascio et al., 2012b, 2015; Foss-Feig et al., 2012).

Sensory associative regions. Consistent with some prior accounts, we also found morphological changes in associative parietal regions, including the superior parietal lobule and precuneus (Wallace et al., 2013). Findings in these regions both significantly interacted with age and autism-related behaviors, further emphasizing potential differences in sensory association in autism and the relation of structure in these regions to complex social and communicative skills such as theory of mind, as precuneus activation has previously been linked to theory of mind processing in individuals with autism (Dufour et al., 2013).

Together, these concordant patterns of sensory region morphology in autism suggest first, that there might be some common biology shaping sensory processing patterns in

autism across the different sensory systems. Second, these changes may cascade onto each other; e.g., altered processing in unimodal sensory region may impact the signals that get sent to associative sensory regions. Third, morphology in many primary and associative sensory areas related to complex autism-related behaviors, such as social cognition, preference for routines, and interests. This provides further support for the developmental cascades model, such that primary processing of sensory cues may cascade onto these higher-order skills (Cascio et al., 2016).

2.4.2 Implications for interoceptive brain networks: Cortical morphological changes in autism depend on both autism behaviors and developmental timing

Primary interoceptive perception. Gyrification was decreased in autism in the posterior insula and parietal/central operculum regions, which are involved in basic and associative sensory processing, particularly of interoceptive stimuli (Craig, 2002). Further, patterns of cortical thickness in these areas interacted with age such that individuals with autism showed greater declines with age than individuals with typical development. Functional MRI analyses have found relationships between posterior insula response with age and social traits in autism (Failla et al., 2020), consistent with the present structural findings. These findings implicate the primary perception of interoceptive cues as altered in autism, perhaps increasingly so across development. Apparent decreases in cortical thickness may be associated with increased myelination (Natu et al., 2019), and the finding that gyrification was also decreased rather than increased (as these vary inversely; (Mota and Herculano-Houzel, 2015)) might point towards myelination as well. This would be consistent with predictive coding theories of autism that suggest heightened primary perception of sensations (Pellicano and Burr, 2012).

Interoceptive planning and associations. The anterior cingulate and anterior insular cortices are considered to be part of the salience network (Seeley et al., 2007; Menon and

Uddin, 2010). This account is consistent with the Embodied Predictive Interoception Coding (EPIC) model, in which these areas are considered hubs for predicting and planning responses to bodily needs, informed by current environmental sensations (Barrett and Simmons, 2015). In both accounts, these regions process broad environmental stimuli and determine its relationship to the bodily self. Structural differences within the anterior cingulate have been identified in several prior studies involving individuals with autism (Ecker et al., 2014; Yang and Hofmann, 2016; Kohli et al., 2019a; Laidi et al., 2019) and decreased insular and orbitofrontal gyrification has been found in adults with autism, correlating with executive functioning ratings (ages 40-61; Kohli et al., 2019b). In our sample, we found increased cortical thickness in autism in both of the anterior insula and anterior cingulate, which may relate to either increased cell bodies or decreased myelination (Rakic, 1995; Natu et al., 2019). Decreased myelination in particular may relate to prior findings of altered structural and functional salience network connectivity in autism, which has been suggested as a particularly distinguishing feature of autism that relates to both sensory reactivity and socioemotional processing (Uddin et al., 2013; Abbott et al., 2016; Green et al., 2016; Chen et al., 2017).

Findings across insular cortex. The finding that spanned the largest number of vertices, and corresponding functional regions, was a significant interaction between sulcal depth and age bilaterally in large areas between the superior temporal gyrus and Sylvian fissure, such that sulcal depth in these areas was particularly decreased in older individuals with autism relative to NT adults. The size of the significant clusters suggest that a broader structural shift rather than local cellular circuitry may be contributing to increasing differences in these areas with age, which may impact function in the many comprising regions.

Insular cortex is a prominent component of this broad region; thus, this evidence suggests that functional organization of primary and associative interoceptive regions develop differently in autism. Yamada et al. (2016) found an overall reduced number of data-derived

subregions along the insular cortex in autism when analyzing the homogeneity of the functional MRI signal, which is consistent with these structural findings.

Further, one of only two clusters in which LGI significantly covaried with autism-related behaviors spanned both posterior and anterior insula. In this area, decreased gyrification related to greater autism-related behaviors. This provides some evidence to distinguish interoceptive processing in autism from other sensations, in which relationships to autism-associated behaviors were only observed in cortical thickness or sulcal depth. The underlying cellular differences in which these interoceptive regions co-vary with autism-related behaviors may occur across a broader range of features, such as cell body size, count, and myelination. The other cluster in which LGI covaried with autism-related behaviors, localized to superior temporal gyrus, showed a positive rather than negative relationship. This suggests that there may be a balance between how internal and external sensory processing may contribute to the overall autism phenotype. Potentially, tipping this balance (i.e., too strong or too weak of associations formed for how we use environmental sensations to contextualize our internal stimuli) might lead to a greater number of autism-related challenges.

2.4.3 Limitations

Our approach to local gyrification indexing addresses several limitations in prior approaches, and as mentioned there is emerging evidence that, as intended, this approach identifies regions of group differences that are more precisely localized to specific curves than the frequently used FreeSurfer approach (Płonka et al., 2020). However, we are limited when comparing this approach to studies using FreeSurfer or similar packages, given that all MRI approaches simply estimate "true" gyrification. Additionally, we are limited in a thresholded whole-brain when trying to thoroughly understand cortical structure in a specific region, as sub-threshold trends may also inform the underlying structure. Thus, region-of-interest studies are needed to confirm the exact relation between indices in a given region

and thus to clarify to a greater extent what the underlying neural features in autism may be.

Though both age and biological sex are accounted for in our models, our groups did differ somewhat on these factors, and there are several additional considerations based on demographic factors that may also inform future research. Given that this project spanned multiple distinct cohorts, IQ measures were not standardized across protocols and so were not included as a covariate in analyses; thus, the identified group differences in IQ may account for some of the between-group regions of differences. As our sample includes a greater proportion of young males (i.e., under 10 years old) and generally IQ within average ranges, additional research is necessary to ascertain a more thorough characterization of changes in older individuals and persons with below average IQ. Additionally, we have accounted for linear effects of age in our modeling, but not non-linear terms. This is supported as an adequate control by our data distribution (see Supplemental Figure 2), and the largest recent study to date supports linear effects as the best model fit across a broad age range (see model comparisons in MRC AIMS Consortium et al., 2020). However, non-linear trajectories may be particularly important to consider for certain developmental windows (e.g., 1.5-5 years; Schumann et al., 2010); as such, non-linear trends may be promising for future studies to explore. Finally, though our study identifies several regions in which changes in these indices interact with age, it is limited by its cross-sectional design in understanding developmental trajectories, as these effects have been inferred across individuals. Further, though our work presents some broad patterns across our wide age range, these patterns may qualitatively differ at different developmental points. Thus, longitudinal studies using our adaptive approach to gyrification are thus a highly promising area of future research, with the potential to facilitate our efforts to more fully understand cortical developmental trajectories in autism.

While our findings contribute to a broader understanding of cortical morphology in individuals with autism, relations between these cortical indices and individual variability in autism-related behaviors and related domains such as language, IQ, and co-occurring

conditions are further areas to explore. As the ADOS CSS was only collected on our AUT group, one possible direction for future research to explore is the extent to which the identified structure-behavior relationships generalize to autism-related behaviors in the general population or whether they are specific to those who have received a diagnosis. Additionally, the ADOS CSS represents a broad measure of autism-related behaviors; thus, precise relations between structural indices and finer-grained behavioral measures of symptom domains may further elucidate the relation between brain structure and behavior in autism.

2.4.4 Conclusions

The results of this study have extended prior findings of cortical structure in autism to identify patterns of morphological differences with improved spatial resolution. Overall patterns of differences suggested complex cortical patterns that varied with age and autism-related behaviors in several sensory, limbic, and frontoparietal regions in persons with autism relative to neurotypical controls. Many of these identified structural changes were in interoceptive network regions, including one of the only clusters in which local gyrification correlated with autism-related behaviors. These results provide support for sensory cascade models of autism and inform ways in which interoceptive processing in autism may be distinct from neurotypical development. Future work may further examine the associations between these structural changes and other behavioral outcomes in individuals with autism, such as reported interoceptive experiences. This will provide greater insights into how the prominent structural alterations in sensory and broader regions relate to phenotypic variation in autism.

CHAPTER 3

Insular connectivity in autistic and non-autistic development

3.1 Introduction

The sensory perception of cues signaling biological needs (i.e., interoception) presents an interesting paradox: these are the most crucial cues for our survival, yet we are often unaware of them (Ainley et al., 2016; Allen et al., 2022; Barrett and Simmons, 2015; Craig, 2002; Kleckner et al., 2017; Paulus and Stein, 2006). Barrett and Simmons (2015) propose how efficient design of the neural circuits for interoception may explain this paradox. These circuits perform the crucial role of meeting the body's needs efficiently by continually anticipating those needs based on past experiences and current state. Communication between interoceptive cortex in the posterior insula and limbic regions such as the anterior insula and dorsal amygdala underlies the continual comparison of predicted with actual bodily needs (Barrett and Simmons, 2015; Paulus and Stein, 2006). In this model, successfully predicted physiological changes may not rise to the level of conscious awareness, but unpredicted changes require conscious awareness for two important purposes: to meet the body's newly-perceived need and to learn from current circumstances to predict this need in the future. Thus, the brain systems that underlie the prediction of interoceptive sensations may reveal more about altered interoceptive experiences than awareness measures on their own.

Fundamentally, our expectations for our bodily states are learned across the course of development. Starting in infancy, our caregivers help us meet our bodily needs, forming a basis for how social cues shape our interoceptive expectations (Atzil et al., 2018; Zoltowski et al., 2022). Other contextual cues may thus become associated with fulfilled needs over later development as we gradually become independent in maintaining homeostasis. There is indeed evidence that developmental differences may influence the relationship between

interoception, emotional awareness, and mental health (Trevisan et al., 2019), including for individuals on the autism spectrum. Thus, considering the development of interoceptive brain systems in autistic and non-autistic individuals may be especially important to understand the mixed interoceptive challenges reported by autistic individuals (DuBois et al., 2016; Failla et al., 2020; Fiene and Brownlow, 2015; Garfinkel et al., 2016; Palser et al., 2018; Quadt et al., 2021; Trevisan et al., 2021b; Williams et al., 2022).

The development of different aspects of interoception may be revealed by examining the specialized subregions along the insular cortex that coordinate to process, predict, and contextualize bodily sensations (Craig, 2008; Farb et al., 2013). Cytoarchitectural analysis of insular cortex reveals eight distinct subregions as divided by number of cortical layers (granularity) and location relative to the long, short, and accessory insular gyri (Craig, 2008; Farb et al., 2013). These are commonly grouped into three major subdivisions that each map to a broader function: the posterior, middle, and anterior insula (Figure 1). The posterior insula receives inputs from subcortical regions about bodily sensations and these cell circuits involve the greatest number of cortical layers (dorsal and ventral granular in the 8-division model), which allows this area to process detailed information about bodily signals. The middle insula has a medium number of cortical layers ("dysgranular") and receives diverse multimodal sensory inputs which may then be associated with interoceptive cues. Ultimately, information that reaches the anterior insula reflects an abstracted "gist" of bodily state as interpreted within the current environmental context and is processed at the broadest level of cell circuitry, reflected in its agranular (i.e., least layered) structure (Barrett and Simmons, 2015; Kleckner et al., 2017).

There also may be interesting patterns to consider based on laterality of interoceptive system development. Typically, the laterality of external sensory systems reflects the side of the body from which sensory information originates. However, interoceptive signals tend to originate from common (and often centralized) organs like the heart or lungs, but may be lateralized for distinct purposes. The most prominent model of insular lateraliza-

Figure 3.1: Correspondence of detailed and major subregions of the human insula

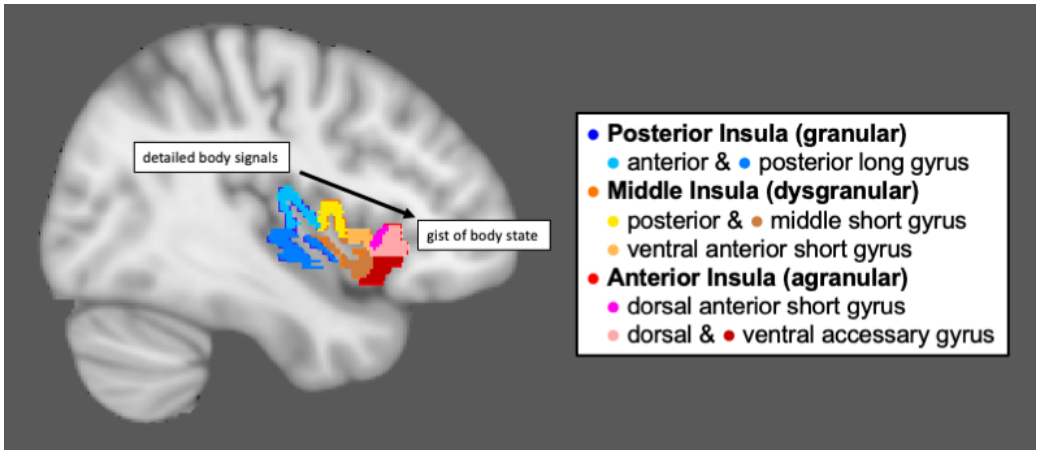

Subregions of the human insula are shown for both detailed (8-subregion) and major (posterior, middle, anterior) categorizations. The figure legend shows corresponding granularity (granular, dysgranular, or agranular) of each subregion.

tion comes from Craig (2005, 2008, 2002) neuroanatomic work establishing interoceptive pathways that the right insula specializes in sympathetic nervous system control and the left insula specializes in parasympathetic nervous system control. Evidence for this model comes from differential insular activation when stimulating the vagus nerve (Narayanan et al., 2002) and differential autonomic response patterns when stimulating the left versus right insula in neurosurgery patients (Oppenheimer et al., 1992). Thus, differentiating between right and left insula development may inform the relationships between interoception, stress, and anxiety.

Of the three major insular subregions, the anterior insula has been the best studied in autism (Di Martino et al., 2014; Uddin, 2015; Uddin and Menon, 2009). This region has received attention as it is considered part of the salience network for dynamically allocating attention towards environmental stimuli that are deemed most relevant to the bodily self (Uddin and Menon, 2009), consistent with its status as a high-level hub of the interoceptive network (Klapwijk et al., 2017). Uddin (2015) reviews prominent differences in anterior insular connectivity in autism, though findings in terms of specific regions of differences have been heterogeneous between samples. Considering development is key to

finding patterns within this heterogeneity (Nomi et al., 2019; Uddin et al., 2013). In general neurodevelopment, connectivity patterns vary across the lifespan such that the number of functional connections is increasing across childhood but prunes (i.e., selectively decreases) towards specialized communication patterns starting in adolescence and continuing throughout adulthood (Hua and Smith, 2004; Innocenti and Price, 2005; Katz and Shatz, 1996). Nomi et al. (2019) model for anterior insular connectivity in autism is that aggregate findings suggest a shift from hyper- connected in childhood to hypo- connected in adolescence and adulthood. Mechanistically, this would suggest that anterior insular connections are pruned more readily in autism compared to neurotypical development.

These anterior insula findings suggest differences in autistic individuals in how the "gist" of bodily information is constructed and developed. However, less is known about how communication patterns of primary interoceptive cortex in the posterior insula develop and whether that pattern diverges in autism. Whereas processing in the anterior insula reflects an abstracted sense of bodily state, processing in the posterior insula reflects internal (bodily) signals that may or may not rise to the level of conscious awareness. Thus, these patterns may reveal insights about the subconscious parts of interoceptive processing that have been difficult to otherwise study. Failla et al. (2017) have found that altered anterior insula connectivity in autism may be related to posterior insular processing, specifically pinpointing differences in the white matter connecting the posterior to anterior insula in autistic compared to non-autistic individuals. As a complement to this structural approach, measuring functional communication patterns of the posterior insula may broaden our understanding of how the insula coordinates with a variety of regions to adaptively tune interoceptive awareness.

Studies thus far of posterior insular (PI) functional connectivity in autism have mostly been completed in smaller adolescent samples. Findings included reduced PI connectivity with somatosensory areas in one autistic sample (Ebisch et al., 2011) and with visual, integrative, and striatal areas in another (Francis et al., 2019). Xu et al. (2018) analyzed con-

nectivity using an 8 subregion model and did not find significant connectivity differences in either their hypergranular or dorsal granular insula seed regions, which most closely align with the PI seeds used in other studies. Though Francis et al. (2019) combined left and right seeds, Ebisch et al. (2011) found differential pattern strength by insula seed hemisphere. Though both left and right insula seeds showed reduced connectivity with somatosensory areas, they found that a greater number of somatosensory subregions were hypo-connected to the left posterior insula than to the right. These differences are interesting to consider within models of insular specialization for sympathetic (right) versus parasympathetic (left) specialization (Craig, 2005, 2008, 2002). Potentially, Ebisch et al. (2011) findings suggest that autistic individuals may maintain a greater number of sympathetic processing connections relative to neurotypical individuals, as compared to parasympathetic.

Further, developmental patterns of connectivity differences have only been examined in a limited subset of these studies. These may be especially relevant to consider, given patterns of anterior insula connectivity with age (Nomi et al., 2019; Uddin et al., 2013) and other known developmental changes in surrounding limbic regions (Gabard-Durnam et al., 2014). Francis et al. (2019) found that in all three regions with which the autistic group showed reduced posterior insular connectivity (fusiform, putamen, and intraparietal lobule), connectivity within the autistic group increased with age, narrowing the difference between autistic and neurotypical samples at older ages. This mirrors patterns found in other behavioral (Feldman et al., 2018) and neural (Dunham et al., 2023) studies of multisensory processing in autism.

However, before we can understand how posterior insula development diverges in autism, we must better understand its typical development. Thus, in this sample we examine age-related trends in posterior insula connectivity across our autistic and non-autistic samples. We will also examine dimensional relationships with self-reported body awareness. To begin to understand patterns in autism, we will further examine group-based differences in PI connectivity in autistic versus neurotypical individuals, independent of age. Though we

are underpowered to address age-specific group differences in the current sample, these findings will provide important background on how posterior insula connectivity develops across individuals, to compare with autistic development in the future.

3.2 Methods

3.2.1 Participants

Participants included in full-sample analyses were n = 59 autistic individuals (AUT, ages 7-54) and n = 71 non-autistic individuals (N-AUT, ages 7-53). Individuals were included in the autism group if diagnoses were confirmed by a licensed clinical psychologist, via the Autism Diagnostic Observation Schedule, General or Second Edition (ADOS-G or ADOS-2, Lord et al., 2000, 2012 and clinical judgment. Individuals were recruited across multiple functional magnetic resonance imaging (fMRI) cohorts, which include prior reports of functional results (Failla et al., 2020). All participants assented/consented to study participation and all parent studies were approved by the Vanderbilt University Institutional Review Board.

Individuals were excluded from participating in the parent MRI studies if intellectual quotient (IQ) was below 70 or contraindications to MRI scanning were present (see Supplemental Information), with final decisions made by staff MRI technicians. Of an initial n = 68 autistic and n = 79 non-autistic individuals who completed scanning procedures, n = 9 autistic and n = 8 non-autistic participants were excluded due to failed quality assurance, defined below for structural (n = 2 AUT, n = 3 N-AUT excluded) and functional (n = 7 AUT, n = 5 N-AUT excluded) preprocessing steps.

Participants were included in interoceptive self-report analyses if they had completed the Body Perception Questionnaire (BPQ; Porges, 1993). This is a questionnaire designed to measure reported awareness of bodily sensations in everyday contexts, and comprises subscales for “Body Awareness” and “Autonomic Reactivity”. The “Body Awareness” subscale was analyzed.

Table 3.1: Participant characteristics by diagnostic group

Group	n	Age (years)	Sex (% female)	Motion			BPQ
				mFD	DVARS	n	Awareness
N-AUT	71	20.2 (7-53)	28.2%	0.185 (0.08-0.36)	1.99 (1.19-2.94)	24	2.87 (1.77-3.46)
AUT	59	16.9 (7-54)	28.8%	0.196 (0.09-0.37)	1.92 (1.46-2.54)	32	2.75 (1.12-4.42)
p		0.06	0.94	0.36	0.23		0.49

Characteristics per group are summarized as mean, range for continuous variables and percentage (%) for categorical variables. No participant characteristics (age, gender, head motion) significantly differed between the groups, though the autistic participants were somewhat younger on average. Abbreviations: N-AUT: non-autistic, AUT: autistic, n: included sample size, mFD: median framewise displacement (millimeters), DVARS: derivative of temporal variance, BPQ: Body Perception Questionnaire (Porges, 1993)

Figure 3.2: Distribution of sample ages by diagnostic group

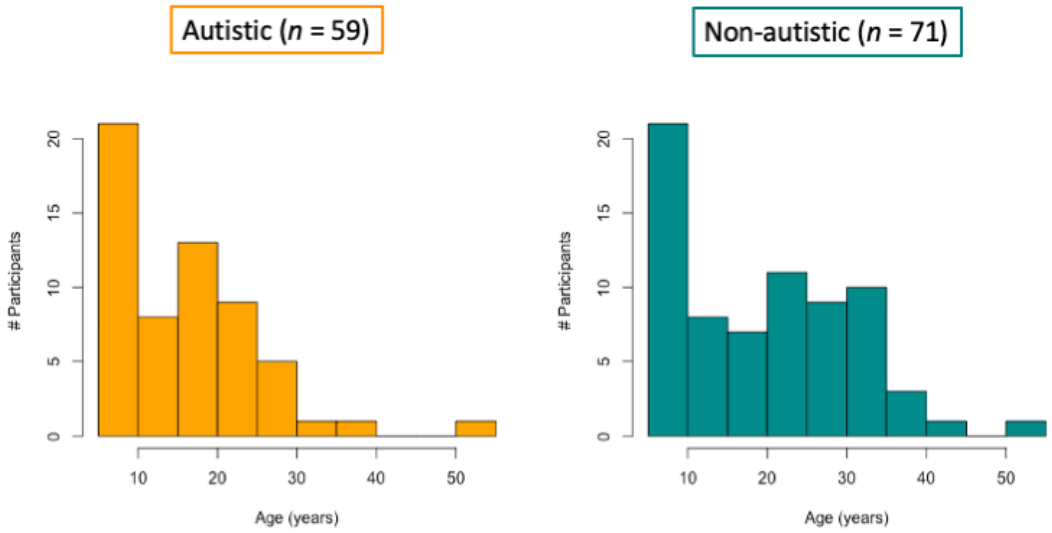

Histograms of participant age per group (Autistic versus Non-Autistic) are plotted, as number of participants (y-axis) per five-year age groups (x-axis). Autistic group is in orange and non-autistic group is in teal.

3.2.2 Image Collection

Anatomical and resting state functional images were acquired via one of three protocols:

Protocol 1 (n = 27 autistic, n = 24 non-autistic):

- High-resolution T1-weighted anatomical images were acquired via sagittal slices with 1mm^3 voxel resolution, TR = 9.0 msec, TE = 4.6 msec, flip angle = 8o, and acquisition matrix = 256 x 256 x 170.
- Resting state images were acquired using an echo planar imaging (EPI) sequence (3 mm^3 isotropic voxels, TR = 2s, flip angle 90) for approximately 6min 46s duration (203 volumes).

Protocol 2 (n = 29 autistic, n = 36 non-autistic) and Protocol 3 (n = 3 autistic, n = 11 non-autistic):

- High-resolution T1-weighted anatomical images were acquired via sagittal slices with 1mm^3 voxel resolution, TR = 8.0 msec, TE = 3.7 msec, flip angle = 7o, and acquisition matrix = 256 x 256 x 170.
- Resting state images were acquired using an echo planar imaging (EPI) sequence (3x3x4 mm voxels, TR = 2s, flip angle 79, and acquisition matrix 80 x 80 x 28) for approximately 6min 46s duration (203 volumes).

Though Protocols 2 and 3 had identical acquisition parameters, these were considered separate covariates in all analyses due to differences in the preceding task (interoception task or special interests task), per parent study design.

Since some participants completed multiple of these protocols, the total number of resting state runs ranged between 1-7, though the median was 1 resting state run. Participants completed between 1-3 anatomical scans at each study visit. For analyses, the functional scan with lowest average motion (median framewise displacement) out of any study visit and the highest quality structural scan at that same visit (determined via visual inspection,

with Computational Anatomy Toolbox (CAT) output considered when inconclusive, see below) were chosen for analysis. Thus, a total of one structural and one functional run were analyzed per participant.

3.2.3 MRI Preprocessing

Neuroimage data storage and processing took place on the Vanderbilt University Institute of Imaging Science Center for Computational Imaging XNAT (Harrigan et al., 2016; Huo et al., 2018). The processing pipelines are available through github (https://github.com/baxpr/connprep; https://github.com/baxpr/conncalc).

Structural preprocessing. T1-weighted anatomical images were preprocessed using the CAT12 extension to Statistical Parametric Mapping (SPM, version 12) software (Gaser et al., 2022). Anatomical images were skull stripped and normalized to MNI space. Quality assurance measures at this stage included the overall rated image quality (IQR) value, computed as part of the CAT12 toolbox and representing a quality measure across signal noise and bias. These numbers range from 0-100 and are interpreted on a letter grade scale (Gaser et al., 2022). Participants with IQR $<$70 were excluded from further analyses (n = 2 AUT, n = 1 N-AUT). Additionally, original structural images and MNI-normalized structural images were visually examined for quality by two trained raters, resulting in 2 exclusions for artifacts (both N-AUT).

Functional preprocessing. For each functional run, head motion realignment was completed using a two-stage SPM procedure with six head motion parameters. These motion parameters and their first derivates were also included as nuisance regressors in subsequent analyses. Functional images were co-registered to structural images using a rigid body transform and then normalized to MNI space using the previously computed CAT12 transform. Additional steps taken to reduce noise in the fMRI signal include bandpass filtering

(between 0.01 and 0.10 Hz), COMPCOR, and mean gray matter signal regression (Parkes et al., 2018).

Quality assurance for functional preprocessing included two criteria for determining acceptable levels of motion/noise due to motion. Framewise displacement (FD) and derivative of temporal variance (DVARS) were calculated. Individuals were excluded for either high average motion (FD >0.5mm, n = 3 AUT) or a high number of volumes with extreme motion (FD >1mm and DVARS ¿ 5%, n = 3 AUT) or both (n = 3 N-AUT). The quality of co-registration between structural and functional images was also visually examined by two trained raters, resulting in 3 additional exclusions (n = 1 AUT, n = 2 N-AUT).

3.2.4 Statistical Analysis

Left and right posterior insula seed regions of interest (ROIs) were defined following protocols used previously in Failla et al. (2017) and following Farb et al. (2013) cytoarchitectonic subdivisions among the insular gyri. The posterior seed maps onto the posterior long gyrus of the insula. Whole brain seed-based connectivity was analyzed with the left and right posterior insula ROIs, respectively, as seeds. In the first analytic stage, correspondence between each voxel and the average posterior insular seed signals were computed, resulting in a Z map per individual scan.

In the second analytic stage, individual predictors were used to assess the correspondence with connectivity strength. The covariates used in this analysis were: group, age, protocol, motion (median FD), and biological sex. Two different models were run to assess different potential terms of age, with other covariates kept constant: linear associations (t test for Age) and non-linear associations (F test for Age+Age^2). However, there was only one region in which age associations were significant for nonlinear effects that was not identified with the linear term; thus, age-related findings are primarily presented from the results of the linear model. Lastly, a model to assess interoceptive self-report was run using the BPQ Awareness subscale scores, in the subset of participants (n = 56) that had

completed this measure. Threshold-free cluster enhancement (TFCE) was implemented to determine significant clusters per predictor, using n = 5000 permutations and a family-wise error rate of p <0.1 to detect significant clusters. A voxel threshold of k >5 voxels was further applied to increase result interpretability. (Note, see Appendix 1: Chapter 3 supplement for a comparison of age-related clusters identified with a false discovery rate threshold of p <0.05. Ultimately, these approaches converged on similar regions with differing stringency).

3.3 Results

3.3.1 Findings by age: Combined sample

For the left posterior insula seed, there was one cluster of significantly increased linear associations with age, though this area was predominantly within the white matter (Table 2, Figure 2). There were several more areas of significantly decreased linear associations with age. The most prominent, in terms of both voxel size and significance, was within contralateral (right) thalamus, in which a cluster of k = 292 voxels was identified (p_{FWE} = 0.016). The remaining identified areas included the middle and anterior insula, ipsilateral thalamus, caudate, putamen, frontal operculum, and inferior frontal gyrus, pars opercularis. There was one additional region identified as showing a nonlinear association with age, of k = 15 voxels in the precentral gyrus (MNI_{peak} = 0, -16, 72, TFCE = 5040, p_{FWE} = 0.045).

For the right posterior insula seed, there were numerous clusters of significantly increased linear associations with age. The most prominent was in the ipsilateral (right) precuneus, in which a cluster of k = 209 voxels was identified (p_{FWE} = 0.036). Most of the other regions identified were also in associative sensory regions spanning both hemispheres, including left precuneus, right supplementary motor cortex, posterior cingulate gyrus, right supracalcarine cortex, and left lateral occipital cortex. There were also numerous clusters of significantly decreased associations with age. Similarly to the left hemisphere, these were prominently in the putamen and thalamus, though all identified clusters

were ipsilateral. Cortical areas included two visual areas, occipital pole and lingual gyrus. For the right posterior insula seed, there were no new regions of association identified via the nonlinear term of age.

3.3.2 Differences in posterior insula connectivity by group

The only group-specific findings were identified for the left posterior insula seed, not the right seed (Figure 3, Table 2). There was one cluster within the left lateral occipital gyrus that was associated with increased connectivity in the AUT group compared to the N-AUT group.

3.3.3 Relationships with bodily awareness

The most prominent cluster relating to increased BPQ awareness scores was the same for both the left and right posterior insula seeds, localized to right lateral occipital cortex (both peaks at 28, -62, 32; k = 78 voxels, p_{FWE} = 0.033 left seed and k = 35 voxels, p_{FWE} = 0.041 right seed). A couple other smaller clusters in neighboring and mirrored areas were identified, including the left and right angular gyrus for the left seed and left superior parietal lobule for the right seed.

However, the left posterior insula seed showed many more areas of association with decreased bodily awareness scores. The largest of these was in the right mid insula (k = 63, p_{FWE} = 0.030). The other areas identified included several frontal/prefrontal areas, specifically the anterior cingulate, precentral gyrus, supplementary motor cortex, and middle frontal gyrus. There were also a few temporal areas identified, including the temporal pole and primary auditory cortex. For the right posterior insula seed, there were no significant relationships identified with decreased bodily awareness.

Figure 3.3: Posterior insula connectivity by age

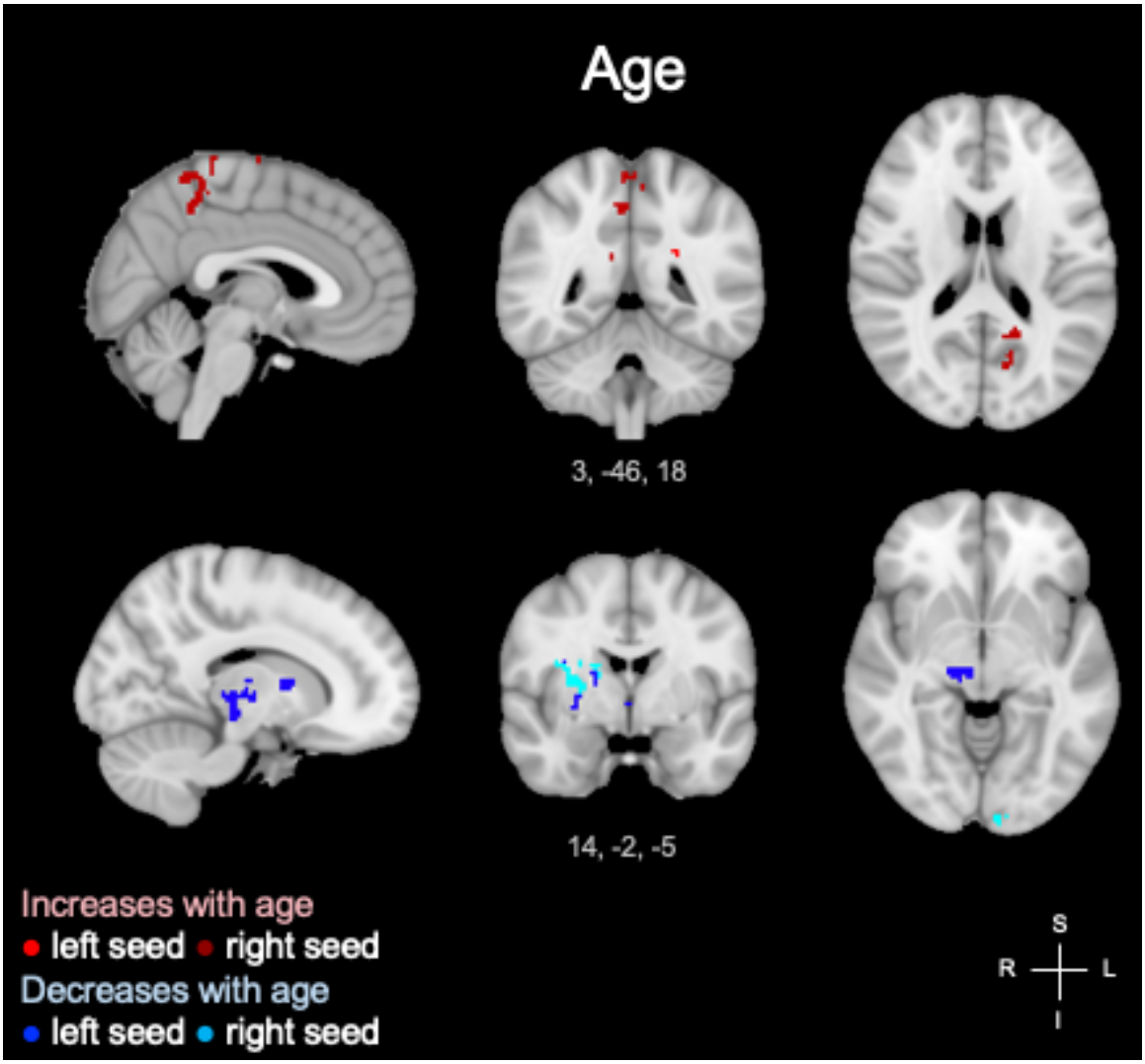

Significant clusters in which posterior insula functional connectivity increases (red) and decreases (blue) with age are shown (using threshold-free cluster enhancement, $p_{FWE} < 0.10$). Increasing connectivity with age is shown in areas including precuneus, supplementary motor cortex, and posterior cingulate. Decreasing connectivity with age is shown in areas including the thalamus, insula, and putamen. Color intensity varies by seed hemisphere as shown in figure legend. Images are shown in radiological convention.

Table 3.2: Summary of significant clusters for full sample linear age model

Term	Seed	# Voxels	Location	MNI_{peak}	TFCE	p_{FWE}
Age+	L	14	White matter (L)	-24, -44, 26	464.34	0.057
	R	209	Precuneus (R)	4, -44, 50	491.62	0.036
		39	Precuneus (L)	-16, -54, 18	485.69	0.040
		19	Precuneus / lingual gyrus	0, -54, 8	453.63	0.066
		36	Precuneus (L)	-14, -64, 18	449.73	0.070
		20	Precuneus (L)	-4, -72, 34	447.20	0.073
		5	Precuneus (L)	-10, -78, 38	436.37	0.086
		5	Precuneus (L)	-4, -44, 48	430.91	0.093
		19	Supp. motor cortex (R)	2, -10, 72	465.92	0.054
		6	Posterior cingulate (R)	10, -46, 22	434.66	0.088
		5	White matter (L)	-24, -42, 26	434.54	0.088
Age-	L	292	Thalamus (R)	8, -18, 2	536.69	0.016
		19	Thalamus (R)	18, -10, 12	450.68	0.064
		10	Thalamus (L)	-18, -14, 18	433.54	0.084
		14	Thalamus (L)	-12, -22, 10	435.29	0.082
		67	Insula (Anterior, R)	30, 10, 14	486.53	0.036
		19	Insula (Mid-Anterior, L)	-32, 14, 6	453.26	0.062
		10	Insula (Mid, R)	38, 4, 4	432.35	0.086
		36	Frontal operculum (R)	42, 10, 12	470.62	0.047
		39	Caudate (R)	14, 4, 8	450.02	0.065
		20	Putamen (R)	26, -2, 4	440.24	0.076
		9	Putamen (L)	-24, 4, 8	435.11	0.082
		5	Inferior frontal gyrus, pars opercularis (R)	46, 14, 14	427.63	0.093
	R	255	Putamen (R)	26, -6, 8	578.57	0.010
		45	Occipital pole (V1, L)	-8, -96, -2	469.13	0.052
AUT > N-AUT	L	62	Lateral occipital (L)	-12, -62, 58	520.57	0.017
	R	n/a				
AUT < N-AUT	L	n/a				
	R	n/a				

Model: Age + Group + Biological Sex + Motion + Protocol. Entries are grouped by location and then ordered by peak TFCE. Locations were assigned as the top match using the Harvard-Oxford Cortical and Subcortical Atlases. If a second match differed by less than 5% probability, this area was included as well. Other columns include the number of voxels (#) per cluster and for the peak cluster, the corresponding MNI coordinates (MNI_{peak}), threshold-free cluster enhancement score, and family-wise error p-value. Abbreviations: AUT = autism; N-AUT: non-autism, Supp. = Supplementary, Age+ = increasing term of age; Age- = decreasing term of age

Table 3.3: Summary of significant clusters for BPQ model

Term	Seed	# Voxels	Location	MNI_{peak}	TFCE	p_{FWE}
BPQ+	L	78	Lateral occipital (R)	28, -62, 32	600.84	0.033
	R	35	Lateral occipital (R)	28, -62, 32	516.62	0.041
		5	Lateral occipital (R)	26, -66, 44	462.34	0.089
BPQ-	L	63	Insula (Mid, R)	42, 4, -4	596.24	0.030
		28	White matter (R)	22, -24, 30	557.44	0.053
		18	White matter (R)	22, -10, 36	556.55	0.054
		24	White matter (L)	-16, 2, 34	551.77	0.058
		17	Supp. motor cortex; Anterior cingulate (R)	14, 6, 40	554.86	0.055
		7	Anterior cingulate (R)	6, 12, 36	526.09	0.084
		25	Precentral gyrus (L)	-54, 6, 8	554.79	0.055
		10	Precentral gyrus (L)	-30, -10, 42	536.68	0.072
		10	Temporal pole (R)	50, 14, -16	544.21	0.064
		16	Temporal pole (R)	60, 6, -2	533.14	0.076
		11	Frontal operculum, temporal pole (R)	48, 16, -6	521.25	0.090
		25	Paracingulate gyrus (L)	-6, 18, 38	537.10	0.071

Model: Age + Group + Biological Sex + Motion + Protocol + BPQ. Locations were assigned as the top match using the Harvard-Oxford Cortical and Subcortical Atlases. If a second match differed by less than 5% probability, this area was included as well. Other columns include the number of voxels (#) per cluster and for the peak cluster, the corresponding MNI coordinates (MNI_{peak}), threshold-free cluster enhancement score, and family-wise error p-value. Abbreviations: BPQ+ = increasing BPQ term, BPQ- = decreasing BPQ term, Supp. = Supplementary

Figure 3.4: Differences in posterior insula connectivity by group

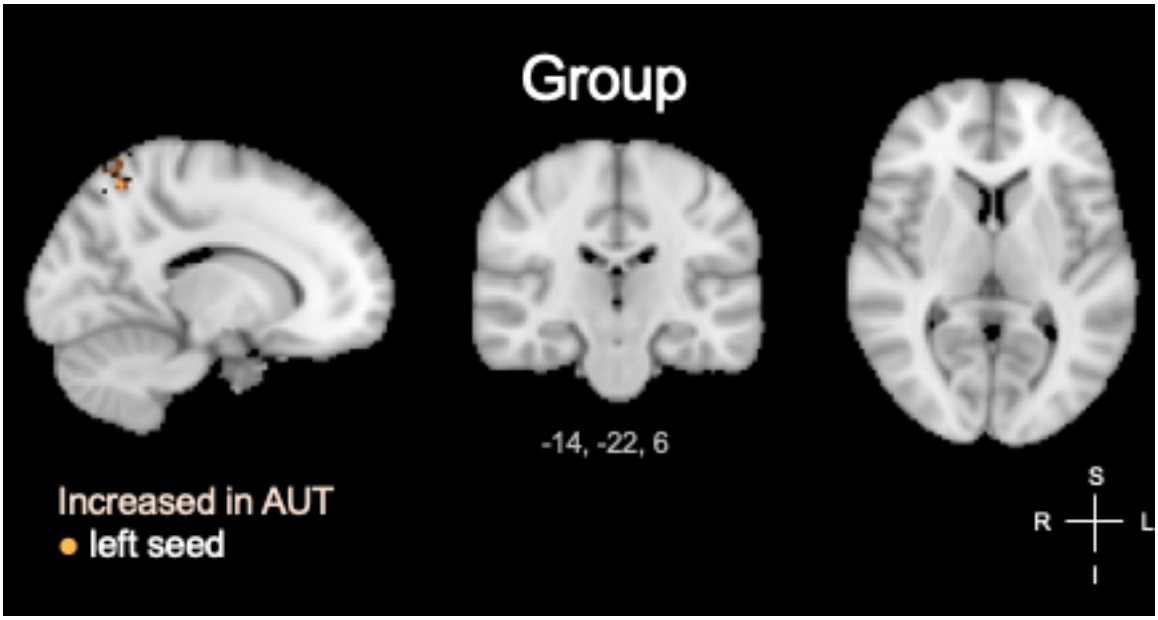

Differences in posterior insula functional connectivity by group were limited to one cluster, between left posterior insula and left lateral occipital cortex, shown here in orange. Functional connectivity with this region was increased in the autistic compared to non-autistic group (using threshold-free cluster enhancement, $p_{FWE} < 0.10$). Images are shown in radiological convention.

3.4 Discussion

3.4.1 General development of posterior insula connectivity

When looking at age-related connectivity patterns combined across groups, a few common themes emerged. There were more clusters of decreasing than increasing posterior insula (PI) connectivity with age, driven by the left PI seed. This is consistent with our sample including adolescents and adults whose brains have undergone widespread pruning of cortical connections (Hua and Smith, 2004; Innocenti and Price, 2005; Katz and Shatz, 1996). The specific areas of decreases are also consistent with a developmental perspective on interoceptive learning (Ainley et al., 2016; Barrett and Simmons, 2015). In both hemispheres, the areas of decreases were generally other insula subregions or sub-cortical regions, including thalamus, striatum, and brainstem. This would imply that, over time, our interoceptive perception becomes a less direct representation of our bodily signals as conveyed in these subcortical regions. Ideally, this may reflect adaptive learning: our ex-

Figure 3.5: Posterior insula connectivity by bodily awareness

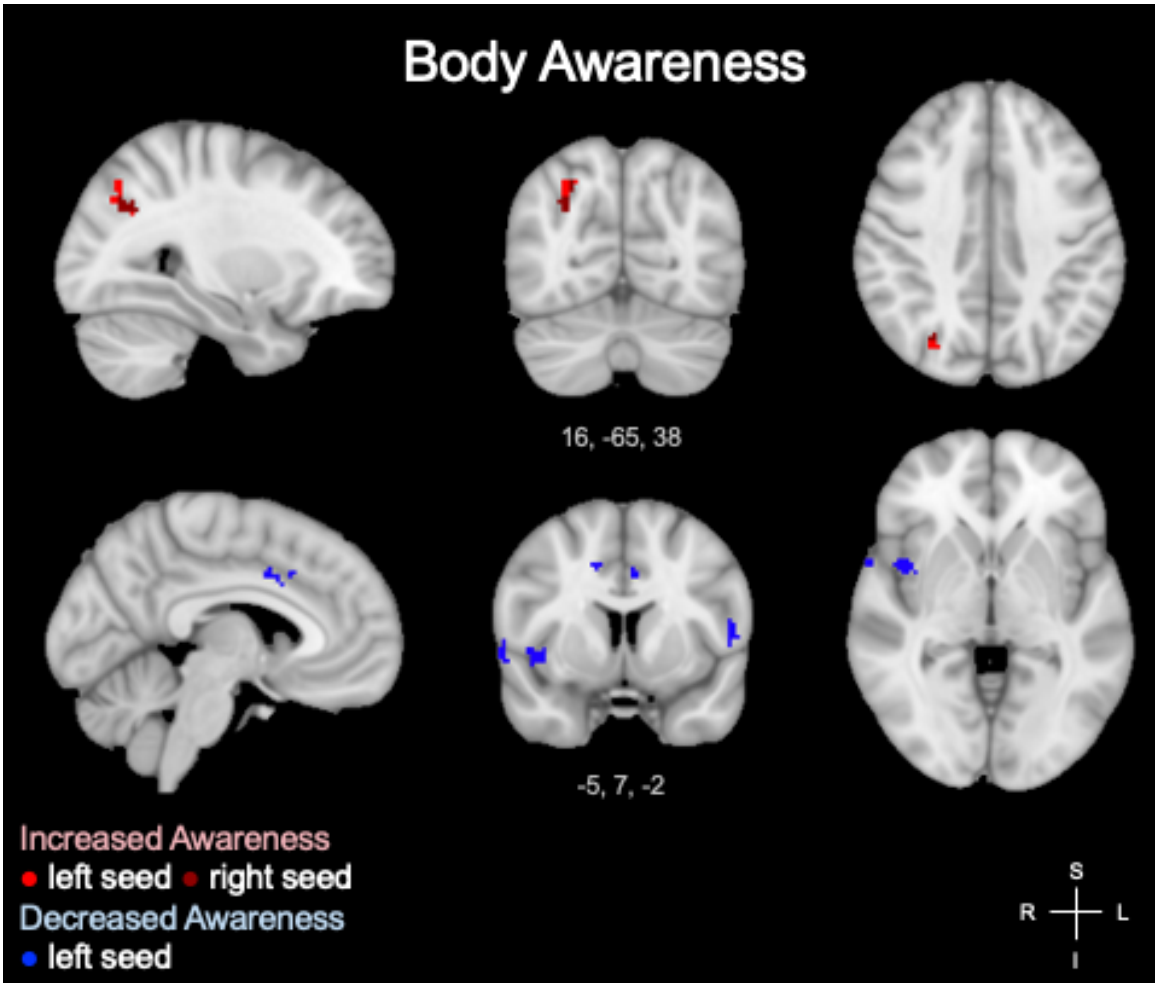

Significant clusters in which posterior insula functional connectivity increases (red) and decreases (blue) with bodily awareness as measured by the BPQ (Porges, 1993) are shown (using threshold-free cluster enhancement, $p_{FWE} < 0.10$). Increasing connectivity with BPQ scores is shown in right lateral occipital cortex. Decreasing connectivity with BPQ scores is shown in areas including mid-insula, white matter, anterior cingulate, precentral gyrus, and temporal pole. Color intensity varies by seed hemisphere as shown in figure legend. Images are shown in radiological convention.

pectations for these signals become well-tuned and thus less conscious effort is required to process and respond to homeostatic needs. Cardiovagal autonomic control has been shown to increase in efficiency from childhood to early adulthood (Lénárd et al., 2005), which may enable less effortful monitoring of these signals. Further, interoceptive task findings support an increasing distinction between baseline processing and intentional processing of cardiac signals with age (Failla et al., 2020). Failla et al. (2020) found that adults showed greater increases in insula responsiveness from baseline during heartbeat counting, but achieved similar accuracy levels as did children (i.e., this enhanced processing did not correspond to better performance). This would suggest that heartbeats may be processed in adults when needed (e.g., when explicitly asked by an experimenter to do so or during abnormal heart rhythms), but fewer neural resources are engaged towards each heartbeat during baseline, non-critical conditions.

Patterns of connectivity with the right posterior insula showed clues as to what types of associations may be used to refine our interoceptive models over time as we age. Particularly, there were several significant clusters that increased with age between right posterior insula and posterior parietal cortex, covering broad multimodal areas. This is in line with how we might expect the cues we use to interpret our bodily needs to become increasingly integrated among our multiple senses over time. Particularly, the strongest findings were in the right and left precuneus, which has been proposed to be involved in visuospatial imagery and consciousness (e.g., Cavanna and Trimble, 2006; Wenderoth et al., 2005). This might reflect that the actions required to maintain homeostasis into adulthood involve increasingly complex actions and advanced planning, such as seeking a job to buy food. Further, interoception may be processed increasingly within an abstracted sense of self identity (Palmer and Tsakiris, 2018).

The one cluster identified in which connectivity with the left posterior insula seed increased with age was localized to areas of broad white matter. Though right insula included more cortical connections, there was one mirroring white hemisphere region as well. Gore

et al. (2019) have found evidence that functional connectivity identified in white matter does reflect neural activity as conveyed along specific pathways. The areas connected by these exact tracts requires advanced modeling to approximate (Gore et al., 2019). However, the posterior white matter locations we identified could conceivably link towards multimodal sensory areas, strengthening an increasingly integrated sense of interoception as we age.

Similar to Ebisch et al. (2011) findings for diagnostic group differences, our findings for connectivity by age suggest qualitatively similar patterns between the hemispheres, but of varying strength and number of regions. The right posterior insula showed a balance of increasing and decreasing connections with age, with an overall greater number of connections that increased with age. On the other hand, the left posterior insula showed predominantly decreasing connectivity with age. This suggests that cortical pruning may occur more readily for parasympathetic than sympathetic nervous system regulation, with a greater level of baseline processing maintained for sympathetic regulation. Correspondingly, the right posterior insula was the only insula subregion in Failla et al. (2020) that did not show increasing responsiveness with age during heartbeat counting. Thus, cues relative to sympathetic activation might require more ongoing maintenance than for parasympathetic activation. This makes sense from a survival standpoint, given the critical nature of threat response.

3.4.2 Autistic differences in posterior insula connectivity

Group differences in insular connectivity were localized to just the left posterior insula seed, identifying one main cluster in left lateral occipital cortex. Unlike findings in prior samples (Ebisch et al., 2011; Francis et al., 2019), connectivity was increased with these areas in our autistic compared to non-autistic group. Though we were limited by sample size in exploring age-dependent differences in posterior insula connectivity, the relatively older age of our sample (e.g., extending past adolescence into middle adulthood) may contribute

to the directionality of these findings. For example, Francis et al. (2019) found increasing posterior insula connectivity with age in their areas of initially decreased connectivity. Thus, it is possible that in autistic individuals, the posterior insula might show the opposite developmental pattern from the anterior insula (Nomi et al., 2019), shifting from hypo- connected to hyper- connected. Particularly, our finding suggests that left PI connectivity is increased in autism in an area related to mental imagery, especially processing speed and time estimation (Forn et al., 2013; Sack et al., 2002). Craig (2009) notes the essential role of the insula in time perception, as linked to the cardiac cycle. Thus, increased connectivity between these areas in the autistic group might suggest that self-referential processing, particularly as related to the self in time, may be especially grounded in interoceptive processing in autistic individuals. Otherwise, these generally null findings by group further call into question whether findings of reduced interoceptive accuracy in autism might be more nuanced than common behavioral measures, such as heartbeat counting accuracy, suggest (Williams et al., 2022).

3.4.3 Relationship with bodily awareness

We identified several regions in which posterior insular connectivity covaried with either enhanced or reduced self-reported body awareness. For both our right and left posterior insula seeds, trends with increased bodily awareness were found with coinciding lateral occipital cortex clusters. This lateral occipital region is in a similar, though not identical, area as the self-referential parietal areas that showed increasing connectivity with age (e.g., Cavanna and Trimble, 2006). Potentially, this may suggest that individuals who more closely relate interoception with their sense of self perceive these cues more readily. Further, the correspondence of the same region as identified with the right and left insula seed may relate to the specific subscale that we used. Though there are other scales that better differentiate sympathetic versus parasympathetic nervous system functioning, the "Awareness" subscale we used is the most general subscale of everyday awareness across both

types of sensations (Porges, 1993). Thus, this lateral occipital region may be an interesting area related to generalized awareness of bodily sensations and less specific to context or threat response.

On the other hand, the areas related to reduced body awareness were in key interoceptive network regions, including the mid/anterior insula and anterior cingulate. Several of these findings were in white matter regions as well, which is interesting to consider relative to recent findings that support the role of glial cells for efficient interoceptive processing (Fabbri et al., 2023). The negative relationship between body awareness and connectivity in these areas is surprising, however, since one might hypothesize increasing connectivity within the insular network to relate to increased awareness. Previously, enhanced within-interoceptive network connectivity was found to relate to individuals' attunement with their stress responses, measured by the concordance between galvanic skin response and reported stress levels (Kleckner et al., 2017). Notable for interpreting these findings, however, is that the BPQ "Awareness" subscale does not clearly map onto the extent to which this awareness is adaptive. Specifically, the BPQ Awareness subscale reflects reported frequency and strength of a broad number of interoceptive sensations, without a focus on the interpretation that individuals are assigning to these sensations. Therefore, these findings might highlight the distinction between efficiency of interoceptive processing and awareness. In everyday situations, individuals with strong within-interoceptive network connectivity may meet their needs readily, bringing fewer of these signals to enough awareness to remember and report. However, individuals who relate these signals to a broader sense of self (e.g., via parietal cortex connections) may report greater general awareness of these signals.

Revisiting autistic group patterns with the dimensional relationship between body processing and neural connectivity in mind, one reason for limited group differences might be the broad range of scores seen in the autistic compared to non-autistic group. Autistic participants showed extreme scores at both ends of the scale, including enhanced and re-

duced awareness. Thus, it may be likely that autistic individuals group towards both ends of these neural processing profiles, rather than showing a uniform profile of differences from neurotypical processing. Further, the consideration of adaptive interoceptive processing relative to different body awareness levels may be ripe for future studies to explore as well. For example, Paulus and Stein (2006) and Ainley et al. (2016) suggest increased awareness of bodily sensations in anxious individuals because of less flexibly tuned expectations for these signals. Whereas, interoceptive awareness as developed from mindfulness interventions may have more beneficial purposes (Walsh et al., 2019). Thus, these findings represent a start in understanding how neural communication with interoceptive regions leads to bodily awareness, but further work is needed to understand when these differences reach clinical significance.

3.4.4 Limitations

Though our overall sample allowed us to look at broader trends in posterior insula connectivity by age as compared to prior work (Ebisch et al., 2011; Francis et al., 2019), we were underpowered in this sample to understand differential trends in autistic versus non-autistic development. Ideally, even larger samples may be able to better address the differences rather than cross-diagnostic trends.

Another limitation is that it is unclear whether our sample reflects how interoceptive processing diverges in individuals with the greatest challenges in interpreting and responding to their bodily needs, since the BPQ does not clearly map onto this construct. There have been recent efforts to create measures that delineate the different aspects of interoceptive experiences, including more clearly defined problems and challenges (Fiene et al., 2018). Future work may therefore aim to relate these neural pathways to indices of adaptive versus maladaptive interoceptive processing.

Lastly, autistic heterogeneity may have masked some potential findings due to large individual variability. Notably, the range of the autistic group's BPQ scores was much

wider than the non-autistic group. Thus, subgrouping might be a useful approach to better understand the link between interoceptive brain systems and interoceptive experiences for autistic individuals whose self-reports are either much higher or lower than non-autistic individuals.

3.4.5 Conclusion

These findings extend the existing literature of how posterior insula connectivity changes over development. In general, our findings support theories for how our expectations for these signals better tuned and increasingly multimodal over the course of development. The connections that were best maintained with age also seemed to be those that were most related to increased bodily awareness. However, within-interoceptive network connections, especially with subcortical sensorimotor regions, were shown to be decreased with both age and body awareness. This especially highlights that adaptive interoceptive processing may indeed involve effective tuning out of certain interoceptive sensations. Identified differences between the autistic and non-autistic groups were minimal, but those that were found were both localized to left posterior insula rather than right and may specifically relate to sense of time. Thus, our findings suggest that distinctions between parasympathetic and sympathetic processing may be especially relevant to consider when understanding interoceptive processing development in autism.

CHAPTER 4

Perceiving the self in context

4.1 Introduction

Though many of our biological signals (heartbeats, breathing, autonomic changes) are processed implicitly, the ability to perceive and respond to unexpected changes in these signals is crucial for well-being (Craig, 2002; Kleckner et al., 2017; Quadt et al., 2018; Tsakiris and Critchley, 2016). However, it has been far from straightforward to measure adaptive functioning in this system. Descriptive theories point towards interoceptive concerns broadly in physical and mental health conditions, such as anxious individuals showing increased sensitivity towards bodily changes (Domschke et al., 2010; Paulus and Stein, 2006) and depressed individuals experiencing reduced capacity to address their bodily needs (Barrett et al., 2016). Autistic individuals report a variety of interoceptive concerns, providing statements such as "The best way I can describe this to health professionals is that I receive a signal from somewhere I'm not exactly sure, and I have difficulties interpreting what they might mean" or "I'm super sensitive to little changes in how my body feels" (Trevisan et al., 2021b). Though these descriptions are illustrative, their correspondence to specific aspects of interoceptive system functioning remains elusive. Without a clear index of how, exactly, interoceptive information is being processed differently in individuals who experience interoceptive concerns, supporting these individuals involves substantial guesswork.

Ideally, we might hope to have objective interoceptive tests that map the relationship between stimulus levels and perceptual responses, akin to eye exams or hearing tests, that may be used in clinical practice. These types of tasks can be extremely useful in linking specific nervous system features and behavioral concerns, while being quick and easy to administer. However, there is a major roadblock towards developing these tests compared to other sensory systems: the practical and ethical concerns of manipulating stimulus levels

for stimuli occurring within the body, compared to how we may systematically alter stimuli like lights or tones that occur outside of the body. Researchers have worked on developing indices of interoceptive processing within this limited experimental control (Brener and Ring, 2016). Unfortunately, the interoceptive indices that have been studied thus far have yet to clearly differentiate individuals who do versus do not experience interoceptive concerns (Adams et al., 2022a; Williams et al., 2022; DuBois et al., 2016).

Most interoceptive indices have been developed for heartbeat perception, using scores from one of two paradigms: i) heartbeat counting (Dale and Anderson, 1978; Schandry, 1981)and ii) two-alternative forced choice (2AFC) heartbeat discrimination (Whitehead et al., 1977). In heartbeat counting paradigms, individuals are instructed to count the number of beats they perceive between starting and stopping the trial, and this number is compared to the recorded beats using electrocardiogram (EKG) or pulse oximetry. In 2AFC heartbeat discrimination tasks, individuals are presented with a series of sensory stimuli in another modality (vision or hearing), using one condition synchronous to their heartbeats and one condition asynchronous from their own beats. They are then asked to determine which is which (Whitehead et al., 1977). Though conceptually simple, these tasks have proven difficult for participants to complete. In heartbeat discrimination tasks, many participants perform at chance, limiting the ability to address individual or group differences (Brener and Ring, 2016). In heartbeat counting tasks, this results in many non-interoceptive factors explaining variation in task performance, including working memory, processing speed, knowledge about expected heart rates, and task instructions (e.g., whether one is instructed to report beats they think they might have perceived or are certain they perceived; Desmedt et al., 2018). Further, these tasks do not show particularly high correspondence with each other, with only 4.4% shared variance (Hickman et al., 2020). Thus, the utility of these tasks as a measure of adaptive interoceptive processing has been deeply questioned.

Further, our understanding of interoceptive perception in autism thus far has primarily been built on these heartbeat counting and 2AFC heartbeat discrimination tasks, which

have so far led to a deficit model of interoceptive accuracy in autism (Garfinkel et al., 2016; Palser et al., 2018). Meta-analyzed findings do suggest a true effect of reduced heartbeat counting in autism, though equivalent heartbeat discrimination (Williams et al., 2022). However, there are other known findings that might explain autistic differences in heartbeat counting as not specific to interoception. A greater tendency towards underestimated heartbeats in autism may be readily explained by other well-replicated findings: i) higher average heart rates in autism (Bal et al., 2010; Hollocks et al., 2014; Ming et al., 2005; Watson et al., 2012), ii) slower processing speeds (Zapparrata et al., 2022) and differences in working memory (Wang et al., 2017), and iii) a general tendency towards more cautious perceptual decision-making (Quinde-Zlibut et al., 2020). As the general utility of these tasks has been questioned, so has a strong need to extend our understanding of interoceptive perception in autism beyond these two tasks.

Researchers have therefore re-evaluated the conscious detection of interoceptive signals in terms of their ecological relevance to the individual (Ainley et al., 2016; Allen et al., 2022; Barrett et al., 2016; Trevisan et al., 2021a). Stimuli such as heartbeats and respiration are typically regular and predictable; if they remain within homeostatic ranges, it may be more adaptive to tune these signals out, conserving neural energy (Ainley et al., 2016; Barrett and Simmons, 2015). Thus, focus has begun to shift from measuring detection of interoceptive stimuli towards developing measures that reflect the models one uses to filter and respond to these signals, i.e. interoceptive prediction and tuning. From a mathematical standpoint, this is well-described by Bayesian models (Ainley et al., 2016; Barrett and Simmons, 2015; Huang and Rao, 2011). Bayesian modeling provides a way to estimate sensory expectations based on prior experience (priors) and the updated response to incoming signals, particularly when these diverge from expectations (posteriors). However, estimating prior and posterior distributions necessitates comparison of least two experimental conditions: baseline and altered. Thus, putting this in practice requires facing the challenges of manipulating signals that occur within the participant. Approaches

include medical interventions or targeted manipulations, such as instructing individuals to hold their breath. Khalsa et al. (2009, 2016) and Smith et al. (2020) have started these studies, providing tangible evidence that comparing experimental conditions reveals interoceptive tuning differences in anxiety and depression that were not apparent when using a single experimental condition. However, their difficult and/or invasive nature warrants caution in adapting these for participants with developmental differences or physical health concerns.

A less invasive alternative may be to study the perception of interoceptive signals relative to environmental cues that contextualize their interpretation, such as perceiving and interpreting a heart rate change in a gym versus home environment. Focusing on this contextualization lends several additional benefits. It may be understood as a type of multisensory integration, from which there is a rich literature to draw upon (Calvert et al., 2004; Murray and Wallace, 2012), and these types of paradigms have been especially informative about autistic sensory processing (Baum et al., 2015; Feldman et al., 2018). Multiple facets of integration may be measured by multisensory tasks, as integration occurs across time, spatial location, and signal strength (Rohe and Noppeney, 2016). These properties make up the three major principles of multisensory integration, such that two stimuli are especially likely to be integrated if they occur close together in time (temporal principle) and/or space (spatial principle). The last principle, termed inverse effectiveness, describes how integration is particularly used to boost the comprehension of weaker stimuli, whereas may be less necessary when signals are strong enough to be readily perceived on their own. One's exact parameters for integration are learned over time from one's environment (Stein and Rowland, 2011; Wallace and Stein, 1997). For example, individuals might learn in early language development how closely speakers' voices tend to align with their mouth movements and perceive language accordingly.

Revisiting the interoceptive literature within a multisensory framework reveals further potential for task design. Though 2AFC heartbeat discrimination has been predominantly

considered an interoceptive task, extensions of this task that include a greater number of conditions may serve to reduce the confounds in this task design and align it with common multisensory temporal integration measures. Typically, the stimuli in the synchronous condition are presented 200 milliseconds (ms) after each beat to account for the delay inherent in transducing the signal and propagating it from baroreceptors in cardiac and/or vascular tissue to primary interoceptive cortex. The stimuli in the asynchronous condition are presented 500 ms after each beat, well after this process has occurred. Inherent in the 2AFC design is an assumption that 200 ms is universally the ideal offset for perceived synchrony, which disregards individual variability, including variability in signal strength and the distance of these receptors from the brain (Brener and Kluvitse, 1988; Ring and Brener, 1992). For individuals who may maximally perceive their heartbeats sooner or later than the 200ms condition, a psychometric curve which incorporates multiple offsets can better distinguish interoception from chance performance (Schneider et al., 1998). This approach is known in psychophysics as the method of constant stimuli. Brener and Ring (2016) have noted the advantage of the method of constant stimuli to precisely locate the temporal sensation of the heartbeat relative to a visual stimulus and review strong evidence for validity of this task in neurotypical participants. Using this multi-interval task version in autistic compared to non-autistic participants allows examination of multiple cardioception features beyond accuracy, as we may examine differences in location of peak heartbeat sensation and/or in precision of cardiovisual integration.

Further, several additional paradigms have recently been developed to measure the types of complex integration that individuals may use in their daily lives. Legrand et al. (2022) have developed a measure of heart rate discrimination from an external stimulus, based on the idea that heart rate may be a more robust index of health than beat-to-beat changes. Though beats are a necessary component of rates, this type of task involves hierarchical integration over longer time scales to track relative rates. Another type of task has been developed by Walsh et al. (2019) in a study of the sensory effects of mindfulness

interventions. This task assesses whether controlled breathing improved one's ability to detect subtler changes in visual stimuli, which they found occurred more prominently after the mindfulness training had been completed (Walsh et al., 2019). These tasks may provide a meaningful complement to those from multi-interval heartbeat discrimination.

Prior multisensory studies in other modalities provide a basis for the patterns by diagnostic group that we might expect to see in these tasks. Autistic individuals generally show wider temporal integration compared to non-autistic populations (Baum et al., 2015; Feldman et al., 2018). Noel et al. (2018) have provided initial evidence that this extends to cardiovisual integration, as they found that autistic individuals showed more diffuse binding between cardiac and visual stimuli than non-autistic individuals when analyzed retroactively (thus, the visual stimuli did not directly mirror participants' cardiac rhythms). Additionally, autistic individuals show less susceptibility to multisensory illusions than neurotypical peers, suggesting a greater tendency to segregate information between sensory sources (Baum et al., 2015; Feldman et al., 2018). Further, multisensory findings for auditory and visual stimuli suggest increasing autistic versus non-autistic group differences for stimuli of increasing complexity (such as speech versus tones; Feldman et al., 2018), which may be particularly interesting to examine in regards to heart beats versus heart rate. Lastly, the prior literature suggests that multisensory differences between autistic and non-autistic groups may lessen with age (Feldman et al., 2018). Therefore, in this study, we analyzed interoceptive-exteroceptive perceptual integration in autistic versus non-autistic individuals across varying ages and across tasks of varying complexity.

4.2 Methods

4.2.1 Participants

Our sample included n = 42 adult (25 non-autistic, 17 autistic) and n = 21 youth (10 non-autistic, 11 autistic) participants. Study procedures were approved by the Vanderbilt Institutional Review Board, under protocol #191677. All individuals or their primary care-

Table 4.1: Participant characteristics by diagnostic group

Group	Total (valid)	Gender (% male)	Age (% years)	Interoception (ISQ)	Anxiety (SCARED)	Heart rate (bpm)
Non-autistic	35 (19)	35%	25.6	37.2	0.39	74.7
Autistic	28 (14)	62%	23.2	58.9	0.76	81.7

Sample sizes are summarized per group of total participants (i.e., included in at least one task analysis) and participants with valid parameters on all three tasks (included in composite task analyses). Characteristics of the total sample per group are summarized as percent for categorical variables and mean for continuous variables. Since the number of items on the SCA(A)RED varies between children and adults, these scores have been rescaled by the total number of items.

givers gave informed consent for study participation; any individuals who were not primary medical decision makers (i.e., ineligible to consent) provided informed assent for participation. For either group, individuals between the ages of 8-60 were eligible to participate. Individuals were included in the autistic group if a prior or new autism diagnosis was confirmed using research-reliable administration of the Autism Diagnostic Observation Scale-2 (ADOS-2; Lord et al., 2012) and clinical judgment of a licensed clinical psychologist specializing in autism. Exclusion criteria for both groups included factors that could limit the completion and interpretation of perceptual tasks; specifically, uncorrected sensory impairments unrelated to autism (e.g., vision or hearing loss), atypical cardiac rhythms (e.g., arrhythmias or premature contractions), a full-scale intellectual quotient score (IQ) $<$70, or genetic, psychiatric, or neurologic conditions (other than ADHD, depression, or anxiety). Lastly, individuals were excluded from either group if an autism diagnosis was inconclusive per the study clinician (though, participants who were evaluated for autism but did not receive a diagnosis were eligible for the non-autistic group).

Participants were also excluded from subsets of analyses if their task parameters were not in interpretable ranges (see **Tasks** for a description of these criteria per task). This led to a total of n = 33 (19 non-autistic, 14 autistic) participants included in joint analyses of all three tasks.

Figure 4.1: Anxiety levels by age and diagnostic groups

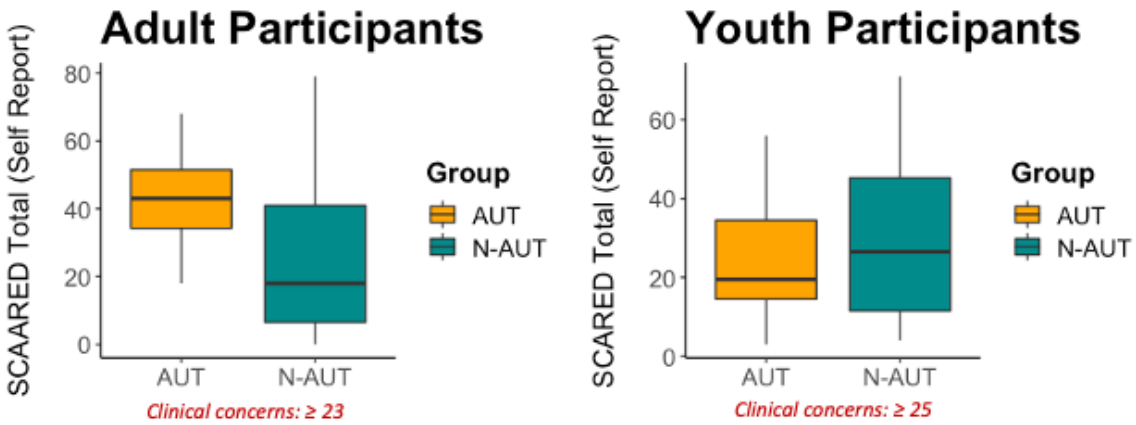

Total anxiety scores using the SCAARED self-report (adults, 18+) and SCARED self-report (youth, ages 8-17 years) are shown in box plots by diagnostic group. The autistic group is shown in orange and non-autistic group is shown in teal. In red, the scores above which anxiety levels are concerned a clinical concern are labeled for each age group.

4.2.2 Questionnaire measures

Participants completed self- and/or parent- report surveys to characterize their interoceptive processing experiences and anxiety levels. Interoceptive challenges were measured using the Interoception Sensory Questionnaire (ISQ; Fiene et al., 2018) a 20-item questionnaire that is interpreted as bodily state confusion related to interoceptive hypo- awareness. This measure was designed specifically for autistic populations. Anxiety was measured using three different scales. The Anxiety Scale for Children-ASD (ASC-ASD; Rodgers et al., 2016) and Anxiety Scale for Adults-ASD (ASA-ASD; Rodgers et al., 2020) were used to measure aspects of anxiety that may be specific to autism, as these have been specifically developed and validated for use in autistic individuals. The SCA(A)RED Child (Birmaher et al., 1997) and Adult (Angulo et al., 2017)) were used to measure typical presentations of anxiety, as these questionnaires are derived closely from Diagnostic and Statistical Manual (DSM; American Psychiatric Association, 2013) criteria for anxiety disorders. The State-Trait Anxiety Inventory (STAI; Spielberger, 1983) was also used to measure state anxiety levels at the time of the study visit. Since the number of items on the ASC/A-ASD and

SCA(A)RED vary between children and adults, these scores have been rescaled by the total number of items.

4.2.3 Tasks

Participants completed three perceptual tasks to characterize different aspects of interoceptive-exteroceptive integration.

Method of constant stimuli (MCS) heartbeat discrimination task. The goal of this task is to determine how precisely individuals perceive visual cues relative to their heartbeats. This task was adapted from Yates et al. (1985). In this task, a trial consists of a series of 6 flashes presented in the center of a screen at one of 7 intervals of offset (0, 100, 200, 300, 400, 500, 600 milliseconds (ms)) from the R wave, as measured by electrocardiogram (EKG). On each trial, participants are asked to judge whether the stimuli occur at the same time (synchronous) or different time (asynchronous) as their heartbeat. The adult version of the task includes 25 presentations per offset condition. A shortened version for children includes 15 presentations per offset condition.

We analyzed this task by fitting a Gaussian curve to the proportion of synchronous ratings per offset condition, resulting in three parameters: temporal location of heartbeat sensation (the peak of the curve, i.e. which offset was perceived as most synchronous), perceptual strength (the proportion of trials in which participants reported synchrony at this peak offset), and temporal binding window (TBW, defined here as the width of the full curve at 50% of its peak). The TBW indicates the variation in offsets over which participants still tended to rate these stimuli as generally occurring at the same time. Though the first two parameters (location and perceptual strength) help characterize different aspects of perception, we focused on binding window width as our measure of interoceptive-exteroceptive integration.

Participants with valid curve parameters were defined as having location of heartbeat sensation >0 ms, perceptual strength <1.1 (i.e., reporting near 100% of trials as syn-

Figure 4.2: Design of method of constant stimuli (MCS) heartbeat discrimination task

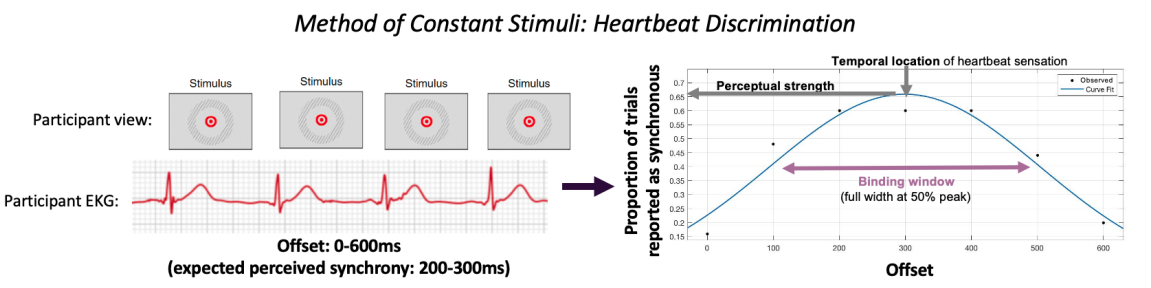

The experimental design (left) and analytic parameters (right) of the method of constant stimuli (MCS) heartbeat discrimination task are shown. In this task, participants judge the simultaneity between their heartbeats and visual stimuli of varying offsets. The three resulting parameters from this task are: temporal location of heartbeat sensation (which offset from the heartbeat was perceived as most synchronous), perceptual strength (the proportion of trials in which participants reported synchrony at this peak offset), and temporal binding window (TBW, defined here as the width of the full curve at 50% of its peak).

chronous at their peak offset) and binding window width <1000 ms. Parameter values outside these ranges reflected poor curve fits that were extrapolated far beyond the experimental offsets (e.g., erroneously suggesting that synchronous perception occurred anywhere from seconds to minutes after one's R wave). Participants with invalid MCS parameters (n = 9 autistic and n = 14 non-autistic) were excluded from further MCS task analyses, though participant characteristics (group, age, gender, interoception/anxiety, heart rate, blood pressure, and number of trials) were compared between participants with and without valid task parameters. This left n = 40 (n = 20 autistic and n = 20 non-autistic) participants analyzed for the MCS task.

Heart rate discrimination task (HRD). This task was developed by Legrand et al. (2022). The goal of this task is to determine the precision with which individuals can identify their heart rate, relative to the rate of auditory tones. In this task, a trial consists of first, a 5 second window in which participants are asked to pay attention to their heart. In the next phase, the participant hears a series of tones and are asked whether these are faster or slower than their heart rate. A staircase procedure is completed, starting with bigger rate differences, and then providing smaller differences until the smallest difference the

Figure 4.3: Design of heart rate discrimination task

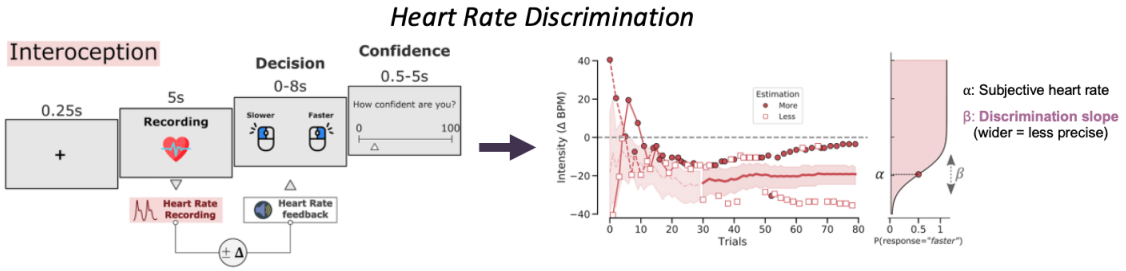

The experimental design (left) and analytic parameters (right) of Legrand et al.'s (2022) heart rate discrimination task are shown. In this task, a staircase procedure is completed to determine the precision (larger slopes (β) = less precise) with which participants can discriminate their heart rate from a series of auditory tones. Components of this figure have been reproduced with permission from Legrand et al. (2022).

participant can reliably detect between their heart rate and tones is determined. An additional, exteroceptive condition of this experiment is included for comparison. This task is designed equivalently to the interoceptive version, but instead of an initial heart rate phase, participants are presented with two series of auditory tones and asked to discern whether the second series are slower or faster than the first.

The parameters resulting from this task include a subjective heart rate estimate (i.e., the rate at which participants are equally likely to say the tones were faster or slower than their heart rate) and the slope of heart rate estimation, indicating the degree to which participants' discriminative judgments change in response to each increment in tone rate. Larger values correspond to decreased precision, since these indicate that a greater difference in presented tone rate is required for the participants to perceive a change. There were no participants with outlying or uninterpretable parameters on this task; however, a total of n = 7 autistic and n = 2 non-autistic participants were excluded due to task incompletion, leaving a total of n = 54 participants in our analyzed sample. Task incompletion was due to auditory sensitivities, issues with task pacing, and/or general time constraints.

Respiration integration task (RIT). This task was developed by Walsh et al. (2019). The purpose of this task is to measure the specific ability to integrate interoceptive information

and map it to visual information, controlling for visual ability alone. In this task, a circle is presented at the center a screen; the circle expands and contracts rhythmically. On each trial, participants view 2 cycles of expansion and contraction, the reference and the target. The reference circle always expands and contracts at a constant rate, and the rate of the target is varied. After each pair of stimuli, participants indicate whether the target is faster or slower than the reference. A staircase procedure is used to titrate the difficulty and converge on a threshold (just noticeable difference (JND), the smallest difference in speed that participants can reliably discern). The task is completed in 3 phases. First, participants use vision alone to perform the task. Once this threshold is established, participants spend 60 seconds practicing matching their breathing to the movement of the circle as it pulses at the reference frequency. Afterwards, in the integration period, participants repeat the task while matching their breathing to the expansion and contraction of the sphere.

A respiratory integration score is calculated by using a linear model to predict breath condition thresholds from visual alone thresholds; thus, adjusting empirically for factors such as practice effects. The residuals of this model are then considered the respiratory integration score. Negative residual values indicate that an individual was better (i.e., discerned smaller differences in speed) in the breath condition than predicted from their visual score, reflecting increased integration. Positive residual values indicate that an individual was worse in the breath condition than predicted from their visual score, indicated decreased integration. In some cases, the staircase does not converge or converges on extreme values, often in cases of participant inattention. Parameters on this task were considered invalid if scores on either condition were extreme outliers (i.e., more than 4 standard deviations above the average). A total of n = 2 non-autistic and n = 2 autistic participants were excluded from RIT task analysis due to an outlying score or task incompletion, leaving n = 59 participants analyzed.

Figure 4.4: Design of respiration integration task

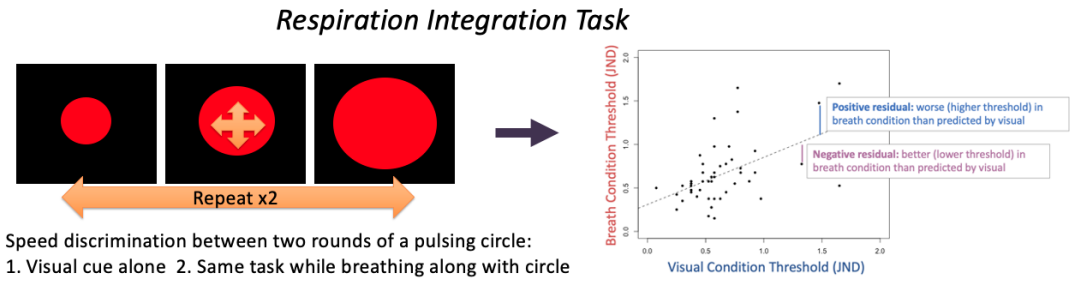

The experimental design (left) and analytic parameters (right) of Walsh et al.'s (2019) respiration integration task are shown. In this task, participants complete two rounds of a visual speed discrimination task, with and without matched breathing. This task results in a respiratory integration score reflecting the degree to which participants improved their visual speed judgments (lower scores) when using matched breathing.

4.3 Single task analysis

To examine how perceptual patterns on each of these tasks relate to individual characteristics, we analyzed a linear regression model with terms of group, age, and gender for each of our three outcome parameters (MCS: binding window width, HRD: interoception slope, RIT: threshold change in breath condition). For the two cardiac tasks, we also covaried for perceptual patterns by heart rate, as collected before task performance. To further describe the evidence for each of these terms, we calculated inclusion Bayes factors ($BF_{inclusion}$) for each of these terms as compared to the full model. These values are interpreted as a ratio of the evidence for including (numerator) or excluding (denominator) the given term based on the strength of its contributions to the model, with values > 1 favoring including the term and values < 1 favoring excluding the term.

4.4 Combined task analysis

We further aimed to combine the information gained from each of these measures into a composite score reflecting generalized interoceptive-exteroceptive integration. To do this, we completed a principal components decomposition on our three parameters of interest: i) MCS: binding window width, ii) HRD: heart rate discrimination precision, and iii) RIT: respiratory integration score. Individuals' scores on the components from this decomposition

were compared between diagnostic groups and with self-reported interoceptive challenges.

Correlations between interoceptive confusion as reported by the ISQ and our two trait measures of total anxiety (ASC/A-ASD total and SCA(A)RED total) were assessed to determine whether these should be analyzed as distinctive versus overlapping constructs. Since these correlations were quite high (ISQ and ASC/A-ASD: r = 0.68 and ISQ and SCA(A)RED: r = 0.70), we focus on presenting the results between task parameters and the ISQ, as these reflect a proximal report of interoceptive behavioral experiences.

4.5 Results

4.5.1 Single task results

Method of constant stimuli task. Of the 63 total study participants, 40 (63%) had MCS parameters within interpretable, valid ranges. This number is slightly above findings reviewed in Brener and Ring (2016) of around 50% of the population perceiving their heartbeat above chance, with the highest numbers coming from similar multi-interval tasks. No participant demographic characteristics (age, gender, diagnostic group) differed between participants with valid versus invalid task parameters. Individuals with stronger cardiac signals (i.e., faster heart rate and higher blood pressure) were more likely to have valid task parameters; these three effects were each statistically significant (See Table 2). Additionally, though not significant, state anxiety (STAI) ratings were somewhat higher in participants with valid parameters. Surprisingly, individual who reported greater interoceptive challenges were more likely to have valid task parameters, though this effect was not significant either.

Among the participants with valid parameters, model results showed that no terms significantly corresponded with cardiovisual binding window width. The term with the strongest evidence was increased heart rate with narrower widths ($BF_{inclusion}$ = 1.04). Contrary to our hypotheses, the term for group showed narrower widths in autistic participants than in non-autistic participants (Figure 5A), though with substantial variability such that

Table 4.2: Method of constant stimuli parameter validity by participant characteristics

	Number (AUT, N-AUT)	Gender (% male)	Age (years)	ISQ	STAI	Blood pressure (Sys./Dias.)	Heart rate (bpm)
Invalid	9, 14	52%	25.2	42.2	28.6	109.2 / 64.9	72.6
Valid	20, 20	45%	24.2	48.0	32.6	118.8 / 73.4	80.7
p	0.41	0.59	0.77	0.45	0.08	0.04*/0.007*	0.005*

Characteristics of participants categorized as having valid versus invalid MCS parameters. These are summarized as percent for categorical variables (gender) and mean for continuous variables (age, interoceptive hypo-awareness as measured by the ISQ, state anxiety as measured by the STAI). Characteristics that significantly differed between those with valid and invalid parameters are marked with an asterisk.

Table 4.3: Method of constant stimuli binding window width by participant characteristics

	Estimate	Std. Error	t	p	$BF_{inclusion}$
(Intercept)	860.64				
AUT >N-AUT	-7.77	54.05	-0.14	0.89	0.47
Age	-0.67	1.92	-0.35	0.73	0.45
Heart rate	-3.98	2.60	-1.53	0.14	1.04
Male >Other	-33.16	57.70	-0.58	0.57	0.47

Regression table for the model of heartbeat discrimination by group, age, heart rate, and gender. Columns include unstandardized slope estimate (ms), standard error, t, p and Bayes inclusion factor. No terms showed significant correspondence with cardiovisual binding width at $p < 0.05$..

the evidence for this effect was weak ($BF_{inclusion} = 0.47$). The term for gender was a similar size as diagnostic group, showing narrower widths for males than female or non-binary participants ($BF_{inclusion} = 0.47$). There was the least evidence to support any relationship between binding window width and age ($BF_{inclusion} = 0.45$).

Though binding window width varied independently from the other two parameters (temporal location of heartbeat sensation: r = 0.15 and perceptual strength: r = -0.34), there was one significant relationship between these two parameters with participant features. Specifically, individuals with higher heart rates had a moderate tendency to perceive synchrony sooner (r = -0.55, Figure 5B).

Figure 4.5: Method of constant stimuli heartbeat discrimination parameters

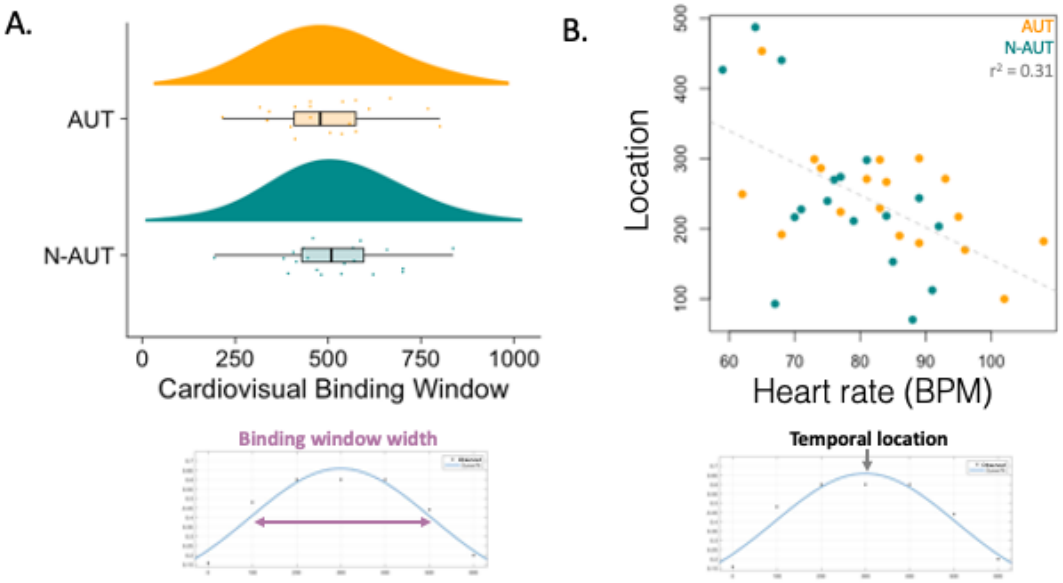

In panel A, raincloud plots of cardiovisual binding window width (ms) by are shown by group. In panel B, a scatter plot of the temporal location of peak heartbeat sensation (ms) by heart rate (bpm) is shown. For both plots, group is color coded as autistic (AUT) = orange; non-autistic (N-AUT) = teal.

Heart rate discrimination task. For the n = 54 participants who completed this task, model results showed that age was a strongly significant predictor of heart rate estimation slope, such that older individuals showed greater precision (t = -4.99, $p < 0.001$, $BF_{inclusion}$ = 1690, Figure 6B). Heart rate secondarily predicted slope estimates, with individuals showing increased precision with increased heart rate (t = -2.02, p = 0.049, $BF_{inclusion}$ = 1.05). There was not evidence suggesting group differences, though the estimates were towards decreased precision in the autistic compared to non-autistic group (t = 1.07, p = 0.29, $BF_{inclusion}$ = 0.35, Figure 6A). There was the least evidence to support any differences in heart rate discrimination by gender ($BF_{inclusion}$ = 0.28).

Heart rate discrimination slope estimates only weakly correlated with slope estimates from the tone rate discrimination task (r = 0.30); thus, findings were equivalent with and without adjusting for tone rate slope.

Respiration integration task. Of the n = 59 participants analyzed, groups did not sig-

Table 4.4: Heart rate discrimination slope by participant characteristics

	Estimate	Std. Error	t	p	$BF_{inclusion}$
(Intercept)	27.83				
AUT >N-AUT	1.47	1.37	1.07	0.29	0.35
Age	-0.24	0.05	-4.99	0.00*	1690
Heart rate	-0.12	0.06	-2.02	0.049*	1.05
Male >Other	-0.70	1.27	-0.55	0.59	0.28

Regression table for the model of heart rate discrimination by group, age, heart rate, and gender. Columns include unstandardized slope estimate (bpm), standard error, t, p and Bayes inclusion factor. Age and heart rate both showed significant associations with heart rate discrimination scores at p <0.05.

Figure 4.6: Heart rate discrimination by group and age

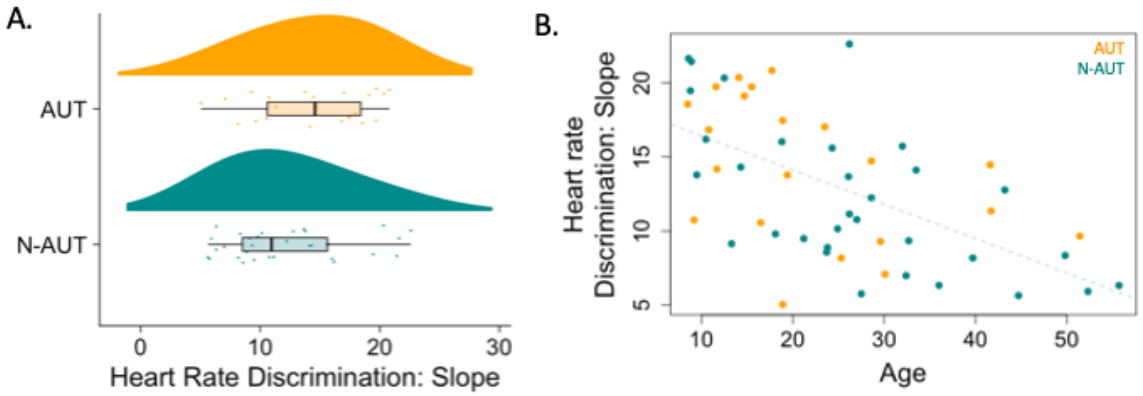

In panel A, raincloud plots of heart rate discrimination slope (β, larger = less precise) are shown by group. In panel B, a scatter plot of heart rate discrimination by age (years) is shown. For both plots, group is color coded as autistic (AUT) = orange; non-autistic (N-AUT) = teal.

Table 4.5: Respiration integration score by participant characteristics

	Estimate	Std. Error	t	p	$BF_{inclusion}$
(Intercept)	0.21				
AUT >N-AUT	-0.21	0.08	-2.68	0.0097*	3.37
Age	-0.01	0.00	-2.31	0.025*	2.62
Male >Other	0.10	0.08	1.32	0.193	0.63

Regression table for the model of respiration integration score (breath condition: threshold change) by group, age, and gender. Columns include unstandardized slope estimate (change in threshold), standard error, t, p and Bayes inclusion factor. Age and group showed significant associations with respiration integration scores at $p < 0.05$.

nificantly differ for initial visual discrimination scores, though there was a trend towards less precise initial scores in the autistic group (mAUT = 0.74, mN-AUT = 0.61, p = 0.15). Model results showed that the two groups significantly differed in respiration integration as indexed by improvement in the breath condition (t = -2.68, p = 0.0097, $BF_{inclusion}$ = 3.37, Figure 7A). The autistic group showed greater integrative tendencies than the non-autistic group, i.e., a lower JND in the breath condition than predicted from the visual. Older individuals also showed greater integrative tendencies (t = -2.31, p = 0.025, $BF_{inclusion}$ = 2.62, Figure 7B). Gender did not significantly correspond with integrative tendencies ($BF_{inclusion}$ = 0.63).

4.5.2 Patterns between tasks

Heartbeat discrimination and heart rate discrimination showed a positive correlation (r^2 = 0.13), though neither task substantially correlated with respiration integration (r^2 = 0.005 for MCS and r^2 = 0.07 for HRD, see Figure 8).

The principal components derived from these three measures reflected these relationships accordingly, as about half of individual variation (49%) was explained by a first component loading strongly with all three tasks (method of constant stimuli: -0.57; heart rate discrimination: -0.68; and respiration integration task: -0.46). Further, distinctive variation

Figure 4.7: Respiratory integration scores by group and age

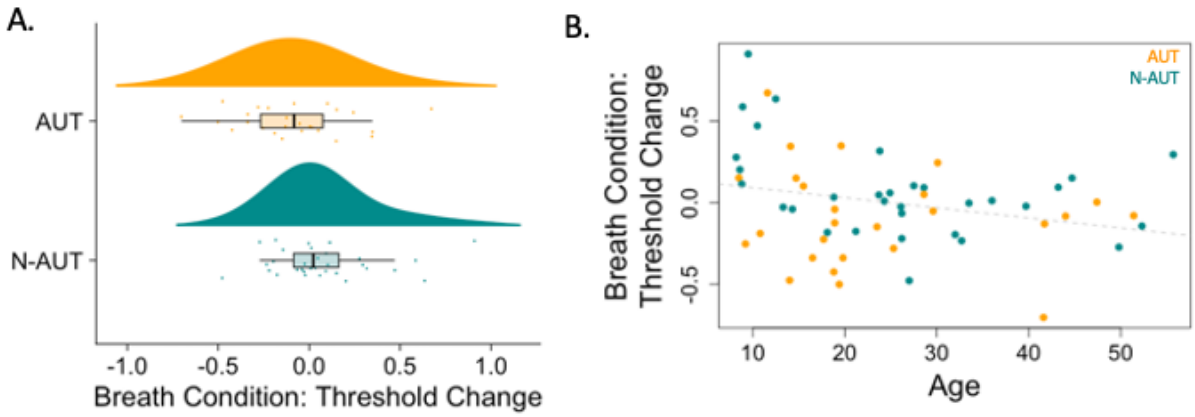

In panel A, raincloud plots of respiratory integration scores (i.e., the change in thresholds between breath and visual only conditions, lower = better in matched breathing condition) are shown by group. In panel B, a scatter plot of respiratory integration scores by age (years) is shown. For both plots, group is color coded as autistic (AUT) = orange; non-autistic (N-AUT) = teal.

in the respiration integration task was primarily reflected in the second component (respiration loading -0.81), which explained 31% of individual variation. A last component reflected idiosyncratic integration with the heart rate integration task, such that individuals showed a similar pattern between heartbeat (loading: -0.57) and respiration (loading: -0.38) integration but opposing pattern with heart rate discrimination (loading: 0.73).

4.5.3 Relationships with interoceptive confusion

No single task parameter significantly correlated with interoceptive confusion as measured by ISQ scores (MCS width: r = 0.01, HRD slope: r = 0.16, RIT integration score: r = 0.14). Using the principal components decomposition scores, however, a group-specific relationship between combined task parameters and interoceptive confusion emerges. In a model testing the association between group, generalized integration scores (principal component 1, PC1), and their interaction term, the interaction term was the main significant predictor (t = -2.66, p = 0.01, $BF_{inclusion}$ = 2.84). The term of group and the generalized integration score alone did not show significant relationships with interoceptive difficulties,

Table 4.6: Principal component decomposition of interoceptive-exteroceptive measures

Task: index	Component 1: Combined	Component 2: Diverging RIT	Component 3: Diverging HRD
MCS: width	-0.57	0.59	-0.57
HRD: slope	-0.68	0.05	0.73
RIT: breath threshold change	-0.46	-0.81	-0.38
% variance	49%	31%	19%

Rows 1-3 show the loading scores of each interoceptive-exteroceptive index (heartbeat discrimination: width, heart rate discrimination: slope, and respiration integration: breath threshold change) with the three derived principal components. The absolute value of these loading scores reflects the strength to which the given parameter contributes to that component. Their directionality (positive or negative) reflects whether parameters are co-varying in the same or opposing directions from each other. Values occur on a -1 to 1 scale. The last row indicates the variance in participant data explained by each component.

Figure 4.8: Interoceptive-exteroceptive index correspondence

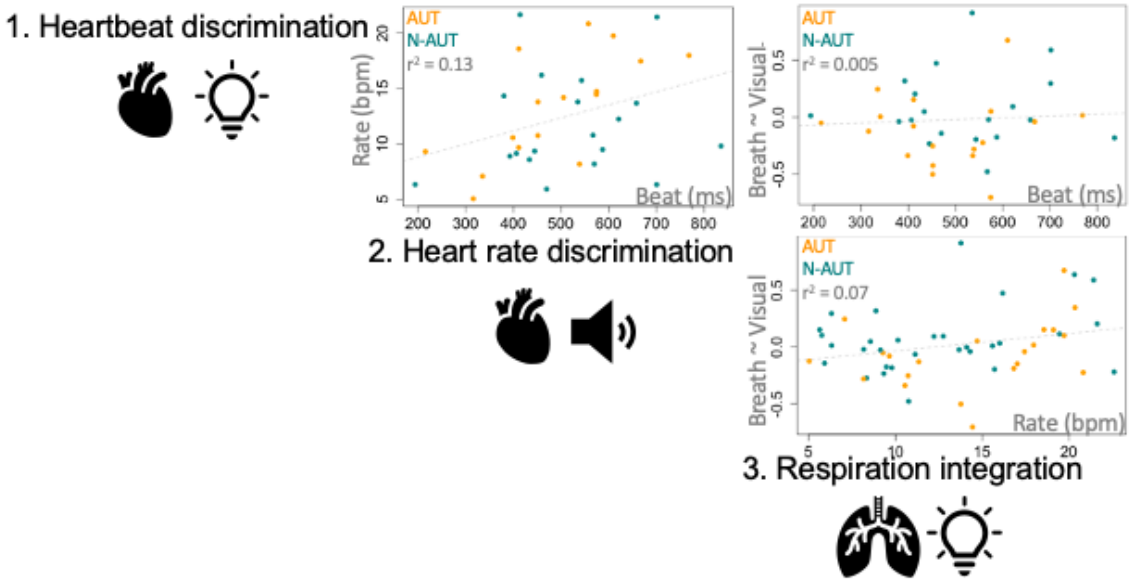

Correlation plots between method of constant stimuli: width (ms), heart rate discrimination: slope (bpm), and respiration integration: breath integration score (residual) interoceptive-exteroceptive indices. Autistic individuals are plotted in orange, non-autistic individuals are plotted in teal. Lines of best fit across all participants are plotted and corresponding r-squared values are summarized.

Table 4.7: Interoceptive hypo- awareness as predicted by principal component scores and group

	Estimate	Std. Error	t	p	$BF_{inclusion}$
Intercept	52.2				
AUT >N-AUT	13.6	8.8	1.55	0.11	1.51
General integration (PC1)	9.3	5.6	1.65	0.13	0.91
Group x PC1	-19.3	7.2	-2.66	0.01*	2.84

Regression table for the model of interoceptive hypo-awareness (ISQ; Fiene et al., 2018) with general interoceptive-exteroceptive integration scores (PC1, first principal component derived from heartbeat discrimination width, heart rate discrimination slope, and respiratory integration score measures) by group. The term of the interaction effect of group and interoceptive-exteroceptive integration scores was significant at p $<$0.05.

though there was evidence to support greater interoceptive confusion in the autistic than non-autistic group (AUT >N-AUT: $BF_{inclusion}$ = 1.51). Shown in Figure 9, these patterns were similar when analyzed in regard to anxiety levels as measured by the SCA(A)RED total.

4.6 Discussion

This study is the first to characterize interoceptive-exteroceptive integration across multiple psychophysical measures and further, to compare autistic and non-autistic populations. Our measures included both cardiac and respiratory integration, measured in both youth and adults. Our findings help build a taxonomy of interoceptive-exteroceptive integration compares among the different tasks and provide evidence for how development occurs along this taxonomy. Some, but not all, of these tasks differed by diagnostic group. Further, there are several implications for how heightened cardiac signaling and anxiety may specifically impact interoception in autistic compared to non-autistic populations.

4.6.1 Towards a taxonomy of interoceptive-exteroceptive integration

In accordance with emerging findings in interoception research (Crucianelli et al., 2022), we found that one's interoceptive-exteroceptive integration precision may not be a single

Figure 4.9: Interaction effects of combined interoceptive-exteroceptive scores, group, interoceptive confusion and anxiety

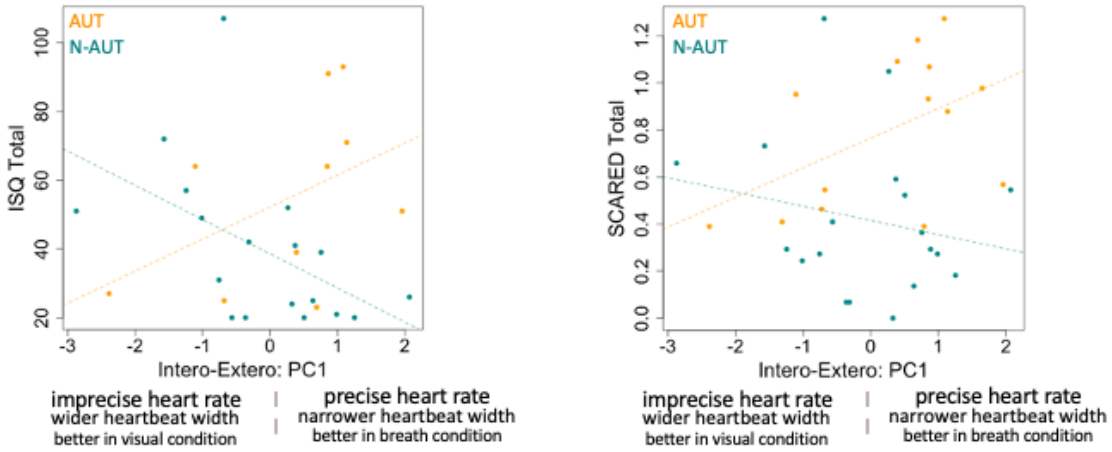

For both panels, the x-axis reflects individual scores on the first principal component of our three interoceptive-exteroceptive indices (Intero-Extero PC1), reflecting generalized integration. Positive scores = precise integration and negative scores = imprecise integration. The degree to which heart rate, heartbeat, and respiration indices is reflected in each component is scaled to the size of the axis text. On the left panel, the correspondence between principal component scores and interoceptive confusion as measured by the ISQ is shown. On the right panel, the correspondence between principal component scores and total anxiety as measured by the SCA(A)RED (re-scaled by number of items) is shown. Individuals and trend lines are coded by group, with orange = autistic and teal = non-autistic.

trait across all possible combinations of stimuli and task design. The two measures of overlapping stimuli (i.e., cardiac) and constructs (temporal integration, at beat versus rate levels) showed a moderate correlation within participants. Unfortunately, the method of constant stimuli task showed some similar limitations as prior heartbeat-focused task designs, as around a third of the participants had uninterpretable task parameters (Brener and Ring, 2016). Fortunately, however, the moderate shared variance (13%) between heartbeat and heart rate integration tasks provides information beyond these limitations. This estimate is thus far higher than the estimated concordance between 2AFC heartbeat discrimination and heartbeat counting tasks of 4.4% shared variance (Hickman et al., 2020), though has yet to be estimated in as large of a sample as those two prior tasks. This provides support initial support that an interoceptive tuning framework, describing one's integration parameters along a possible continuum, more cohesively describes varying task performance than an interoceptive accuracy-focused framework. Further, frameworks that only describe 2AFC and HBC tasks as interoceptive accuracy measures do not meaningfully explain the large diverging variance between the two, including the many confounds. On the other hand, the diverging variance in beat-based and rate-based integration may occur in ways that relate to their relational hierarchy, as beats are a necessary component of rates but one's focus may shift between these levels of resolution. One possibility is a developmental shift, such that some individuals who shift their focus to rate-based processing may do so at the expense of tracking beat-based patterns with external stimuli. Another possibility is that heart rate variability, which we did not derive in this study but is an important direction of future work, differentially influences the priors placed on heartbeats versus heart rates such that individuals may vary from each other in whether beats or rates are providing more stable information. Altogether, the heart rate discrimination task provides strong concurrent evidence about individuals who integrate their heartbeats in an interpretable manner and a promising path towards understanding those who cannot.

On the other hand, the respiratory integration task, measuring both a different intero-

ceptive stimulus and a different multisensory principle, showed minimal correlations with either of the two cardiac tasks. One difference with the prior two tasks is that, as the inverse effectiveness principle suggests, the ability for interoceptive input to improve visual speed discrimination is more prominent in those who are worse initially. Thus, this relationship with initial visual ability may represent one source of diverging variance between individuals. Also, unlike the other two tasks, this task requires visuo-visceromotor integration from the participant to match their breathing to the circles before being able to receive a boost from this added signal. Thus, the effectiveness of this breath control might be one area in which participants' abilities diverge from the passive cardiac perceptual conditions. This lastly also may relate to individuals' varied life experiences, since activities such as musical training may especially build rhythmic breath control skills.

Nevertheless, the principal component analysis findings suggest a meaningful extent to which all three of these tasks tap into a common construct, including respiration integration. Thus, it does appear that some participants have general trends in their interoceptive-exteroceptive integration across all tasks (e.g., all precise or all broad) whereas others show patterns that are specific to interoceptive modality or specific task demands. This might have meaningful implications for intervention work involving interoception. Previously, these types of cardiac (Quadt et al., 2021) and respiration (Walsh et al., 2019) tasks have been used in separate studies of interventions for anxiety. Based on our three-factor findings, it might be desirable to administer several of these tasks to get a balanced profile of someone's interoceptive-exteroceptive processing and tailor potential interventions to this profile.

4.6.2 Developmental progression of interoceptive-exteroceptive integration

There has not been a strong prior literature of how interoceptive task parameters vary by age. When meta-analyzed for heartbeat counting and discrimination, the evidence did not suggest that individuals improved by age (Williams et al., 2022). Mash et al. (2017) found

an interaction between age and IQ for heartbeat counting scores, such that the degree to which IQ confounds heartbeat counting may contribute to the patterns that do exist for age. Thus, this study builds upon the literature to show how multiple different types of interoceptive-exteroceptive indices change from childhood to adulthood.

Of our three paradigms, heart rate discrimination and respiration integration both significantly improved with age. This effect was especially striking for heart rate discrimination, with an inclusion Bayes Factor of 1690. Notably, both tasks seemed to improve with age equivalently across our groups, contrary to prior audiovisual findings (Feldman et al., 2018). However, MCS heartbeat discrimination varied independently of age. In terms of cardiac processing, this provides further support for a developmental progression between these levels, suggesting that at some point, processing of heart beats gets aggregated into a sense of rate. Individuals may then contextualize their internal functioning relative to this sense of rate, without further refinement of beat-based integration. Notably, the youngest age in our sample is eight years. Though there is necessarily some developmental period in which lower-level cardiac integration gets tuned, is likely that the critical period to tune heartbeat-based integration parameters occurs younger than this age. On the other hand, we found that rate-based integration is still being refined into adolescence and adulthood.

The other task in which improvements were shown by age was the respiration integration task. This is also a more complex task than heartbeat integration, including cyclical skills between using visual cues to guide breathing and then using those breathing cues to guide rate detection. Given this level of complexity, it makes sense that the ability to complete this complex cycle would continue to improve into adulthood. Like heart rate discrimination, there are examples of how this type of skill may be used in everyday circumstances in older individuals. Musical training is one example, but driving is an example in which visual speed discrimination may be critical for survival. It would be an interesting extension of this paradigm to study the extent to which individuals naturally tune their breathing in this type of critical sensory discernment paradigm. Thus, our findings suggest

that interoceptive-exteroceptive integration does not uniformly refine with age but refines in accordance with task complexity and ecological utility.

4.6.3 Interoceptive-exteroceptive integration in autism: The role of physiology

Reported interoceptive confusion was highly elevated in our autistic compared to non-autistic participants, which is consistent with prior qualitative reports (Trevisan et al., 2021b) and further suggests that interoception does differ somehow between autistic and non-autistic individuals. However, individual task findings don't suggest that the degree of interoceptive confusion in autism is best explained by group-level perceptual differences. Based on other multisensory integration findings in autism, we hypothesized that our autistic group would show broader integration patterns between interoceptive and exteroceptive stimuli. Further, we hypothesized that they would perform relatively better in unimodal than multimodal conditions. We did not find significant evidence that this is the case. Rather, our one significant group finding was in the opposite direction: better performance in multimodal visual-breath condition than in a unimodal visual condition. However, several aspects of our results provide evidence as to why interoceptive-exteroceptive integration in autism as measured via these three tasks may show different patterns than hypothesized based on other sensory modalities.

First, respiration integration findings were significant in the opposite direction of our hypotheses. One consideration is that the ability to improve in the breath condition depends on initial visual performance. Our results suggest that the autistic group does show somewhat less precise initial visual performance compared to the non-autistic group, which may contribute to some of these findings. Detailed visual processing has been supported as a perceptual strength in autism; however, processing of visual motion especially as an abstracted sense of speed, which must be held in working memory for the next trial, may be considerably more challenging for autistic individuals thus may especially benefit from an added stimulus (Robertson and Baron-Cohen, 2017). In Chapter 3, we found enhanced

links in autistic compared to non-autistic individuals between interoceptive cortex and visual areas that process time and motion, providing a neural mechanism via which this enhanced breathing effect may occur. The degree of voluntary control that one has over their breathing may also explain why this integration is especially helpful for autistic participants. Given an experience of increased sensory uncertainty of the external world (Pellicano and Burr, 2012), such percepts that are under conscious control may be especially grounding to autistic individuals.

Second, both of our cardiac task findings suggest that diagnostic group on its own is not a meaningful differentiator of perceptual reports, but instead that the divergence in average heart rate by group contributes to different experiences. Autistic individuals on average have higher resting heart rates than neurotypical individuals (Bal et al., 2010; Hollocks et al., 2014; Ming et al., 2005; Watson et al., 2012), which was replicated in our sample. Across our sample, higher heart rates corresponded with a strong tendency to perceive heartbeats more quickly and a moderate tendency to integrate both beats and rates more precisely. The tendency for individuals with higher heart rates to perceive beats sooner has previously been shown by Ring and Brener (1992), which they note is in line with general tendencies to perceive stronger stimuli sooner, though it has not been well accounted for in the modern interoceptive literature (Brener and Ring, 2016). Further, the potential for these heart rate effects to impact how we understand interoception in autistic individuals has not been widely discussed. Thus, our insignificant group differences may represent a trade-off between a general broader tendency in integrating multisensory stimuli versus the demands of tracking a relatively faster cardiac signal. Notably, elevated heart rates in autism are proposed to relate to a variety of features, including anxiety, psychotropic medication use, the degree of sensorimotor challenges, and physical activity levels, which may all interact (Hollocks et al., 2014; Thapa et al., 2021). Thus, future work may examine whether each of these factors mediate cardiac interoception in distinct ways and what the according impacts may be for autistic individuals.

4.6.4 Interoceptive confusion: Composite findings

When composite patterns across our three tasks were considered, self-reported interoceptive confusion did seem to relate to our generalized measure of interoceptive-exteroceptive integration. Further, this relationship significantly diverged in autistic versus non-autistic individuals. In non-autistic individuals, this relationship went in the expected direction: individuals who report being less aware of their interoceptive sensations (and more confused) showed broader patterns of interoceptive-exteroceptive integration. However, the direction of this relationship for autistic individuals is not initially intuitive, since we found that individuals who report the greatest interoceptive confusion show narrower integration between internal and external cues across all our paradigms.

The unexpected direction of this relationship in autism is reminiscent of findings from Simon and Corbett (2013) who found that autistic children's self-reported anxiety levels corresponded substantially less with their measured cortisol than for their non-autistic peers. This may represent the distinction between low-level sensory integration and high-level contextual interpretation of how interoceptive stimuli relate to bodily needs, which there is some evidence to suggest diverges in autism (Garfinkel et al., 2016; Palser et al., 2018). At a neural level, autistic individuals show altered structural connectivity in posterior-anterior insula tracts in autism, along which the transition from sensation to interpretation occurs (Failla et al., 2017). Though diverging perception and behavioral reports of interoception in autism were initially categorized as reduced meta-awareness (Garfinkel et al., 2016; Palser et al., 2018), our selection of tasks as aligned with a predictive coding framework more clearly delineate interoception as another example in which autistic individuals may be perceiving the "trees" at expense of the "forest" (Pellicano and Burr, 2012). Paulus and Stein (2006) provide an initial framework for how enhanced cardioception in anxious individuals may impede rather than aid effective interpretation of bodily needs. Our results suggest that this effect may be exaggerated in autistic individuals, particularly given combined influences of high heart rates, high anxiety, and a general tendency towards sen-

sory overload. Though respiration integration was the lowest contributor to the general component, there are a couple reasons why it may trend with the other two tasks towards increased anxiety in autism. One possibility is that individuals who show greater difficulty in the initial visual condition may have more rigid exteroceptive sensory priors, leading to intolerance of uncertainty and thus anxiety. Another possibility, since we have not controlled for intervention history, is that some of the most anxious autistic participants may have already completed mindfulness interventions. Thus, examining interoception-related intervention history is one meaningful future direction to further unpack these findings.

Importantly, the identified autism-specific relationships between interoceptive perception, reported interoceptive confusion, and anxiety do suggest that interoceptive interventions may be especially helpful for autistic individuals. However, the goal of these interventions may be slightly reframed from prior work (Quadt et al., 2021). Instead of the framework of correcting an interoceptive deficit, it may be especially helpful for autistic individuals to receive support in interpreting the bigger picture from their wealth of internal signals. Further, it may be especially calming to leverage signals they can control such as breathing, as in mindfulness settings (Walsh et al., 2019).

4.6.5 Limitations

Though the composite findings from these tasks have begun to predict interoceptive behavioral reports, the limitation remains that none of these tasks are a strong predictor of reported interoceptive confusion alone. Though we have made progress in analyzing patterns across the three measures combined, one major limitation with the combined sample size is poor heartbeat discrimination curve fits for two-fifths of our sample. We have explored alternative curve fitting options (see Appendex: Chapter 4 Supplement), but without evidence for improved parameter interpretability. However, principal component analysis findings do not necessarily support dropping this task entirely, since this contributed to an understanding of interoceptive confusion as reported by the ISQ. Thus, we continue to aim

for sufficient sample sizes to account for this degree of data loss.

As mentioned, for cardiac tasks, it is challenging to differentiate the effects of anxiety on performance from simply elevating cardiac signaling (faster heart rates) versus broader rewiring of interoceptive circuits. One promising direction of future research may be from longitudinal or test-retest designs that enable utilization of the Bayesian framework for truly analyzing these same tasks across different interoceptive contexts.

Another limitation is that we have not yet addressed potential contributions of IQ to task performance, which has been shown to be related to heartbeat counting scores (Desmedt et al., 2018). While we can make the case that none of these tasks have the same degree of working memory load as the heartbeat counting task, it will still be important to test directly. However, since we had predominantly null or improved findings in autism, we can still note that a tendency towards working memory differences and slower processing speeds in autism (Zapparrata et al., 2022; Wang et al., 2017) do not provide a compelling alternative explanation for this pattern of findings.

Additionally, patterns observed by age are cross-sectional in this design. Though we hypothesize for these effects to occur within individuals, e.g., in response to environmental stressors, longitudinal designs are also needed to test these hypotheses.

4.6.6 Conclusions

Overall, this study characterizes both shared and distinctive aspects of interoceptive-exteroceptive integration across stimuli (cardiac and respiratory) and integrative complexity. Our findings suggest that complex, but not simple, integration is increasingly refined into adulthood. Further, a composite measure across all tasks showed group-specific relationships with interoceptive confusion and anxiety. These results suggest that interoceptive integration may be a perceptual strength in autism, supporting the utility of interventions that contextualize the meaning of interoceptive sensations among the potential wealth of signals.

CHAPTER 5

Discussion

5.1 The road taken: A contextual, systems-based analysis of interoception in autism

In this dissertation, we used multiple complementary approaches to understand how the sense of interoception develops from childhood to adulthood and how this relates to the types of interoceptive challenges commonly experienced by autistic individuals. These approaches were designed to bridge the gap between the limited prior perceptual literature and emerging predictive coding frameworks of interoception (Ainley et al., 2016; Allen et al., 2022; Barrett and Simmons, 2015), which account for the efficiency of filtering some of these signals from our awareness. First, we examined the properties of interoceptive brain systems, which informs how we process information beyond our conscious awareness. In Chapter 2, we examined the structure of interoceptive brain regions in autistic and non-autistic individuals, which gives information about the organization of cell circuits that perform the detailed computations that give rise to interoceptive awareness. In Chapter 3, we analyzed communication between primary interoceptive regions with the rest of the brain, which informs the type of broader external cues that are being integrated with our sense of interoception. Then in Chapter 4, to link these findings back to behavior and perceptual experiences, we analyzed interoception using a new generation of interoceptive perceptual tasks that links the study of interoception with the multisensory literature. Using these approaches, we found evidence supporting developmental trends in interoception across our groups. We found some surprising ways in which the groups differed. Lastly, we found several ways to account for individual features in understanding interoception and supporting individuals who experience interoceptive challenges.

5.2 The combined picture: interoceptive development

5.2.1 What we learned: The development of interoceptive efficiency

Though existing interoceptive frameworks provide hypotheses about how interoception might develop (Barrett and Simmons, 2015; Palmer and Tsakiris, 2018), there is little empirical evidence to describe how this occurs in practice. Heartbeat counting has been the most thoroughly tested across a wide age range, but the improvements with age that one might expect for any skill have been mysteriously unsupported for this task (Williams et al., 2022; Mash et al., 2017). In Chapters 3 and 4, we provide evidence for how interoceptive perception develops instead: not as a progression of single stimulus detection, but a refinement of the time, planning, and levels of complexity required to address bodily needs. In Chapter 3, we found that with age, primary interoceptive cortex becomes less tightly coupled with subcortical regions providing internal receptor input and more tightly coupled with cortical motor imagery regions involved in broader self-reflection and planning. In Chapter 4, we found that the integration parameters of heartbeat-based integration were stable with age, but integration across a broader, heart rate-focused time scale continued to refine into adulthood. These findings provide concrete examples of how our sense of interoception evolves to serve us as we grow and take increasing responsibility for our own homeostatic regulation within a complex world (Zoltowski et al., 2022; Atzil et al., 2018; Fotopoulou et al., 2022).

Most prominently, our results inform how to developmentally tailor studies of interoceptive processing and how this may lead to interoceptive issues. Findings from both Chapter 3 and Chapter 4 suggest a developmental progression between tuning "in" to individual interoceptive stimuli (most notably heartbeats) and tuning "out" towards a broader picture of what these stimuli mean for health within the environment. Thus, the emerging literature of improved heartbeat perception paradigms (Fittipaldi et al., 2020; Körmendi et al., 2022) may particularly aid in understanding childhood interoception beyond what we have studied here. Further, our findings of correspondence between heartbeat and heart

rate integration paradigms do suggest that some initial focus towards heartbeat integration may be a stepping stone towards adaptive heart rate integration. However, our findings also suggest that sometime around adolescence, it may be more appropriate to shift experimental focus to gestalt interoceptive measures, including heart rate and respiration integration, rather than lower-level perception such as identifying individual heartbeats.

5.2.2 Future directions I: A younger understanding of interoceptive development

A particular remaining gap in the understanding of interoceptive system development is the understanding of how this system is tuned before ages seven or eight. Given the especially early development of the interoceptive brain system (Jönsson et al., 2018), it is hypothesized that critical tuning of the foundations of this system occurs during earliest life. Researchers have surmounted some of the challenges of completing magnetic resonance imaging (MRI) with infants and young children (The IBIS Network et al., 2017), so future work may extend similar structural and resting state approaches as completed here towards these younger samples. For the specific understanding of temporal heartbeat integration, another promising measure is the heartbeat evoked potential (HEP, Park and Blanke, 2019) as derived from electroencephalogram (EEG). Studies have supported the consistent identification of an evoked potential shortly following the R peak of the heartbeat as measured during tasks (Al et al., 2020; Banellis and Cruse, 2020; Marshall et al., 2017) and at rest (Dirlich et al, 1997), which correlates with behavioral interoception measures (Fittipaldi et al., 2020). This measure has greatly aided our understanding of both the temporal location and variability of the heartbeat sensation. Thus, the possibility of collecting resting HEPs in infants may give important information about the earliest temporal properties of heartbeat perception and integration.

5.3 Group comparisons

5.3.1 Revising a deficit model of interoception in autism

Our comparisons of interoceptive-exteroceptive integration between our two diagnostic groups first and foremost challenge the budding deficits model of interoception in autism (Williams et al., 2022; Garfinkel et al., 2016). Based primarily from findings of reduced heartbeat counting accuracy in autism, the literature has hypothesized a general tendency towards reduced interoception in autism that extends into reduced emotional awareness (Trevisan et al., 2019). Questionnaire and qualitative report findings certainly make this seem like a possibility, though the qualitative reports suggest there is not a single autistic phenotype of interoception (Trevisan et al., 2021b). As described in Chapter 4, the heartbeat counting task has substantial limitations that call into question a framework built solely on these findings (Desmedt et al., 2018). Though meta-analyzed findings do suggest a true difference in autism (Williams et al., 2022), there are other known findings that might explain these differences as not necessarily driven by interoceptive differences specifically, such as IQ (Desmedt et al., 2018; Williams et al., 2022), heart rate differences (Bal et al., 2010; Hollocks et al., 2014; Ming et al., 2005; Watson et al., 2012), and perceptual decision-making tendencies (Quinde-Zlibut et al., 2020). Thus, the results of our analyses via approaches that reduce these confounds suggest much greater nuance as to how interoception differs in autism.

In Chapter 4, we did find a much higher level in our autistic than non-autistic group of reported interoceptive confusion as measured by the Interoception Sensory Questionnaire (ISQ, Fiene et al., 2018). However, neither of the significant differences we observed by group in Chapter 3 or Chapter 4 suggest that a deficit in primary interoceptive perception explains this reported confusion. Instead, our only significant group findings suggested potential areas of enhanced interoceptive-exteroceptive integration in the autistic compared to non-autistic groups. In Chapter 3, we found increased connectivity in autism between the posterior insula and lateral occipital cortex, in areas related to mental imagery and

processing speed (Forn et al., 2013; Sack et al., 2002). In Chapter 4, we found increased respiration integration improvement in autism, such that matched breathing helped with processing of relative visual rates. These findings combine to suggest that some areas of interoceptive-exteroceptive integration may be a relative strength in autism, particularly with certain types of visual processing.

However, in the one sample in which we were powered to look at age by group interactions, we found evidence for diverging insular structural trends such that sulcal depth in this region decreased with age more prominently in autistic than non-autistic individuals. First, these findings suggest that there might be some tradeoff between how autistic interoceptive processing develops within the insular gradient, compared to integrating interoception with information from other sensory sources. Though it is not yet clear how to map this accelerated sulcal depth decrease with strengths or weaknesses in interoception, these findings do suggest the potential for some interoceptive weaknesses in autism as well as interoceptive strengths. Thus, the ability to extend our connectivity and perceptual approaches into large enough samples to examine age-specific group differences would aid in integrating the information from these complementary approaches into a development-specific model of interoception in autism.

As proposed by Pellicano and Burr (2012), Bayesian theories of autism have suggested that autistic individuals rely less on their past experience to interpret current sensations than non-autistic individuals do. The proposed consequences are that autistic individuals process sensory information more veridically than non-autistic individuals (e.g., seeing the trees), but with a cost in terms of efficient interpretation (e.g., missing the forest). What our findings do indeed point towards is that interoception in autism may reflect Bayesian differences in sensory processing (Pellicano and Burr, 2012; Palmer et al., 2017). Specifically, the contrast between perceptual integration (as equal or better) and interoceptive interpretation (as greatly reduced) is consistent with hypothesized patterns from this Bayesian framework (Pellicano, 2013). However, the group trends compared to other multisensory

findings were surprising. Based on prior multisensory studies, we had hypothesized that even at the lowest levels (i.e., beat-based integration) we would see wider, broader temporal binding windows in autism that would further diverge with increasing complexity (Feldman et al., 2018). This leads us to consider that interoception may diverge from other common sensory trends in autistic individuals.

5.3.2 Future directions II: Linking sensory systems via the middle insula

Our findings thus far have built up a greater understanding of posterior insula-mediated interoceptive processing in autistic and non-autistic development. Further, there is a broader extant literature on anterior insula processing in autism and resulting relationships with self-focused and emotional processing (Uddin, 2011; Uddin et al., 2017; Uddin and Menon, 2009). However, between these two regions is the middle insula, situated at the very heart of interoceptive-exteroceptive integration. Though this region is generally characterized as blending interoception with multimodal processing, early studies showed that this area receives very quick and direct sensory inputs that circumvent the usual primary to associative pathways, including auditory and visual inputs (Mesulam and Mufson, 1982). Further, one functional homogeneity study of the insula found evidence that this area is expanded in autistic compared to non-autistic individuals (Yamada et al., 2016). Last, the middle insula in rodents shows specific links between motor cortex and the bed nucleus of the stria terminalis (BNST, a key anxiety region; Avery et al., 2016) during anxiety-related escape attempts (Luchsinger et al., 2021). Together, these findings suggest that the middle insula might be an especially important structure for understanding autistic interoceptive processing. Further, this region may provide specific links to how exteroceptive sensitivities, interoceptive processing, and anxiety levels in autism relate to each other.

5.3.3 Future directions III: Extending the Bayesian framework

First, we were limited to examine age-specific differences in autism in two of our three studies, so extending these samples will also help build the profile describing whether,

how, and when interoception diverges in autism. Other resources exist that may help complete some of these purposes as well, such as the Autism Brain Image Database Exchange (ABIDE) I (Di Martino et al., 2014) and II (Di Martino et al., 2017) samples that may provide an important opportunity to replicate our resting state findings, with appropriate caution in interpreting site-based variability. Second, test-retest and longitudinal designs may especially help with understanding how interoceptive models develop over time and adapt to different situations. Though we may be limited in using some invasive approaches to alter interoception (Khalsa et al., 2016), the increasing creativity in interoceptive task design suggests that there may be some future avenues by which we may look at differential interoceptive processing in different situations. Interoceptive processing before, during, and after physical activity may be one set of conditions that is especially relevant to health and wellbeing.

5.4 Towards dimensionality: A consideration of differential autistic features

5.4.1 The role of differential autism behaviors and anxiety

Individual variability is also a complicated part of understanding sensory processing in autism, since different autistic individuals may show hypo- or hyper- responsiveness to the same type of sensory stimulus (Ausderau et al., 2016; Chen et al., 2022a). We examined dimensional relationships with participant characteristics in each chapter to understand some of this variability. One feature we considered was the overall level of autism-related behaviors, since we hypothesized that due to its developmental primacy, our interoceptive measures may show cascading relationships with both social (Atzil et al., 2018) and sensorimotor domains of autism (Park and Tallon-Baudry, 2014; Tallon-Baudry et al., 2018). In addition, we were especially interested in the relationship between interoception and anxiety. Researchers have hypothesized that altered tuning of our interoceptive system may correspond to a pervasive sense of bodily threat (Paulus and Stein, 2006; Domschke et al., 2010; Ainley et al., 2016; Barrett and Simmons, 2015), though this has been thus far hard to

characterize in practice (Adams et al., 2022a). Thus, our results augment this prior literature by finding unique interactions between our diagnostic groups, interoceptive-exteroceptive integration, and anxiety that further a dimensional understanding.

Consistent with autistic heterogeneity, we did observe substantial variability in both our perceptual and behavioral report measures of interoception in autism, such that there were few clear trends of differences between our autistic and non-autistic groups. However, we did find several dimensional relationships with participant characteristics. In Chapter 2, we found that local gyrification in the insula significantly covaried with autism-related behaviors, as measured by the Autism Diagnostic Observation Schedule, Calibrated Severity Score (ADOS CSS, (Gotham et al., 2009)). This finding supports a link between interoception and behavioral features across the broader social-communicative and sensorimotor domains of autism. Further, in Chapter 4, we found that resting heart rate was a consistent predictor of cardioception indices rather than group; thus, attention to factors such as arousal levels, medications, and activity levels that influence heart rate is one important piece of understanding interoception in autism. We also found a strong correlation between total anxiety levels and interoceptive confusion, as measured by the ISQ, supporting a relationship between interoception and anxiety. However, our groups strikingly differed in how interoceptive-exteroceptive integrative tendencies as generalized across our three tasks related to both interoceptive confusion and anxiety. Particularly, we found that the most anxious autistic individuals have the hardest time interpreting their interoceptive sensations, even while showing particularly high integrative tendencies. Thus, our results point towards something other than perceptual deficits explaining this sense of bodily confusion in autism and that there may indeed be unique interoception-anxiety links in autism.

Together, our identified links between interoception, autism-related behaviors, and anxiety suggest that interoceptive processing covaries dimensionally with other areas of challenges for autistic individuals. Though this is consistent with models that predict cascading effects of sensory differences (Cascio et al., 2016), these effects become difficult to disen-

tangle when it comes to supporting individuals. Our findings are correlative and thus do not confirm whether greater interoceptive challenges cause greater social, sensorimotor, or anxiety-related challenges or vice versa. It is quite possible that both may contribute to each other, in a vicious cycle.

5.4.2 Future directions IV: Generalizing across cognitive ability

Prior heartbeat counting research has also highlighted that the cognitive demands involved in completing common interoceptive tasks introduce a confound in clinical populations with cognitive differences, including autism (Desmedt et al., 2018); testing the relationships between IQ and our interoceptive-exteroceptive measures will be one future direction. In addition, the biased inclusion of autistic individuals without intellectual disability in many autism research studies (Russell et al., 2019) has severely limited the ability to understand interoceptive differences in this subset of the autistic population. Including this population in interoception research will broaden this understanding. Though our multifaceted approach has helped us understand interoception in autism beyond some of the heartbeat counting limitations, these tasks still require a certain level of receptive and expressive language to complete. Thus, reducing the language levels required in interoception paradigms, including options such as the HEP (Park and Blanke, 2019), so that we can better understand how interoceptive processing intersects with cognitive differences is one very important extension of this work.

5.4.3 How we can help: Towards a new generation of interoceptive supports

Though some of our understanding of how interoception varies between individuals remains to be filled by these future gaps, these results provide hope that we can ultimately support individuals who struggle with interoceptive processing. Prior findings do suggest interoceptive-focused interventions, such as cardioception interventions (Quadt et al., 2021) and mindfulness interventions (Hattfield et al., 2023) result in reduced anxiety and enhanced calmness for autistic individuals. In particular, our findings in Chapter 4 of en-

hanced respiration integration in autism are consistent with the promising effects of mindfulness interventions in this population. Our findings suggest that two of the directions that may enhance these current efforts are i) revising a deficit perspective, as discussed above and ii) efforts towards personalization.

Our findings implicate some practical approaches for personalizing interoceptive interventions to unique individuals' needs. First, our findings by age suggest that the progressing complexity of interoceptive processing with age is one consideration for designing optimal intervention approaches. Further, the principal component analysis findings in Chapter 4 suggest that one useful approach is to administer several types of interoceptive-exteroceptive tasks to get a balanced profile of an individual's interoceptive-exteroceptive processing. This can then be used to tailor intervention goals between the possible types of tasks and stimuli. For example, the component scores of cardiac- versus respiration-focused integration could be compared in advising a cardioception-specific or mindfulness based approach. These findings start to provide some ideas for how to personalize an approach to interoceptive challenges, but our future directions provide even more avenues by which these ideas may be extended.

5.5 Final conclusions

In this dissertation, we built a deeper understanding of how interoception is developed and tuned along a gradient of complexity at the neural and perceptual levels. We found only a few areas in which interoceptive-exteroceptive integration, or its neural correlates, differed in autism as a whole. Further, these average differences generally pointed towards areas of potential integrative strengths in autism, suggesting a need to revise models considering primary interoception to be a deficit in autism. Importantly, our findings suggests that interactions between autism and individual characteristics (age, the degree of autism-related behaviors, physiology, and anxiety levels) may explain more about interoceptive integration and tuing than diagnosis alone. Specifically, our findings suggest that

interoceptive-exteroceptive integration in autism may vary dimensionally with other features or challenges in autism, including the general degree of autism-related behaviors and total anxiety levels. These findings provide ideas for how to personalize a new generation of interoceptive supports for individuals who experience interoceptive challenges.

References

Abbott, A. E., Nair, A., Keown, C. L., Datko, M., Jahedi, A., Fishman, I., and Müller, R.-A. (2016). Patterns of Atypical Functional Connectivity and Behavioral Links in Autism Differ Between Default, Salience, and Executive Networks. *Cerebral Cortex*, 26(10):4034–4045.

Aboud, K. S., Huo, Y., Kang, H., Ealey, A., Resnick, S. M., Landman, B. A., and Cutting, L. E. (2019). Structural covariance across the lifespan: Brain development and aging through the lens of inter-network relationships. *Human Brain Mapping*, 40(1):125–136.

Adams, K. L., Edwards, A., Peart, C., Ellett, L., Mendes, I., Bird, G., and Murphy, J. (2022a). The association between anxiety and cardiac interoceptive accuracy: A systematic review and meta-analysis. *Neuroscience & Biobehavioral Reviews*, 140:104754.

Adams, K. L., Murphy, J., Catmur, C., and Bird, G. (2022b). The role of interoception in the overlap between eating disorders and autism: Methodological considerations. *European Eating Disorders Review*, 30(5):501–509.

Ainley, V., Apps, M. A. J., Fotopoulou, A., and Tsakiris, M. (2016). 'Bodily precision': a predictive coding account of individual differences in interoceptive accuracy. *Philosophical Transactions of the Royal Society B: Biological Sciences*, 371(1708):20160003.

Al, E., Iliopoulos, F., Forschack, N., Nierhaus, T., Grund, M., Motyka, P., Gaebler, M., Nikulin, V. V., and Villringer, A. (2020). Heart–brain interactions shape somatosensory perception and evoked potentials. *Proceedings of the National Academy of Sciences*, 117(19):10575–10584.

Allen, M., Levy, A., Parr, T., and Friston, K. J. (2022). In the Body's Eye: The computational anatomy of interoceptive inference. *PLOS Computational Biology*, 18(9):e1010490.

Amaya, Y., Abe, T., Kanbara, K., Shizuma, H., Akiyama, Y., and Fukunaga, M. (2021). The effect of aerobic exercise on interoception and cognitive function in healthy university students: a non-randomized controlled trial. *BMC Sports Science, Medicine and Rehabilitation*, 13(1):99.

American Psychiatric Association (2013). *Diagnostic and Statistical Manual of Mental Disorders*. American Psychiatric Association, Arlington, VA, 5 edition.

Angulo, M., Rooks, B. T., Gill, M., Goldstein, T., Sakolsky, D., Goldstein, B., Monk, K., Hickey, M. B., Diler, R. S., Hafeman, D., Merranko, J., Axelson, D., and Birmaher, B. (2017). Psychometrics of the screen for adult anxiety related disorders (SCAARED)- A new scale for the assessment of DSM-5 anxiety disorders. *Psychiatry Research*, 253:84–90.

Asman, A. J. and Landman, B. A. (2012). Non-local STAPLE: An Intensity-Driven Multi-atlas Rater Model. In Hutchison, D., Kanade, T., Kittler, J., Kleinberg, J. M., Mattern, F., Mitchell, J. C., Naor, M., Nierstrasz, O., Pandu Rangan, C., Steffen, B., Sudan, M., Terzopoulos, D., Tygar, D., Vardi, M. Y., Weikum, G., Ayache, N., Delingette, H., Golland, P., and Mori, K., editors, *Medical Image Computing and Computer-Assisted Intervention – MICCAI 2012*, volume 7512, pages 426–434. Springer Berlin Heidelberg, Berlin, Heidelberg.

Asperger, H. (1944). Die "Autistischen Psychopathen" im Kindesalter. *European archives of psychiatry and clinical neuroscience*, 117(1):76–136.

Atzil, S., Gao, W., Fradkin, I., and Barrett, L. F. (2018). Growing a social brain. *Nature Human Behaviour*, 2(9):624–636.

Ausderau, K. K., Furlong, M., Sideris, J., Bulluck, J., Little, L. M., Watson, L. R., Boyd, B. A., Belger, A., Dickie, V. A., and Baranek, G. T. (2014). Sensory subtypes in children with autism spectrum disorder: latent profile transition analysis using a national survey of sensory features. *Journal of Child Psychology and Psychiatry*, 55(8):935–944.

Ausderau, K. K., Sideris, J., Little, L. M., Furlong, M., Bulluck, J. C., and Baranek, G. T. (2016). Sensory subtypes and associated outcomes in children with autism spectrum disorders: Sensory subtypes and outcomes in children with ASD. *Autism Research*, 9(12):1316–1327.

Avery, S. N., Clauss, J. A., and Blackford, J. U. (2016). The Human BNST: Functional Role in Anxiety and Addiction. *Neuropsychopharmacology*, 41(1):126–141.

Bal, E., Harden, E., Lamb, D., Van Hecke, A. V., Denver, J. W., and Porges, S. W. (2010). Emotion Recognition in Children with Autism Spectrum Disorders: Relations to Eye Gaze and Autonomic State. *Journal of Autism and Developmental Disorders*, 40(3):358–370.

Banellis, L. and Cruse, D. (2020). Skipping a beat: heartbeat-evoked potentials reflect predictions during interoceptive-exteroceptive integration. preprint, Neuroscience.

Baranek, G. T. (1999). Autism During Infancy: A Retrospective Video Analysis of Sensory-Motor and Social Behaviors at 9-12 Months of Age. *Journal of Autism and Developmental Disorders*, 29(3):213–224.

Baranek, G. T., David, F. J., Poe, M. D., Stone, W. L., and Watson, L. R. (2006). Sensory Experiences Questionnaire: discriminating sensory features in young children with autism, developmental delays, and typical development: SEQ. *Journal of Child Psychology and Psychiatry*, 47(6):591–601.

Baranek, G. T., Sideris, J., Chen, Y., Crais, E. R., Turner-Brown, L., and Watson, L. R. (2022). Early measurement of autism risk constructs in the general population: A new factor structure of the First Years Inventory (FYIv3.1) for ages 6–16 months. *Autism Research*, 15(5):915–928.

Barrett, L. F., Quigley, K. S., and Hamilton, P. (2016). An active inference theory of allostasis and interoception in depression. *Philosophical Transactions of the Royal Society B: Biological Sciences*, 371(1708):20160011.

Barrett, L. F. and Simmons, W. K. (2015). Interoceptive predictions in the brain. *Nature Reviews Neuroscience*, 16(7):419–429.

Bastos, A., Usrey, W., Adams, R., Mangun, G., Fries, P., and Friston, K. (2012). Canonical Microcircuits for Predictive Coding. *Neuron*, 76(4):695–711.

Baum, S. H., Stevenson, R. A., and Wallace, M. T. (2015). Behavioral, perceptual, and neural alterations in sensory and multisensory function in autism spectrum disorder. *Progress in Neurobiology*, 134:140–160.

Bayly, P., Taber, L., and Kroenke, C. (2014). Mechanical forces in cerebral cortical folding: A review of measurements and models. *Journal of the Mechanical Behavior of Biomedical Materials*, 29:568–581.

Behrmann, M., Thomas, C., and Humphreys, K. (2006). Seeing it differently: visual processing in autism. *Trends in Cognitive Sciences*, 10(6):258–264.

Birmaher, B., Khetarpal, S., Brent, D., Cully, M., Balach, L., Kaufman, J., and Neer, S. M. (1997). The Screen for Child Anxiety Related Emotional Disorders (SCARED): Scale Construction and Psychometric Characteristics. *Journal of the American Academy of Child & Adolescent Psychiatry*, 36(4):545–553.

Bos, D. J., Merchán-Naranjo, J., Martínez, K., Pina-Camacho, L., Balsa, I., Boada, L., Schnack, H., Oranje, B., Desco, M., Arango, C., Parellada, M., Durston, S., and Janssen, J. (2015). Reduced Gyrification Is Related to Reduced Interhemispheric Connectivity in Autism Spectrum Disorders. *Journal of the American Academy of Child & Adolescent Psychiatry*, 54(8):668–676.

Boyd, B. A., Baranek, G. T., Sideris, J., Poe, M. D., Watson, L. R., Patten, E., and Miller, H. (2010). Sensory features and repetitive behaviors in children with autism and developmental delays. *Autism Research*, pages n/a–n/a.

Brener, J. and Kluvitse, C. (1988). Heartbeat Detection: Judgments of the Simultaneity of External Stimuli and Heartbeats. *Psychophysiology*, 25(5):554–561.

Brener, J. and Ring, C. (2016). Towards a psychophysics of interoceptive processes: the measurement of heartbeat detection. *Philosophical Transactions of the Royal Society B: Biological Sciences*, 371(1708):20160015.

Brown, L., Sherbenou, R. J., and Johnsen, S. K. (2010). *Test of Nonverbal Intelligence*. Pearson, 4th ed edition.

Calvert, G. A., Spence, C., and Stein, B. E., editors (2004). *The Handbook of Multisensory Processes*.

Camarata, S., Miller, L. J., and Wallace, M. T. (2020). Evaluating Sensory Integration/Sensory Processing Treatment: Issues and Analysis. *Frontiers in Integrative Neuroscience*, 14:556660.

Carper, R. (2002). Cerebral Lobes in Autism: Early Hyperplasia and Abnormal Age Effects. *NeuroImage*, 16(4):1038–1051.

Cascio, C. J., Foss-Feig, J. H., Burnette, C. P., Heacock, J. L., and Cosby, A. A. (2012a). The rubber hand illusion in children with autism spectrum disorders: delayed influence of combined tactile and visual input on proprioception. *Autism*, 16(4):406–419.

Cascio, C. J., Foss-Feig, J. H., Heacock, J. L., Newsom, C. R., Cowan, R. L., Benningfield, M. M., Rogers, B. P., and Cao, A. (2012b). Response of neural reward regions to food cues in autism spectrum disorders. *Journal of Neurodevelopmental Disorders*, 4(1).

Cascio, C. J., Gu, C., Schauder, K. B., Key, A. P., and Yoder, P. (2015). Somatosensory Event-Related Potentials and Association with Tactile Behavioral Responsiveness Patterns in Children with ASD. *Brain Topography*, 28(6):895–903.

Cascio, C. J., Woynaroski, T., Baranek, G. T., and Wallace, M. T. (2016). Toward an interdisciplinary approach to understanding sensory function in autism spectrum disorder: Toward an interdisciplinary approach. *Autism Research*, 9(9):920–925.

Cavanna, A. E. and Trimble, M. R. (2006). The precuneus: a review of its functional anatomy and behavioural correlates. *Brain*, 129(3):564–583.

Caviness, V., Takahashi, T., and Nowakowski, R. (1995). Numbers, time and neocortical neuronogenesis: a general developmental and evolutionary model. *Trends in Neurosciences*, 18(9):379–383.

Chen, H., Uddin, L. Q., Duan, X., Zheng, J., Long, Z., Zhang, Y., Guo, X., Zhang, Y., Zhao, J., and Chen, H. (2017). Shared atypical default mode and salience network functional connectivity between autism and schizophrenia: Shared atypical FC in ASD and schizophrenia. *Autism Research*, 10(11):1776–1786.

Chen, Y., Sideris, J., Watson, L. R., Crais, E. R., and Baranek, G. T. (2022a). Developmental trajectories of sensory patterns from infancy to school age in a community sample and associations with autistic traits. *Child Development*, 93(4).

Chen, Y.-J., Sideris, J., Watson, L. R., Crais, E. R., and Baranek, G. T. (2022b). Early developmental profiles of sensory features and links to school-age adaptive and maladaptive outcomes: A birth cohort investigation. *Development and Psychopathology*, pages 1–11.

Chung, M. K., Robbins, S. M., Dalton, K. M., Davidson, R. J., Alexander, A. L., and Evans, A. C. (2005). Cortical thickness analysis in autism with heat kernel smoothing. *NeuroImage*, 25(4):1256–1265.

Courchesne, E., Karns, C. M., Davis, H. R., Ziccardi, R., Carper, R. A., Tigue, Z. D., Chisum, H. J., Moses, P., Pierce, K., Lord, C., Lincoln, A. J., Pizzo, S., Schreibman, L., Haas, R. H., Akshoomoff, N. A., and Courchesne, R. Y. (2001). Unusual brain growth patterns in early life in patients with autistic disorder. *Neurology*, 57:245–254.

Courchesne, E., Pierce, K., Schumann, C. M., Redcay, E., Buckwalter, J. A., Kennedy, D. P., and Morgan, J. (2007). Mapping Early Brain Development in Autism. *Neuron*, 56(2):399–413.

Craig, A. B. (2005). Forebrain emotional asymmetry: a neuroanatomical basis? *Trends in Cognitive Sciences*, 9(12):566–571.

Craig, A. D. (2002). How do you feel? Interoception: the sense of the physiological condition of the body. *Nature Reviews Neuroscience*, 3(8):655–666.

Craig, A. D. (2004). Human feelings: why are some more aware than others? *Trends in cognitive sciences*, 8(6):239–241.

Craig, A. D. (2008). Interoception and emotion: a neuroanatomical perspective. *Handbook of emotions*, 3(602):272–88.

Craig, A. D. (2009). How do you feel — now? The anterior insula and human awareness. *Nature Reviews Neuroscience*, 10(1):59–70.

Crucianelli, L., Enmalm, A., and Ehrsson, H. H. (2022). Interoception as independent cardiac, thermosensory, nociceptive, and affective touch perceptual submodalities. *Biological Psychology*, 172:108355.

Dale, A. and Anderson, D. (1978). Information Variables in Voluntary Control and Classical Conditioning of Heart Rate: Field Dependence and Heart-Rate Perception. *Perceptual and Motor Skills*, 47(1):79–85.

Dearborn, G. (1932). A case of congenital general pure analgesia. *J Nerv Ment Dis*, 75:612–615.

Desmedt, O., Heeren, A., Corneille, O., and Luminet, O. (2022). What do measures of self-report interoception measure? Insights from a systematic review, latent factor analysis, and network approach. *Biological Psychology*, 169:108289.

Desmedt, O., Luminet, O., and Corneille, O. (2018). The heartbeat counting task largely involves non-interoceptive processes: Evidence from both the original and an adapted counting task. *Biological Psychology*, 138:185–188.

Di Martino, A., O'Connor, D., Chen, B., Alaerts, K., Anderson, J. S., Assaf, M., Balsters, J. H., Baxter, L., Beggiato, A., Bernaerts, S., Blanken, L. M. E., Bookheimer, S. Y., Braden, B. B., Byrge, L., Castellanos, F. X., Dapretto, M., Delorme, R., Fair, D. A., Fishman, I., Fitzgerald, J., Gallagher, L., Keehn, R. J. J., Kennedy, D. P., Lainhart, J. E., Luna, B., Mostofsky, S. H., Muller, R.-A., Nebel, M. B., Nigg, J. T., O'Hearn, K., Solomon, M., Toro, R., Vaidya, C. J., Wenderoth, N., White, T., Craddock, R. C., Lord,

C., Leventhal, B., and Milham, M. P. (2017). Enhancing studies of the connectome in autism using the autism brain imaging data exchange II. *Scientific data*, 4:170010.

Di Martino, A., Yan, C.-G., Li, Q., Denio, E., Castellanos, F. X., Alaerts, K., Anderson, J. S., Assaf, M., Bookheimer, S. Y., Dapretto, M., Deen, B., Delmonte, S., Dinstein, I., Ertl-Wagner, B., Fair, D. A., Gallagher, L., Kennedy, D. P., Keown, C. L., Keysers, C., Lainhart, J. E., Lord, C., Luna, B., Menon, V., Minshew, N. J., Monk, C. S., Mueller, S., Müller, R.-A., Nebel, M. B., Nigg, J. T., O'Hearn, K., Pelphrey, K. A., Peltier, S. J., Rudie, J. D., Sunaert, S., Thioux, M., Tyszka, J. M., Uddin, L. Q., Verhoeven, J. S., Wenderoth, N., Wiggins, J. L., Mostofsky, S. H., and Milham, M. P. (2014). The autism brain imaging data exchange: towards a large-scale evaluation of the intrinsic brain architecture in autism. *Molecular Psychiatry*, 19(6):659–667.

Dierker, D. L., Feczko, E., Pruett, J. R., Petersen, S. E., Schlaggar, B. L., Constantino, J. N., Harwell, J. W., Coalson, T. S., and Van Essen, D. C. (2015). Analysis of Cortical Shape in Children with Simplex Autism. *Cerebral Cortex*, 25(4):1042–1051.

Domschke, K., Stevens, S., Pfleiderer, B., and Gerlach, A. L. (2010). Interoceptive sensitivity in anxiety and anxiety disorders: An overview and integration of neurobiological findings. *Clinical Psychology Review*, 30(1):1–11.

DuBois, D., Ameis, S. H., Lai, M.-C., Casanova, M. F., and Desarkar, P. (2016). Interoception in Autism Spectrum Disorder: A review. *International Journal of Developmental Neuroscience*, 52:104–111.

Dufour, N., Redcay, E., Young, L., Mavros, P. L., Moran, J. M., Triantafyllou, C., Gabrieli, J. D. E., and Saxe, R. (2013). Similar Brain Activation during False Belief Tasks in a Large Sample of Adults with and without Autism. *PLoS ONE*, 8(9):e75468.

Dunham, K., Zoltowski, A., Feldman, J. I., Davis, S., Rogers, B., Failla, M. D., Wallace, M. T., Cascio, C. J., and Woynaroski, T. G. (2023). Neural correlates of audiovisual speech processing in autistic and non-autistic youth. *Multisensory Research*, 36(3):263–288.

Ebisch, S. J., Gallese, V., Willems, R. M., Mantini, D., Groen, W. B., Romani, G. L., Buitelaar, J. K., and Bekkering, H. (2011). Altered intrinsic functional connectivity of anterior and posterior insula regions in high-functioning participants with autism spectrum disorder. *Human Brain Mapping*, 32(7):1013–1028.

Ecker, C., Andrews, D., Dell'Acqua, F., Daly, E., Murphy, C., Catani, M., Thiebaut de Schotten, M., Baron-Cohen, S., Lai, M., Lombardo, M., Bullmore, E., Suckling, J., Williams, S., Jones, D., Chiocchetti, A., the MRC AIMS Consortium, and Murphy, D. (2016). Relationship Between Cortical Gyrification, White Matter Connectivity, and Autism Spectrum Disorder. *Cerebral Cortex*, 26(7):3297–3309.

Ecker, C., Shahidiani, A., Feng, Y., Daly, E., Murphy, C., D'Almeida, V., Deoni, S., Williams, S. C., Gillan, N., Gudbrandsen, M., Wichers, R., Andrews, D., Van Hemert, L., and Murphy, D. G. M. (2014). The effect of age, diagnosis, and their interaction on

vertex-based measures of cortical thickness and surface area in autism spectrum disorder. *Journal of Neural Transmission*, 121(9):1157–1170.

Essen, D. C. V. (1997). A tension-based theory of morphogenesis and compact wiring in the central nervous system. *Nature*, 385(6614):313–318.

Fabbri, R., Spennato, D., Conte, G., Konstantoulaki, A., Lazzarini, C., Saracino, E., Nicchia, G. P., Frigeri, A., Zamboni, R., Spray, D. C., and Benfenati, V. (2023). The emerging science of Glioception: Contribution of glia in sensing, transduction, circuit integration of interoception. *Pharmacology & Therapeutics*, 245:108403.

Failla, M. D., Bryant, L. K., Heflin, B. H., Mash, L. E., Schauder, K., Davis, S., Gerdes, M. B., Weitlauf, A., Rogers, B. P., and Cascio, C. J. (2020). Neural Correlates of Cardiac Interoceptive Focus Across Development: Implications for Social Symptoms in Autism Spectrum Disorder. *Autism Research*, 13(6):908–920.

Failla, M. D., Peters, B. R., Karbasforoushan, H., Foss-Feig, J. H., Schauder, K. B., Heflin, B. H., and Cascio, C. J. (2017). Intrainsular connectivity and somatosensory responsiveness in young children with ASD. *Molecular Autism*, 8(1).

Farb, N. A. S., Segal, Z. V., and Anderson, A. K. (2013). Attentional Modulation of Primary Interoceptive and Exteroceptive Cortices. *Cerebral Cortex*, 23(1):114–126.

Feldman, J. I., Dunham, K., Cassidy, M., Wallace, M. T., Liu, Y., and Woynaroski, T. G. (2018). Audiovisual multisensory integration in individuals with autism spectrum disorder: A systematic review and meta-analysis. *Neuroscience & Biobehavioral Reviews*, 95:220–234.

Fiene, L. and Brownlow, C. (2015). Investigating interoception and body awareness in adults with and without autism spectrum disorder: Investigating interoception and body awareness. *Autism Research*, 8(6):709–716.

Fiene, L., Ireland, M. J., and Brownlow, C. (2018). The Interoception Sensory Questionnaire (ISQ): A Scale to Measure Interoceptive Challenges in Adults. *Journal of Autism and Developmental Disorders*, 48(10):3354–3366.

Fittipaldi, S., Abrevaya, S., Fuente, A. d. l., Pascariello, G. O., Hesse, E., Birba, A., Salamone, P., Hildebrandt, M., Martí, S. A., Pautassi, R. M., Huepe, D., Martorell, M. M., Yoris, A., Roca, M., García, A. M., Sedeño, L., and Ibáñez, A. (2020). A multidimensional and multi-feature framework for cardiac interoception. *NeuroImage*, 212:116677.

Flevaris, A. V. and Murray, S. O. (2015). Orientation-specific surround suppression in the primary visual cortex varies as a function of autistic tendency. *Frontiers in Human Neuroscience*, 8.

Force, N. A. T. (2019). *An independent guide to quality care for autistic people*.

Forn, C., Ripollés, P., Cruz-Gómez, A., Belenguer, A., González-Torre, J., and Ávila, C. (2013). Task-load manipulation in the Symbol Digit Modalities Test: An alternative measure of information processing speed. *Brain and Cognition*, 82(2):152–160.

Foss-Feig, J. H., Heacock, J. L., and Cascio, C. J. (2012). Tactile responsiveness patterns and their association with core features in autism spectrum disorders. *Research in Autism Spectrum Disorders*, 6(1):337–344.

Fotopoulou, A., von Mohr, M., and Krahé, C. (2022). Affective regulation through touch: homeostatic and allostatic mechanisms. *Current Opinion in Behavioral Sciences*, 43:80–87.

Francis, S. M., Camchong, J., Brickman, L., Goelkel-Garcia, L., Mueller, B. A., Tseng, A., Lim, K. O., and Jacob, S. (2019). Hypoconnectivity of insular resting-state networks in adolescents with Autism Spectrum Disorder. *Psychiatry Research: Neuroimaging*, 283:104–112.

Gabard-Durnam, L. J., Flannery, J., Goff, B., Gee, D. G., Humphreys, K. L., Telzer, E., Hare, T., and Tottenham, N. (2014). The development of human amygdala functional connectivity at rest from 4 to 23years: A cross-sectional study. *NeuroImage*, 95:193–207.

Garfinkel, S. N., Seth, A. K., Barrett, A. B., Suzuki, K., and Critchley, H. D. (2015). Knowing your own heart: Distinguishing interoceptive accuracy from interoceptive awareness. *Biological Psychology*, 104:65–74.

Garfinkel, S. N., Tiley, C., O'Keeffe, S., Harrison, N. A., Seth, A. K., and Critchley, H. D. (2016). Discrepancies between dimensions of interoception in autism: Implications for emotion and anxiety. *Biological Psychology*, 114:117–126.

Gargouri, F., Delphine, S., Lehericy, S., and Ben Hamida, A. (2016). The influence of preprocessing steps on functional connectivity in resting state fMRI. In *2016 2nd International Conference on Advanced Technologies for Signal and Image Processing (ATSIP)*, pages 103–107, Monastir, Tunisia. IEEE.

Gaser, C., Dahnke, R., Thompson, P. M., Kurth, F., Luders, E., and Alzheimer's Disease Neuroimaging Initiative (2022). CAT – A Computational Anatomy Toolbox for the Analysis of Structural MRI Data. preprint, Neuroscience.

Geschwind, D. H. and Levitt, P. (2007). Autism spectrum disorders: developmental disconnection syndromes. *Current Opinion in Neurobiology*, 17(1):103–111.

Gilman, S., Iossifov, I., Levy, D., Ronemus, M., Wigler, M., and Vitkup, D. (2011). Rare De Novo Variants Associated with Autism Implicate a Large Functional Network of Genes Involved in Formation and Function of Synapses. *Neuron*, 70(5):898–907.

Gore, J. C., Li, M., Gao, Y., Wu, T.-L., Schilling, K. G., Huang, Y., Mishra, A., Newton, A. T., Rogers, B. P., Chen, L. M., Anderson, A. W., and Ding, Z. (2019). Functional

MRI and resting state connectivity in white matter - a mini-review. *Magnetic Resonance Imaging*, 63:1–11.

Gotham, K., Pickles, A., and Lord, C. (2009). Standardizing ADOS Scores for a Measure of Severity in Autism Spectrum Disorders. *Journal of Autism and Developmental Disorders*, 39(5):693–705.

Green, S. A., Hernandez, L., Bookheimer, S. Y., and Dapretto, M. (2016). Salience Network Connectivity in Autism Is Related to Brain and Behavioral Markers of Sensory Overresponsivity. *Journal of the American Academy of Child and Adolescent Psychiatry*, 55(7):618–626.e1.

Hagler, D. J., Saygin, A. P., and Sereno, M. I. (2006). Smoothing and cluster thresholding for cortical surface-based group analysis of fMRI data. *NeuroImage*, 33(4):1093–1103.

Han, X., Jovicich, J., Salat, D., van der Kouwe, A., Quinn, B., Czanner, S., Busa, E., Pacheco, J., Albert, M., Killiany, R., Maguire, P., Rosas, D., Makris, N., Dale, A., Dickerson, B., and Fischl, B. (2006). Reliability of MRI-derived measurements of human cerebral cortical thickness: The effects of field strength, scanner upgrade and manufacturer. *NeuroImage*, 32(1):180–194.

Han, X., Pham, D. L., Tosun, D., Rettmann, M. E., Xu, C., and Prince, J. L. (2004). CRUISE: Cortical reconstruction using implicit surface evolution. *NeuroImage*, 23(3):997–1012.

Hardan, A. Y., Jou, R. J., Keshavan, M. S., Varma, R., and Minshew, N. J. (2004). Increased frontal cortical folding in autism: a preliminary MRI study. *Psychiatry Research: Neuroimaging*, 131(3):263–268.

Harrigan, R. L., Yvernault, B. C., Boyd, B. D., Damon, S. M., Gibney, K. D., Conrad, B. N., Phillips, N. S., Rogers, B. P., Gao, Y., and Landman, B. A. (2016). Vanderbilt University Institute of Imaging Science Center for Computational Imaging XNAT: A multimodal data archive and processing environment. *NeuroImage*, 124:1097–1101.

Harrison, N. A., Brydon, L., Walker, C., Gray, M. A., Steptoe, A., Dolan, R. J., and Critchley, H. D. (2009). Neural Origins of Human Sickness in Interoceptive Responses to Inflammation. *Biological Psychiatry*, 66(5):415–422.

Hazlett, H. C., Poe, M. D., Gerig, G., Styner, M., Chappell, C., Smith, R. G., Vachet, C., and Piven, J. (2011). Early Brain Overgrowth in Autism Associated With an Increase in Cortical Surface Area Before Age 2 Years. *ARCH GEN PSYCHIATRY*, 68(5):10.

Hickman, L., Seyedsalehi, A., Cook, J. L., Bird, G., and Murphy, J. (2020). The relationship between heartbeat counting and heartbeat discrimination: A meta-analysis. *Biological Psychology*, 156:107949.

Hollocks, M. J., Howlin, P., Papadopoulos, A. S., Khondoker, M., and Simonoff, E. (2014). Differences in HPA-axis and heart rate responsiveness to psychosocial stress in children

with autism spectrum disorders with and without co-morbid anxiety. *Psychoneuroendocrinology*, 46:32–45.

Hsueh, B., Chen, R., Jo, Y., Tang, D., Raffiee, M., Kim, Y. S., Inoue, M., Randles, S., Ramakrishnan, C., Patel, S., Kim, D. K., Liu, T. X., Kim, S. H., Tan, L., Mortazavi, L., Cordero, A., Shi, J., Zhao, M., Ho, T. T., Crow, A., Yoo, A.-C. W., Raja, C., Evans, K., Bernstein, D., Zeineh, M., Goubran, M., and Deisseroth, K. (2023). Cardiogenic control of affective behavioural state. *Nature*.

Hua, J. Y. and Smith, S. J. (2004). Neural activity and the dynamics of central nervous system development. *Nature Neuroscience*, 7(4):327–332.

Huang, Y. and Rao, R. P. N. (2011). Predictive coding. *WIREs Cognitive Science*, 2(5):580–593.

Huo, Y., Blaber, J., Damon, S. M., Boyd, B. D., Bao, S., Parvathaneni, P., Noguera, C. B., Chaganti, S., Nath, V., Greer, J. M., Lyu, I., French, W. R., Newton, A. T., Rogers, B. P., and Landman, B. A. (2018). Towards Portable Large-Scale Image Processing with High-Performance Computing. *Journal of Digital Imaging*, 31(3):304–314.

Huo, Y., Plassard, A. J., Carass, A., Resnick, S. M., Pham, D. L., Prince, J. L., and Landman, B. A. (2016). Consistent cortical reconstruction and multi-atlas brain segmentation. *NeuroImage*, 138:197–210.

Hus, V. and Lord, C. (2014). The Autism Diagnostic Observation Schedule, Module 4: Revised Algorithm and Standardized Severity Scores. *Journal of Autism and Developmental Disorders*, 44(8):1996–2012.

Innocenti, G. M. and Price, D. J. (2005). Exuberance in the development of cortical networks. *Nature Reviews Neuroscience*, 6(12):955–965.

Iverson, J. M. (2021). Developmental Variability and Developmental Cascades: Lessons From Motor and Language Development in Infancy. *Current Directions in Psychological Science*, 30(3):228–235.

Jeste, S. S. and Geschwind, D. H. (2014). Disentangling the heterogeneity of autism spectrum disorder through genetic findings. *Nature Reviews Neurology*, 10(2):74–81.

Jou, R. J., Minshew, N. J., Keshavan, M. S., and Hardan, A. Y. (2010). Cortical Gyrification in Autistic and Asperger Disorders: A Preliminary Magnetic Resonance Imaging Study. *Journal of Child Neurology*, 25(12):1462–1467.

Jönsson, E. H., Kotilahti, K., Heiskala, J., Wasling, H. B., Olausson, H., Croy, I., Mustaniemi, H., Hiltunen, P., Tuulari, J. J., Scheinin, N. M., Karlsson, L., Karlsson, H., and Nissilä, I. (2018). Affective and non-affective touch evoke differential brain responses in 2-month-old infants. *NeuroImage*, 169:162–171.

Kanner, L. (1943). Autistic disturbances of affective contact. *Nervous child*, 2(3):217–250.

Katz, L. C. and Shatz, C. J. (1996). Synaptic Activity and the Construction of Cortical Circuits. *Science*, 274(5290):1133–1138.

Khalsa, S., Rudrauf, D., Sandesara, C., Olshansky, B., and Tranel, D. (2009). Bolus isoproterenol infusions provide a reliable method for assessing interoceptive awareness. *International Journal of Psychophysiology*, 72(1):34–45.

Khalsa, S. S., Adolphs, R., Cameron, O. G., Critchley, H. D., Davenport, P. W., Feinstein, J. S., Feusner, J. D., Garfinkel, S. N., Lane, R. D., Mehling, W. E., Meuret, A. E., Nemeroff, C. B., Oppenheimer, S., Petzschner, F. H., Pollatos, O., Rhudy, J. L., Schramm, L. P., Simmons, W. K., Stein, M. B., Stephan, K. E., Van den Bergh, O., Van Diest, I., von Leupoldt, A., Paulus, M. P., Ainley, V., Al Zoubi, O., Aupperle, R., Avery, J., Baxter, L., Benke, C., Berner, L., Bodurka, J., Breese, E., Brown, T., Burrows, K., Cha, Y.-H., Clausen, A., Cosgrove, K., Deville, D., Duncan, L., Duquette, P., Ekhtiari, H., Fine, T., Ford, B., Garcia Cordero, I., Gleghorn, D., Guereca, Y., Harrison, N. A., Hassanpour, M., Hechler, T., Heller, A., Hellman, N., Herbert, B., Jarrahi, B., Kerr, K., Kirlic, N., Klabunde, M., Kraynak, T., Kriegsman, M., Kroll, J., Kuplicki, R., Lapidus, R., Le, T., Hagen, K. L., Mayeli, A., Morris, A., Naqvi, N., Oldroyd, K., Pané-Farré, C., Phillips, R., Poppa, T., Potter, W., Puhl, M., Safron, A., Sala, M., Savitz, J., Saxon, H., Schoenhals, W., Stanwell-Smith, C., Teed, A., Terasawa, Y., Thompson, K., Toups, M., Umeda, S., Upshaw, V., Victor, T., Wierenga, C., Wohlrab, C., Yeh, H.-w., Yoris, A., Zeidan, F., Zotev, V., and Zucker, N. (2018). Interoception and Mental Health: A Roadmap. *Biological Psychiatry: Cognitive Neuroscience and Neuroimaging*, 3(6):501–513.

Khalsa, S. S., Berner, L. A., and Anderson, L. M. (2022). Gastrointestinal Interoception in Eating Disorders: Charting a New Path. *Current Psychiatry Reports*, 24(1):47–60.

Khalsa, S. S., Feinstein, J. S., Li, W., Feusner, J. D., Adolphs, R., and Hurlemann, R. (2016). Panic Anxiety in Humans with Bilateral Amygdala Lesions: Pharmacological Induction via Cardiorespiratory Interoceptive Pathways. *Journal of Neuroscience*, 36(12):3559–3566.

Klapwijk, E. T., Aghajani, M., Lelieveld, G.-J., van Lang, N. D. J., Popma, A., van der Wee, N. J. A., Colins, O. F., and Vermeiren, R. R. J. M. (2017). Differential Fairness Decisions and Brain Responses After Expressed Emotions of Others in Boys with Autism Spectrum Disorders. *Journal of autism and developmental disorders*.

Kleckner, I. R., Zhang, J., Touroutoglou, A., Chanes, L., Xia, C., Simmons, W. K., Quigley, K. S., Dickerson, B. C., and Feldman Barrett, L. (2017). Evidence for a large-scale brain system supporting allostasis and interoception in humans. *Nature Human Behaviour*, 1(5).

Kohli, J. S., Kinnear, M. K., Fong, C. H., Fishman, I., Carper, R. A., and Müller, R.-A. (2019a). Local Cortical Gyrification is Increased in Children With Autism Spectrum Disorders, but Decreases Rapidly in Adolescents. *Cerebral Cortex*, 29(6):2412–2423.

Kohli, J. S., Kinnear, M. K., Martindale, I. A., Carper, R. A., and Müller, R.-A. (2019b). Regionally decreased gyrification in middle-aged adults with autism spectrum disorders. *Neurology*, page 10.1212/WNL.0000000000008478.

Krishnan, A., Zhang, R., Yao, V., Theesfeld, C. L., Wong, A. K., Tadych, A., Volfovsky, N., Packer, A., Lash, A., and Troyanskaya, O. G. (2016). Genome-wide prediction and functional characterization of the genetic basis of autism spectrum disorder. *Nature Neuroscience*, 19(11):1454–1462.

Kwakye, L. D., Foss-Feig, J. H., Cascio, C. J., Stone, W. L., and Wallace, M. T. (2011). Altered Auditory and Multisensory Temporal Processing in Autism Spectrum Disorders. *Frontiers in Integrative Neuroscience*, 4.

Körmendi, J., Ferentzi, E., and Köteles, F. (2022). A heartbeat away from a valid tracking task. An empirical comparison of the mental and the motor tracking task. *Biological Psychology*, 171:108328.

Laidi, C., Boisgontier, J., de Pierrefeu, A., Duchesnay, E., Hotier, S., d'Albis, M.-A., Delorme, R., Bolognani, F., Czech, C., Bouquet, C., Amestoy, A., Petit, J., Holiga, , Dukart, J., Gaman, A., Toledano, E., Ly-Le Moal, M., Scheid, I., Leboyer, M., and Houenou, J. (2019). Decreased Cortical Thickness in the Anterior Cingulate Cortex in Adults with Autism. *Journal of Autism and Developmental Disorders*, 49(4):1402–1409.

Lee, H., Chen, Y.-J., Sideris, J., Watson, L. R., Crais, E. R., and Baranek, G. T. (2022). Sensory Features of Young Children From a Large Community Sample: Latent Factor Structures of the Sensory Experiences Questionnaire (Version 2.1, Short Form). *The American Journal of Occupational Therapy*, 76(3):7603205140.

Lee, J. M., Kyeong, S., Kim, E., and Cheon, K.-A. (2016). Abnormalities of Inter- and Intra-Hemispheric Functional Connectivity in Autism Spectrum Disorders: A Study Using the Autism Brain Imaging Data Exchange Database. *Frontiers in neuroscience*, 10:191.

Legrand, N., Nikolova, N., Correa, C., Brændholt, M., Stuckert, A., Kildahl, N., Vejlø, M., Fardo, F., and Allen, M. (2022). The heart rate discrimination task: A psychophysical method to estimate the accuracy and precision of interoceptive beliefs. *Biological Psychology*, 168:108239.

Lekander, M., Karshikoff, B., Johansson, E., Soop, A., Fransson, P., Lundström, J. N., Andreasson, A., Ingvar, M., Petrovic, P., Axelsson, J., and Nilsonne, G. (2016). Intrinsic functional connectivity of insular cortex and symptoms of sickness during acute experimental inflammation. *Brain, Behavior, and Immunity*, 56:34–41.

Lénárd, Z., Studinger, P., Mersich, B., Pavlik, G., and Kollai, M. (2005). Cardiovagal autonomic function in sedentary and trained offspring of hypertensive parents. *The Journal of physiology*, 565(3):1031–1038.

Leon, G. R., Fulkerson, J. A., Perry, C. L., and Early-Zald, M. B. (1995). Prospective analysis of personality and behavioral vulnerabilities and gender influences in the later development of disordered eating. *Journal of Abnormal Psychology*, 104(1):140–149.

Lerch, J. P. and Evans, A. C. (2005). Cortical thickness analysis examined through power analysis and a population simulation. *NeuroImage*, 24(1):163–173.

Levitt, J. G. (2003). Cortical Sulcal Maps in Autism. *Cerebral Cortex*, 13(7):728–735.

Libero, L. E., DeRamus, T. P., Deshpande, H. D., and Kana, R. K. (2014). Surface-based morphometry of the cortical architecture of autism spectrum disorders: volume, thickness, area, and gyrification. *Neuropsychologia*, 62:1–10.

Libero, L. E., Schaer, M., Li, D. D., Amaral, D. G., and Nordahl, C. W. (2019). A Longitudinal Study of Local Gyrification Index in Young Boys With Autism Spectrum Disorder. *Cerebral Cortex*, 29(6):2575–2587.

Lilenfeld, L. R., Wonderlich, S., Riso, L. P., Crosby, R., and Mitchell, J. (2006). Eating disorders and personality: A methodological and empirical review. *Clinical Psychology Review*, 26(3):299–320.

Lord, C., Risi, S., Lambrecht, L., Cook, E. H., Leventhal, B. L., DiLavore, P. C., Pickles, A., and Rutter, M. (2000). The Autism Diagnostic Observation Schedule–Generic: A Standard Measure of Social and Communication Deficits Associated with the Spectrum of Autism.

Lord, C., Rutter, M., DiLavore, P. C., Risi, S., Gotham, K., and Bishop, S. (2012). *Autism diagnostic observation schedule-2nd edition (ADOS-2)*. Western Psychological Corporation, Los Angeles, CA.

Lorensen, W. E. and Cline, H. E. (1987). (˜ ˜ ComputerGraphics,Volume21, Number4,July1987. page 7.

Luchsinger, J. R., Fetterly, T. L., Williford, K. M., Salimando, G. J., Doyle, M. A., Maldonado, J., Simerly, R. B., Winder, D. G., and Centanni, S. W. (2021). Delineation of an insula-BNST circuit engaged by struggling behavior that regulates avoidance in mice. *Nature Communications*, 12(1):3561.

Lui, J., Hansen, D., and Kriegstein, A. (2011). Development and Evolution of the Human Neocortex. *Cell*, 146(1):18–36.

Lyu, I., Kang, H., Woodward, N. D., and Landman, B. A. (2018a). Sulcal depth-based cortical shape analysis in normal healthy control and schizophrenia groups. In Angelini, E. D. and Landman, B. A., editors, *Medical Imaging 2018: Image Processing*, page 1, Houston, United States. SPIE.

Lyu, I., Kang, H., Woodward, N. D., Styner, M. A., and Landman, B. A. (2019). Hierarchical spherical deformation for cortical surface registration. *Medical Image Analysis*, 57:72–88.

Lyu, I., Kim, S. H., Girault, J. B., Gilmore, J. H., and Styner, M. A. (2018b). A cortical shape-adaptive approach to local gyrification index. *Medical Image Analysis*, 48:244–258.

Lyu, I., Kim, S. H., Woodward, N. D., Styner, M. A., and Landman, B. A. (2018c). TRACE: A Topological Graph Representation for Automatic Sulcal Curve Extraction. *IEEE Transactions on Medical Imaging*, 37(7):1653–1663.

Mallela, A. N., Deng, H., Gholipour, A., Warfield, S. K., and Goldschmidt, E. (2023). Heterogeneous growth of the insula shapes the human brain. *Proceedings of the National Academy of Sciences*, 120(24):e2220200120.

Marshall, A. C., Gentsch, A., Jelinčić, V., and Schütz-Bosbach, S. (2017). Exteroceptive expectations modulate interoceptive processing: repetition-suppression effects for visual and heartbeat evoked potentials. *Scientific Reports*, 7(1).

Mash, L. E., Schauder, K. B., Cochran, C., Park, S., and Cascio, C. J. (2017). Associations Between Interoceptive Cognition and Age in Autism Spectrum Disorder and Typical Development. *Journal of Cognitive Education and Psychology*, 16(1):23–37.

McGugin, R. W. and Gauthier, I. (2016). The reliability of individual differences in face-selective responses in the fusiform gyrus and their relation to face recognition ability. *Brain Imaging and Behavior*, 10(3):707–718.

McMorris, T. (2021). The acute exercise-cognition interaction: From the catecholamines hypothesis to an interoception model. *International Journal of Psychophysiology*, 170:75–88.

Menon, V. and Uddin, L. Q. (2010). Saliency, switching, attention and control: a network model of insula function. *Brain Structure and Function*, 214(5-6):655–667.

Mesulam, M.-M. and Mufson, E. J. (1982). Insula of the old world monkey. Architectonics in the insulo-orbito-temporal component of the paralimbic brain. *The Journal of Comparative Neurology*, 212(1):1–22.

Ming, X., Julu, P. O., Brimacombe, M., Connor, S., and Daniels, M. L. (2005). Reduced cardiac parasympathetic activity in children with autism. *Brain and Development*, 27(7):509–516.

Minshew, N. J. and Hobson, J. A. (2008). Sensory Sensitivities and Performance on Sensory Perceptual Tasks in High-functioning Individuals with Autism. *Journal of Autism and Developmental Disorders*, 38(8):1485–1498.

Montirosso, R. and McGlone, F. (2020). The body comes first. Embodied reparation and the co-creation of infant bodily-self. *Neuroscience & Biobehavioral Reviews*, 113:77–87.

Mota, B. and Herculano-Houzel, S. (2015). Cortical folding scales universally with surface area and thickness, not number of neurons. *Science*, 349(6243):74–77.

Mottron, L. and Bzdok, D. (2020). Autism spectrum heterogeneity: fact or artifact? *Molecular Psychiatry*, 25(12):3178–3185.

MRC AIMS Consortium, Bedford, S. A., Park, M. T. M., Devenyi, G. A., Tullo, S., Germann, J., Patel, R., Anagnostou, E., Baron-Cohen, S., Bullmore, E. T., Chura, L. R., Craig, M. C., Ecker, C., Floris, D. L., Holt, R. J., Lenroot, R., Lerch, J. P., Lombardo, M. V., Murphy, D. G. M., Raznahan, A., Ruigrok, A. N. V., Smith, E., Spencer, M. D., Suckling, J., Taylor, M. J., Thurm, A., Lai, M.-C., and Chakravarty, M. M. (2020). Large-scale analyses of the relationship between sex, age and intelligence quotient heterogeneity and cortical morphometry in autism spectrum disorder. *Molecular Psychiatry*, 25(3):614–628.

Mul, C.-l., Stagg, S. D., Herbelin, B., and Aspell, J. E. (2018). The Feeling of Me Feeling for You: Interoception, Alexithymia and Empathy in Autism. *Journal of Autism and Developmental Disorders*, 48(9):2953–2967.

Murphy, J., Catmur, C., and Bird, G. (2019). Classifying individual differences in interoception: Implications for the measurement of interoceptive awareness. *Psychonomic Bulletin & Review*, 26(5):1467–1471.

Murray, M. M. and Wallace, M. T., editors (2012). *The neural bases of multisensory processes*. Frontiers in Neuroscience. CRC Press, Boca Raton.

Nagasako, E. M., Oaklander, A. L., and Dworkin, R. H. (2003). Congenital insensitivity to pain: an update. *Pain*, 101(3):213–219.

Narayanan, J., Watts, R., Haddad, N., Labar, D., Li, P., and Filippi, C. (2002). Cerebral Activation during Vagus Nerve Stimulation: A Functional MR Study. *Epilepsia*, 43(12):1509–1514.

Natu, V. S., Gomez, J., Barnett, M., Jeska, B., Kirilina, E., Jaeger, C., Zhen, Z., Cox, S., Weiner, K. S., Weiskopf, N., and Grill-Spector, K. (2019). Apparent thinning of human visual cortex during childhood is associated with myelination. *Proceedings of the National Academy of Sciences*, 116(41):20750–20759.

Nickl-Jockschat, T., Habel, U., Maria Michel, T., Manning, J., Laird, A. R., Fox, P. T., Schneider, F., and Eickhoff, S. B. (2012). Brain structure anomalies in autism spectrum disorder-a meta-analysis of VBM studies using anatomic likelihood estimation. *Human Brain Mapping*, 33(6):1470–1489.

Noel, J.-P., Lytle, M., Cascio, C., and Wallace, M. T. (2018). Disrupted integration of exteroceptive and interoceptive signaling in autism spectrum disorder: Cardiovisual temporal binding window in ASD. *Autism Research*, 11(1):194–205.

Nomi, J. S., Molnar-Szakacs, I., and Uddin, L. Q. (2019). Insular function in autism: Update and future directions in neuroimaging and interventions. *Progress in Neuro-Psychopharmacology and Biological Psychiatry*, 89:412–426.

Nordahl, C. W., Dierker, D., Mostafavi, I., Schumann, C. M., Rivera, S. M., Amaral, D. G., and Van Essen, D. C. (2007). Cortical Folding Abnormalities in Autism Revealed by Surface-Based Morphometry. *Journal of Neuroscience*, 27(43):11725–11735.

Oppenheimer, S. M., Gelb, A., Girvin, J. P., and Hachinski, V. C. (1992). Cardiovascular effects of human insular cortex stimulation. *Neurology*, 42(9):1727–1727.

Palmer, C. E. and Tsakiris, M. (2018). Going at the heart of social cognition: is there a role for interoception in self-other distinction? *Current Opinion in Psychology*, 24:21–26.

Palmer, C. J., Lawson, R. P., and Hohwy, J. (2017). Bayesian approaches to autism: Towards volatility, action, and behavior. *Psychological Bulletin*, 143(5):521–542.

Palser, E., Fotopoulou, A., Pellicano, E., and Kilner, J. (2018). The link between interoceptive processing and anxiety in children diagnosed with autism spectrum disorder: Extending adult findings into a developmental sample. *Biological Psychology*, 136:13–21.

Park, H.-D. and Blanke, O. (2019). Heartbeat-evoked cortical responses: Underlying mechanisms, functional roles, and methodological considerations. *NeuroImage*, 197:502–511.

Park, H.-D. and Tallon-Baudry, C. (2014). The neural subjective frame: from bodily signals to perceptual consciousness. *Philosophical Transactions of the Royal Society B: Biological Sciences*, 369(1641):20130208.

Parkes, L., Fulcher, B., Yücel, M., and Fornito, A. (2018). An evaluation of the efficacy, reliability, and sensitivity of motion correction strategies for resting-state functional MRI. *NeuroImage*, 171:415–436.

Patil, S. and Ravi, B. (2005). Voxel-based Representation, Display and Thickness Analysis of Intricate Shapes. In *Ninth International Conference on Computer Aided Design and Computer Graphics (CAD-CG'05)*, pages 415–422, Hong Kong, China. IEEE.

Paulus, M. P. and Stein, M. B. (2006). An Insular View of Anxiety. *Biological Psychiatry*, 60(4):383–387.

Pellicano, E. (2013). Sensory Symptoms in Autism: A Blooming, Buzzing Confusion? *Child Development Perspectives*, 7(3):143–148.

Pellicano, E. and Burr, D. (2012). When the world becomes 'too real': a Bayesian explanation of autistic perception. *Trends in Cognitive Sciences*, 16(10):504–510.

Pickard, H., Hirsch, C., Simonoff, E., and Happé, F. (2020). Exploring the cognitive, emotional and sensory correlates of social anxiety in autistic and neurotypical adolescents. *Journal of Child Psychology and Psychiatry*, 61(12):1317–1327.

Porges, S. W. (1993). *Body perception questionnaire.* Laboratory of Developmental Assessment, University of Maryland.

Power, J., Cohen, A., Nelson, S., Wig, G., Barnes, K., Church, J., Vogel, A., Laumann, T., Miezin, F., Schlaggar, B., and Petersen, S. (2011). Functional Network Organization of the Human Brain. *Neuron*, 72(4):665–678.

Price, G. R., Wilkey, E. D., Yeo, D. J., and Cutting, L. E. (2016). The relation between 1st grade grey matter volume and 2nd grade math competence. *NeuroImage*, 124:232–237.

Puts, N. A. J., Wodka, E. L., Tommerdahl, M., Mostofsky, S. H., and Edden, R. A. E. (2014). Impaired tactile processing in children with autism spectrum disorder. *Journal of Neurophysiology*, 111(9):1803–1811.

Płonka, O., Krześniak, A., and Adamczyk, P. (2020). Analysis of local gyrification index using a novel shape-adaptive kernel and the standard FreeSurfer spherical kernel – evidence from chronic schizophrenia outpatients. *Heliyon*, 6(6):e04172.

Quadt, L., Critchley, H. D., and Garfinkel, S. N. (2018). The neurobiology of interoception in health and disease: Neuroscience of interoception. *Annals of the New York Academy of Sciences*, 1428(1):112–128.

Quadt, L., Garfinkel, S. N., Mulcahy, J. S., Larsson, D. E., Silva, M., Jones, A.-M., Strauss, C., and Critchley, H. D. (2021). Interoceptive training to target anxiety in autistic adults (ADIE): A single-center, superiority randomized controlled trial. *EClinicalMedicine*, 39:101042.

Quinde-Zlibut, J. M., Okitondo, C. D., Williams, Z. J., Weitlauf, A., Mash, L. E., Heflin, B. H., Woodward, N. D., and Cascio, C. J. (2020). Elevated Thresholds for Light Touch in Children With Autism Reflect More Conservative Perceptual Decision-Making Rather Than a Sensory Deficit. *Frontiers in Human Neuroscience*, 14:122.

Rakic, P. (1995). A small step for the cell, a giant leap for mankind: a hypothesis of neocortical expansion during evolution. *Trends in Neurosciences*, 18(9):383–388.

Rash, B. G., Duque, A., Morozov, Y. M., Arellano, J. I., Micali, N., and Rakic, P. (2019). Gliogenesis in the outer subventricular zone promotes enlargement and gyrification of the primate cerebrum. *Proceedings of the National Academy of Sciences*, 116(14):7089–7094.

Redcay, E. and Courchesne, E. (2005). When Is the Brain Enlarged in Autism? A Meta-Analysis of All Brain Size Reports. *Biological Psychiatry*, 58(1):1–9.

Riddle, K., Cascio, C. J., and Woodward, N. D. (2017). Brain structure in autism: a voxel-based morphometry analysis of the Autism Brain Imaging Database Exchange (ABIDE). *Brain Imaging and Behavior*, 11(2):541–551.

Ring, C. and Brener, J. (1992). The Temporal Locations of Heartbeat Sensations. *Psychophysiology*, 29(5):535–545.

Ritvo, E. R. and Freeman, B. J. (1977). National Society for Autistic Children Definition of the Syndrome of Autism. *Journal of Pediatric Psychology*, 2(4):146–148.

Robertson, C. E. and Baron-Cohen, S. (2017). Sensory perception in autism. *Nature Reviews Neuroscience*, 18(11):671–684.

Rodgers, J., Farquhar, K., Mason, D., Brice, S., Wigham, S., Ingham, B., Freeston, M., and Parr, J. R. (2020). Development and Initial Evaluation of the Anxiety Scale for Autism-Adults. *Autism in Adulthood*, 2(1):24–33.

Rodgers, J., Wigham, S., McConachie, H., Freeston, M., Honey, E., and Parr, J. R. (2016). Development of the anxiety scale for children with autism spectrum disorder (ASC-ASD): Measuring anxiety in ASD. *Autism Research*, 9(11):1205–1215.

Rohe, T. and Noppeney, U. (2016). Distinct Computational Principles Govern Multisensory Integration in Primary Sensory and Association Cortices. *Current Biology*, 26(4):509–514.

Roid, G. H., Miller, L. J., Pomplun, M., and Koch, C. (2013). *Leiter International Performance Scale*. Pearson, Toronto, CA.

Ronan, L. and Fletcher, P. C. (2015). From genes to folds: a review of cortical gyrification theory. *Brain Structure and Function*, 220(5):2475–2483.

Rosen, N. E., Lord, C., and Volkmar, F. R. (2021). The Diagnosis of Autism: From Kanner to DSM-III to DSM-5 and Beyond. *Journal of Autism and Developmental Disorders*, 51(12):4253–4270.

Russell, G., Mandy, W., Elliott, D., White, R., Pittwood, T., and Ford, T. (2019). Selection bias on intellectual ability in autism research: a cross-sectional review and meta-analysis. *Molecular Autism*, 10(1):9.

Sack, A. T., Sperling, J. M., Prvulovic, D., Formisano, E., Goebel, R., Salle, F. D., Dierks, T., and Linden, D. E. J. (2002). Tracking the Mind's Image in the Brain II: Transcranial Magnetic Stimulation Reveals Parietal Asymmetry in Visuospatial Imagery.

Savarese, E. T. (2010). What we have to tell you: A roundtable with self-advocates from AutCom. *Disability Studies Quarterly*, 30(1).

Schaer, M., Cuadra, M., Tamarit, L., Lazeyras, F., Eliez, S., and Thiran, J.-P. (2008). A Surface-Based Approach to Quantify Local Cortical Gyrification. *IEEE Transactions on Medical Imaging*, 27(2):161–170.

Schaer, M., Kochalka, J., Padmanabhan, A., Supekar, K., and Menon, V. (2015). Sex differences in cortical volume and gyrification in autism. *Molecular Autism*, 6(1).

Schaer, M., Ottet, M.-C., Scariati, E., Dukes, D., Franchini, M., Eliez, S., and Glaser, B. (2013). Decreased frontal gyrification correlates with altered connectivity in children with autism. *Frontiers in Human Neuroscience*, 7.

Schandry, R. (1981). Heart Beat Perception and Emotional Experience. *Psychophysiology*, 18(4):483–488.

Schneider, T. R., Ring, C., and Katkin, E. S. (1998). A test of the validity of the method of constant stimuli as an index of heartbeat detection. *Psychophysiology*, 35(1):86–89.

Schultz, R. T. (2005). Developmental deficits in social perception in autism: the role of the amygdala and fusiform face area. *International Journal of Developmental Neuroscience*, 23(2-3):125–141.

Schumann, C. M., Bloss, C. S., Barnes, C. C., Wideman, G. M., Carper, R. A., Akshoomoff, N., Pierce, K., Hagler, D., Schork, N., Lord, C., and Courchesne, E. (2010). Longitudinal Magnetic Resonance Imaging Study of Cortical Development through Early Childhood in Autism. *Journal of Neuroscience*, 30(12):4419–4427.

Seeley, W. W., Menon, V., Schatzberg, A. F., Keller, J., Glover, G. H., Kenna, H., Reiss, A. L., and Greicius, M. D. (2007). Dissociable Intrinsic Connectivity Networks for Salience Processing and Executive Control. *Journal of Neuroscience*, 27(9):2349–2356.

Sestan, N. and State, M. W. (2018). Lost in Translation: Traversing the Complex Path from Genomics to Therapeutics in Autism Spectrum Disorder. *Neuron*, 100(2):406–423.

Shen, M. D., Nordahl, C. W., Young, G. S., Wootton-Gorges, S. L., Lee, A., Liston, S. E., Harrington, K. R., Ozonoff, S., and Amaral, D. G. (2013). Early brain enlargement and elevated extra-axial fluid in infants who develop autism spectrum disorder. *Brain*, 136(9):2825–2835.

Shiee, N., Bazin, P.-L., Cuzzocreo, J. L., Ye, C., Kishore, B., Carass, A., Calabresi, P. A., Reich, D. S., Prince, J. L., and Pham, D. L. (2014). Reconstruction of the human cerebral cortex robust to white matter lesions: Method and validation: Cortical Reconstruction Robust to WM Lesions. *Human Brain Mapping*, 35(7):3385–3401.

Simon, D. M. and Corbett, B. A. (2013). Examining associations between anxiety and cortisol in high functioning male children with autism. *Journal of neurodevelopmental disorders*, 5(1):32.

Smith, R., Kuplicki, R., Feinstein, J., Forthman, K. L., Stewart, J. L., Paulus, M. P., Tulsa 1000 investigators, and Khalsa, S. S. (2020). A Bayesian computational model reveals a failure to adapt interoceptive precision estimates across depression, anxiety, eating, and substance use disorders. *PLOS Computational Biology*, 16(12):e1008484.

Spielberger, C. D. (1983). *Manual for the State-trait anxiety inventory (form Y) ("self-evaluation questionnaire")*. Consulting Psychologists Press, Palo Alto, CA.

Stein, B. E. and Rowland, B. A. (2011). Organization and plasticity in multisensory integration. In *Progress in Brain Research*, volume 191, pages 145–163. Elsevier.

Stevenson, R. A., Segers, M., Ferber, S., Barense, M. D., and Wallace, M. T. (2014). The impact of multisensory integration deficits on speech perception in children with autism spectrum disorders. *Frontiers in Psychology*, 5.

Tallon-Baudry, C., Campana, F., Park, H.-D., and Babo-Rebelo, M. (2018). The neural monitoring of visceral inputs, rather than attention, accounts for first-person perspective in conscious vision. *Cortex*, 102:139–149.

Tavassoli, T., Bellesheim, K., Tommerdahl, M., Holden, J. M., Kolevzon, A., and Buxbaum, J. D. (2016). Altered tactile processing in children with autism spectrum disorder: Tactile processing, inhibition, ASD. *Autism Research*, 9(6):616–620.

Thapa, R., Pokorski, I., Ambarchi, Z., Thomas, E., Demayo, M., Boulton, K., Matthews, S., Patel, S., Sedeli, I., Hickie, I. B., and Guastella, A. J. (2021). Heart Rate Variability in Children With Autism Spectrum Disorder and Associations With Medication and Symptom Severity. *Autism Research*, 14(1):75–85.

The IBIS Network, Hazlett, H. C., Gu, H., Munsell, B. C., Kim, S. H., Styner, M., Wolff, J. J., Elison, J. T., Swanson, M. R., Zhu, H., Botteron, K. N., Collins, D. L., Constantino, J. N., Dager, S. R., Estes, A. M., Evans, A. C., Fonov, V. S., Gerig, G., Kostopoulos, P., McKinstry, R. C., Pandey, J., Paterson, S., Pruett, J. R., Schultz, R. T., Shaw, D. W., Zwaigenbaum, L., and Piven, J. (2017). Early brain development in infants at high risk for autism spectrum disorder. *Nature*, 542(7641):348–351.

Trevisan, D. A., Altschuler, M. R., Bagdasarov, A., Carlos, C., Duan, S., Hamo, E., Kala, S., McNair, M. L., Parker, T., Stahl, D., Winkelman, T., Zhou, M., and McPartland, J. C. (2019). A meta-analysis on the relationship between interoceptive awareness and alexithymia: Distinguishing interoceptive accuracy and sensibility. *Journal of Abnormal Psychology*, 128(8):765–776.

Trevisan, D. A., Mehling, W. E., and McPartland, J. C. (2021a). Adaptive and Maladaptive Bodily Awareness: Distinguishing Interoceptive Sensibility and Interoceptive Attention from Anxiety-Induced Somatization in Autism and Alexithymia. *Autism Research*, 14(2):240–247.

Trevisan, D. A., Parker, T., and McPartland, J. C. (2021b). First-Hand Accounts of Interoceptive Difficulties in Autistic Adults. *Journal of Autism and Developmental Disorders*, 51(10):3483–3491.

Tsakiris, M. and Critchley, H. (2016). Interoception beyond homeostasis: affect, cognition and mental health. *Philosophical Transactions of the Royal Society B: Biological Sciences*, 371(1708):20160002.

Türe, U., Yaşargil, D. C. H., Al-Mefty, O., and Yaşargil, M. G. (1999). Topographic anatomy of the insular region. *Journal of Neurosurgery*, 90(4):720–733.

Uddin, L. Q. (2011). The self in autism: An emerging view from neuroimaging. *Neurocase*, 17(3):201–208.

Uddin, L. Q. (2015). Salience processing and insular cortical function and dysfunction. *Nature Reviews Neuroscience*, 16(1):55–61.

Uddin, L. Q. and Menon, V. (2009). The anterior insula in autism: Under-connected and under-examined. *Neuroscience & Biobehavioral Reviews*, 33(8):1198–1203.

Uddin, L. Q., Nomi, J. S., Hébert-Seropian, B., Ghaziri, J., and Boucher, O. (2017). Structure and Function of the Human Insula:. *Journal of Clinical Neurophysiology*, 34(4):300–306.

Uddin, L. Q., Supekar, K., and Menon, V. (2013). Reconceptualizing functional brain connectivity in autism from a developmental perspective. *Frontiers in Human Neuroscience*, 7.

Wallace, G. L., Robustelli, B., Dankner, N., Kenworthy, L., Giedd, J. N., and Martin, A. (2013). Increased gyrification, but comparable surface area in adolescents with autism spectrum disorders. *Brain*, 136(6):1956–1967.

Wallace, M. T. and Stein, B. E. (1997). Development of Multisensory Neurons and Multisensory Integration in Cat Superior Colliculus. *The Journal of Neuroscience*, 17(7):2429–2444.

Wallman-Jones, A., Perakakis, P., Tsakiris, M., and Schmidt, M. (2021). Physical activity and interoceptive processing: Theoretical considerations for future research. *International Journal of Psychophysiology*, 166:38–49.

Walsh, K. M., Saab, B. J., and Farb, N. A. (2019). Effects of a Mindfulness Meditation App on Subjective Well-Being: Active Randomized Controlled Trial and Experience Sampling Study. *JMIR Mental Health*, 6(1):e10844.

Wang, Y., Zhang, Y.-b., Liu, L.-l., Cui, J.-f., Wang, J., Shum, D. H. K., Van Amelsvoort, T., and Chan, R. C. K. (2017). A Meta-Analysis of Working Memory Impairments in Autism Spectrum Disorders. *Neuropsychology Review*, 27(1):46–61.

Watson, L. R., Roberts, J. E., Baranek, G. T., Mandulak, K. C., and Dalton, J. C. (2012). Behavioral and Physiological Responses to Child-Directed Speech of Children with Autism Spectrum Disorders or Typical Development. *Journal of Autism and Developmental Disorders*, 42(8):1616–1629.

Wechsler, D. (1999). *Wechsler Abbreviated Scales of Intelligence (WASI)*. Pearson, Toronto, CA.

Wechsler, D. (2011). *Wechsler Abbreviated Scales of Intelligence (WASI-II)*. Pearson, Toronto, CA, 2nd ed edition.

Wenderoth, N., Debaere, F., Sunaert, S., and Swinnen, S. P. (2005). The role of anterior cingulate cortex and precuneus in the coordination of motor behaviour. *European Journal of Neuroscience*, 22(1):235–246.

Whitehead, W. E., Drescher, V. M., Heiman, P., and Blackwell, B. (1977). Relation of heart rate control to heartbeat perception. *Biofeedback and Self-regulation*, 2(4):371–392.

Wig, G. S., Laumann, T. O., and Petersen, S. E. (2014). An approach for parcellating human cortical areas using resting-state correlations. *NeuroImage*, 93:276–291.

Williams, K. L., Kirby, A. V., Watson, L. R., Sideris, J., Bulluck, J., and Baranek, G. T. (2018). Sensory features as predictors of adaptive behaviors: A comparative longitudinal study of children with autism spectrum disorder and other developmental disabilities. *Research in Developmental Disabilities*, 81:103–112.

Williams, Z. J., Suzman, E., Bordman, S. L., Markfeld, J. E., Kaiser, S. M., Dunham, K. A., Zoltowski, A. R., Failla, M. D., Cascio, C. J., and Woynaroski, T. G. (2022). Characterizing Interoceptive Differences in Autism: A Systematic Review and Meta-analysis of Case–control Studies. *Journal of Autism and Developmental Disorders*.

Woynaroski, T. G., Kwakye, L. D., Foss-Feig, J. H., Stevenson, R. A., Stone, W. L., and Wallace, M. T. (2013). Multisensory Speech Perception in Children with Autism Spectrum Disorders. *Journal of Autism and Developmental Disorders*, 43(12):2891–2902.

Xu, J., Wang, H., Zhang, L., Xu, Z., Li, T., Zhou, Z., Zhou, Z., Gan, Y., and Hu, Q. (2018). Both Hypo-Connectivity and Hyper-Connectivity of the Insular Subregions Associated With Severity in Children With Autism Spectrum Disorders. *Frontiers in Neuroscience*, 12:234.

Yamada, T., Itahashi, T., Nakamura, M., Watanabe, H., Kuroda, M., Ohta, H., Kanai, C., Kato, N., and Hashimoto, R.-I. (2016). Altered functional organization within the insular cortex in adult males with high-functioning autism spectrum disorder: evidence from connectivity-based parcellation. *Molecular autism*, 7:41.

Yang, J. and Hofmann, J. (2016). Action observation and imitation in autism spectrum disorders: an ALE meta-analysis of fMRI studies. *Brain imaging and behavior*, 10(4):960–969.

Yates, A. J., Jones, K. E., Marie, G. V., and Hogben, J. H. (1985). Detection of the Heartbeat and Events in the Cardiac Cycle. *Psychophysiology*, 22(5):561–567.

Zapparrata, N. M., Brooks, P. J., and Ober, T. M. (2022). Slower Processing Speed in Autism Spectrum Disorder: A Meta-analytic Investigation of Time-Based Tasks. *Journal of Autism and Developmental Disorders*.

Zarza-Rebollo, J. A., Sanabria, D., and Perakakis, P. (2019). Can increased interoception explain exercise-induced benefits on brain function and cognitive performance? preprint, PsyArXiv.

Zhang, J., Meng, Y., He, J., Xiang, Y., Wu, C., Wang, S., and Yuan, Z. (2019). McGurk Effect by Individuals with Autism Spectrum Disorder and Typically Developing Controls: A Systematic Review and Meta-analysis. *Journal of Autism and Developmental Disorders*, 49(1):34–43.

Zoltowski, A. R., Failla, M. D., and Cascio, C. J. (2022). Social touch and allostasis. *Current Opinion in Behavioral Sciences*, 43:69–74.

APPENDIX 1

Supplemental information

.1 MRI scanning criteria

Across all cohorts, each participant was asked by MRI technicians during the study screening phase (i.e., prior to scans being scheduled) whether any of the following criteria was applicable to him/her. Endorsing any of the following conditions without a previous successful MRI scan would cause the MRI technicians to cancel the scan. Possible conditions:

- Alcohol or substance abuse
- Injury by metallic object or foreign body
- History of asthma, allergic reaction, respiratory disease, or reaction to a contrast medium or dye used for an MRI, CT, or X-ray examination
- Anemia or any disease(s) that affects your blood, a history of renal (kidney) disease, renal (kidney) failure, renal (kidney) transplant, high blood pressure (hypertension), liver (hepatic) disease, a history of diabetes, or seizures
- Antipsychotics, mood stabilizers, or noradrenergic-acting medications
- Aneurysm clip(s)
- Cardiac pacemaker
- Implanted cardioverter defibrillator (ICD)
- Electronic implant or device
- Magnetically-activated implant or device
- Neurostimulation system
- Spinal cord stimulator
- Internal electrodes or wires
- Bone growth/bone fusion stimulator
- Cochlear, otologic, or other ear implant
- Insulin or other infusion pump
- Implanted drug infusion device
- Any type of prosthesis (eye, penile, etc.)
- Heart valve prosthesis

- Eyelid spring or wire
- Artificial or prosthetic limb
- Metallic stent, filter, or coil
- Shunt (spinal or intraventricular)
- Vascular access port and/or catheter
- Radiation seeds or implants
- Swan-Ganz or thermodilution catheter
- Medication patch (Nicotine, Nitroglycerine)
- Any metallic fragment or foreign body
- Wire mesh implant
- Tissue expander (e.g., breast)
- Surgical staples, clips, or metallic sutures
- Joint replacement (hip, knee, etc.)
- Bone/joint pin, screw, nail, wire, plate, etc.
- IUD, diaphragm, or pessary
- Dentures or partial plates
- Tattoo or permanent makeup above the waist
- Body piercing jewelry (that cannot be removed)
- Hearing aid (Remove before entering the room)
- Other implant
- Breathing problem or motion disorder
- Claustrophobia
- Prior problems during MRI or CT procedure

.2 Chapter 2 supplement

Table 1: Summary of repeated MRI scans

	AUT (n = 21 repeated scans from n = 19 individuals)	NT (n = 183 repeated scans from n = 113 individuals)
Minimum age difference	0	0
Mean age difference	2	2
Maximum age difference	8	8

Summary of age difference between repeated scans per diagnostic group, with the age difference given as the value of age at the latest scan point minus age at earliest scan point, rounded to the nearest year.

Figure 1: Plot of covariation between cortical indices for clusters in which local gyrification was significantly greater in the autistic than neurotypical group (AUT >NT)

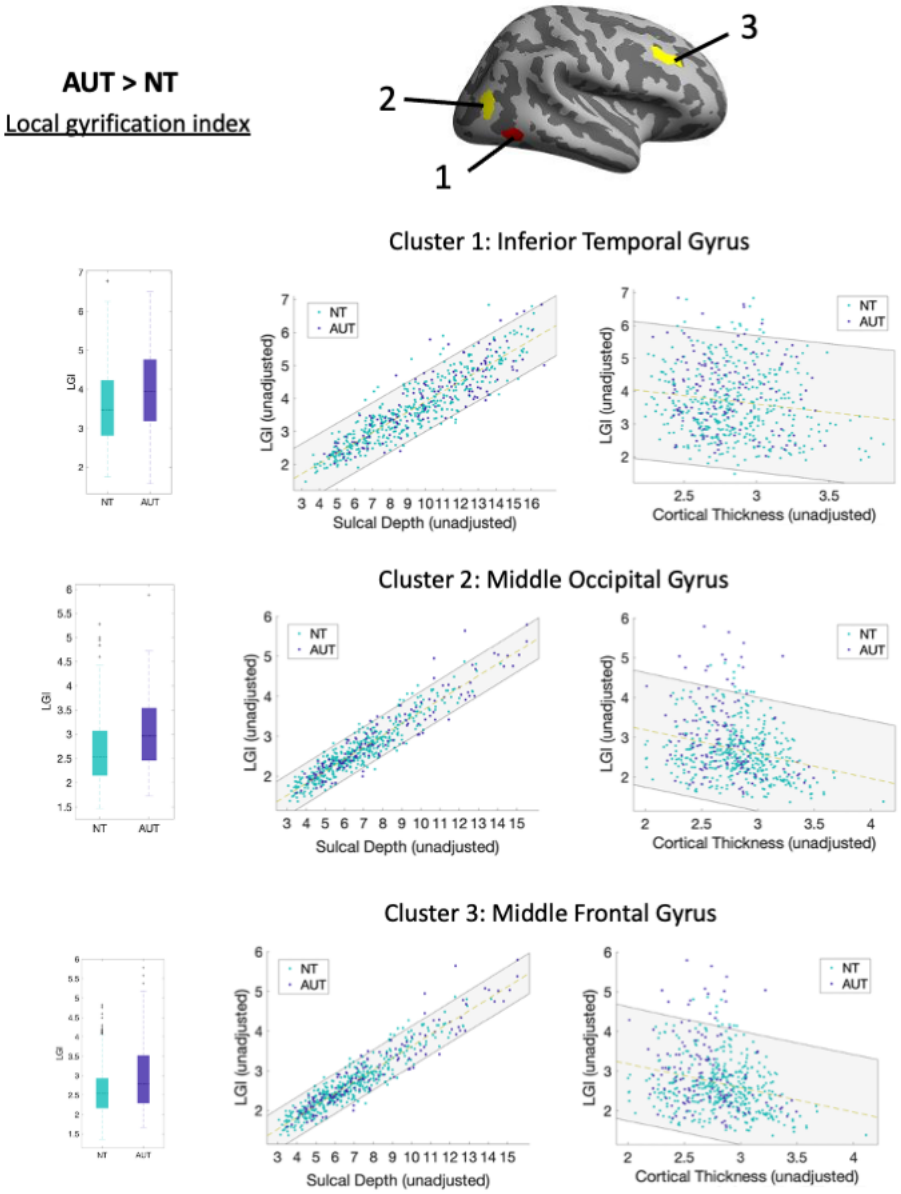

For each of the three significant clusters identified, a box plot is provided for the distribution of LGI, averaged across vertices within this region, by group. Additionally, unadjusted cortical indices (i.e., raw) averaged across vertices within each cluster are plotted, to illustrate correspondence of sulcal depth and cortical thickness, respectively, with LGI. The latter two clusters show closer correspondence between these indices than the first, which is consistent with similar clusters showing significantly greater sulcal depth in the autistic than neurotypical group (see Figure 2, panel B). Indices: local gyrification index (LGI), sulcal depth in mm, and cortical thickness in mm. Gray region indicates 95% confidence interval. Points are colored by participants group, with NT=neurotypical (turquoise) and AUT=autism (purple).

Figure 2: Plot of cortical indices by age, adjusted for diagnosis, biological sex, and scan protocol

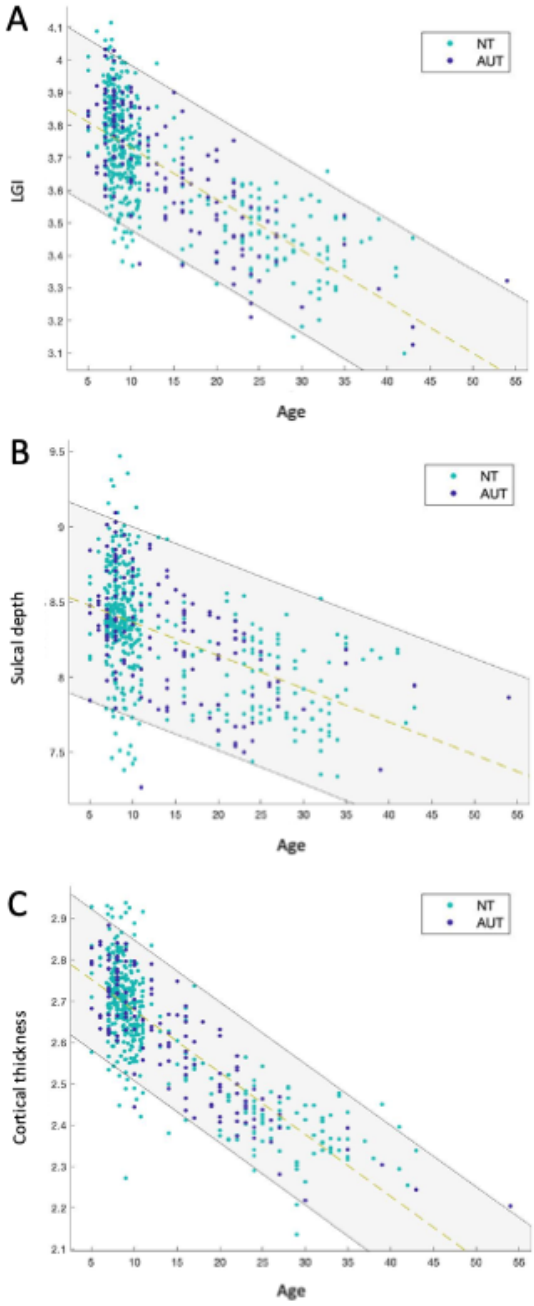

Standardized cortical indices averaged across cortical regions (y-axis) when adjusting for diagnosis, biological sex, participant, and scan protocol are plotted against participant age at scan. All three indices show negative trends with age. Panel A = local gyrification index (LGI), panel B = sulcal depth in mm, and panel C = cortical thickness in mm. Gray region indicates 95% confidence interval. Points are colored by participants group, with NT=neurotypical (turquoise) and AUT=autism (purple).

Figure 3: Morphological indices by scan protocol and biological sex

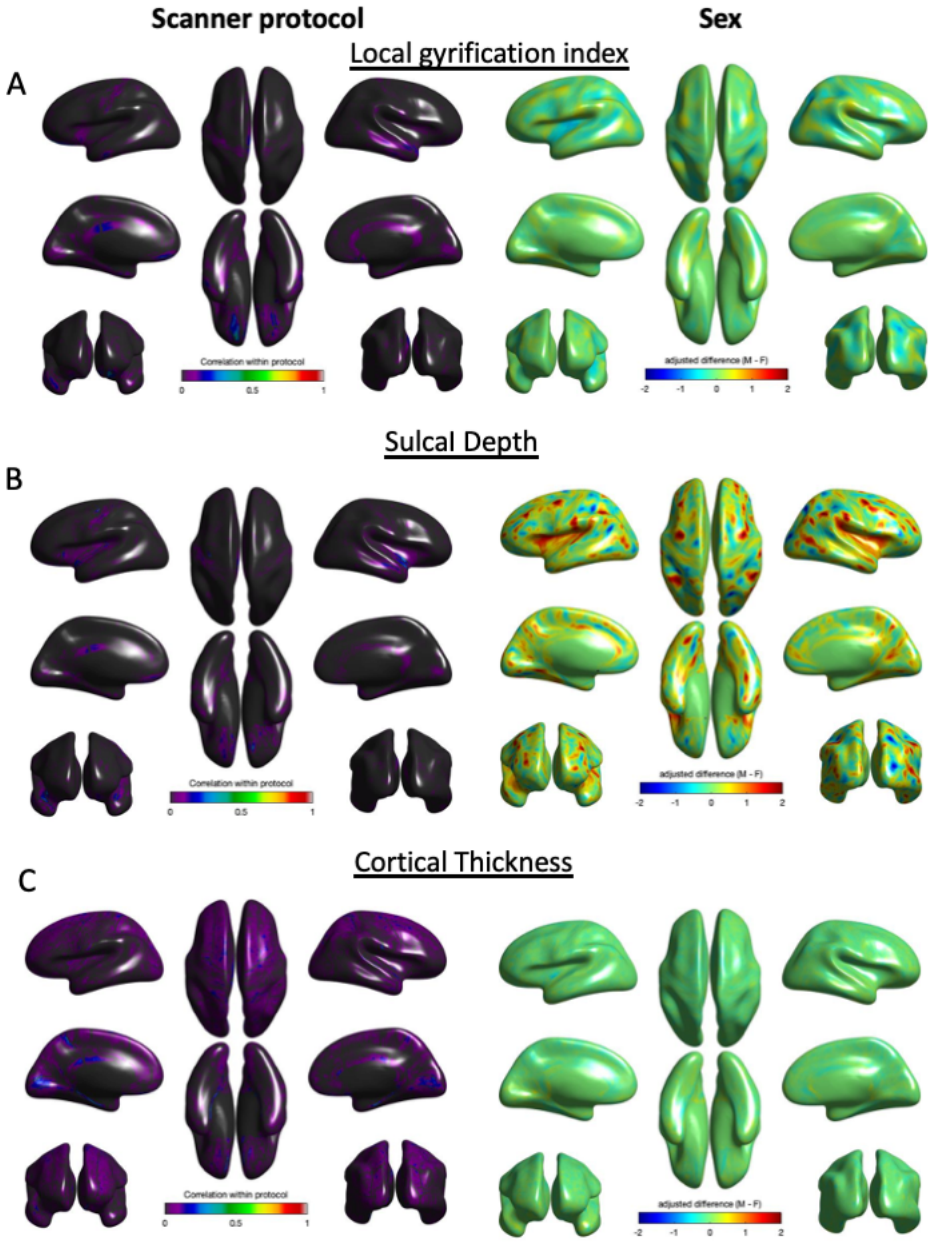

Plot of model terms for cohort scan protocol and biological sex terms. Panel A displays the random effects correlation of the protocol term by index, across brain regions. Panel B displays the average difference in index for males >females (M-F) by index, across brain regions. Note. Values in panel B are plotted on -2 to 2 scale, but relative scale of these differences differs by index (e.g., sulcal depth occurs on 0-30 scale whereas LGI occurs on 1-15 scale).

.3 Chapter 3 supplement

Figure 4: A comparison of FWE and FDR Approaches for posterior insula connectivity by age

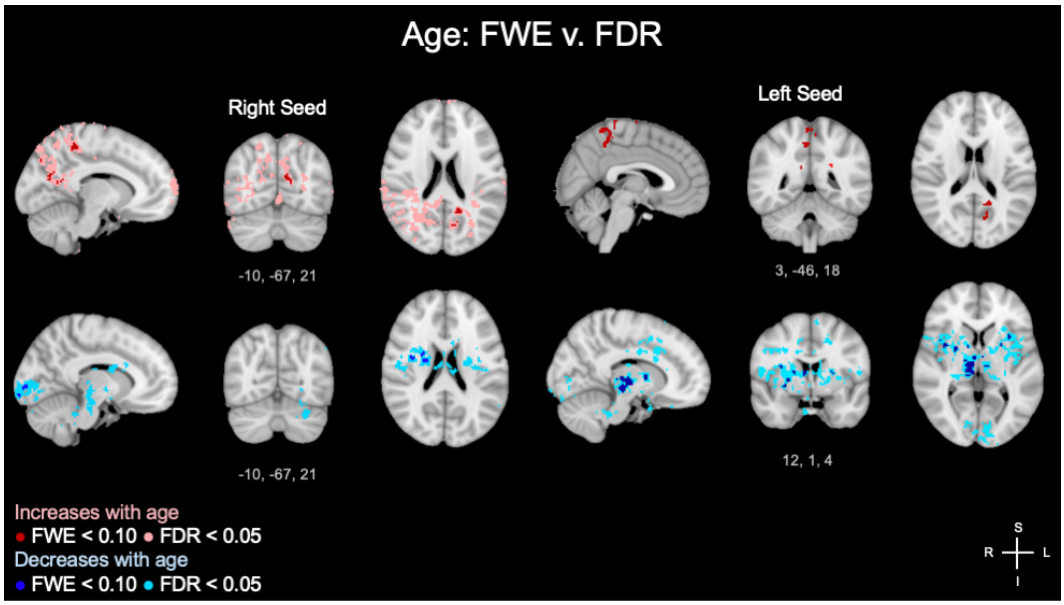

Significant clusters in which posterior insula functional connectivity increases (red) and decreases (blue) with age are shown (using threshold-free cluster enhancement, $p_{FWE} < 0.10$ versus $p_{FDR} < 0.05$). Color intensity varies by multiple corrections approach as shown in figure legend. Clusters corresponding to the right seed are shown on the left and left seed are shown on the right. Images are shown in radiological convention.

.4 Chapter 4 supplement

Figure 5: A comparison of Gaussian and Sine curve fits for an example participant with invalid method of constant stimuli (MCS) parameters

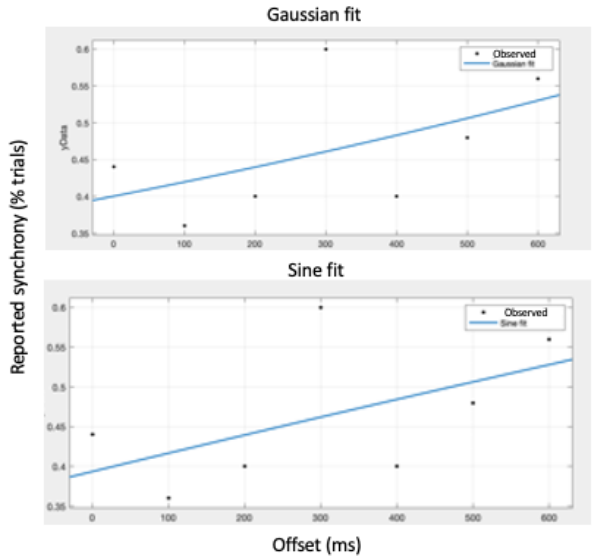

Comparison between a Gaussian curve fit (top panel) and sine wave fit (bottom panel) for one of the participants who was excluded from method of constant stimuli (MCS) task analysis due to invalid curve fit. The sine and Gaussian fits are both outliers. Note that approximately 55% of participants had a valid curve fit using the sine fit approach compared to 63% using the Gaussian approach.